

NORTHWESTERN UNIVERSITY

Mechanisms regulating Astrogliosis and Functional Recovery Following
Spinal Cord Injury.

A DISSERTATION

SUBMITTED TO THE GRADUATE SCHOOL
IN PARTIAL FULFILLMENT OF THE REQUIREMENTS

for the degree

DOCTOR OF PHILOSOPHY

Field of Northwestern University Interdepartmental Neuroscience Program

By

VIBHU VINODCHANDRA SAHNI

EVANSTON, ILLINOIS

December 2008

© Copyright by Vibhu V. Sahni 2008

All rights reserved

ABSTRACT

Mechanisms regulating Astrogliosis and Functional Recovery Following Spinal Cord Injury.

Vibhu V. Sahni

The studies in this thesis are directed towards defining the signaling mechanisms that regulate astrogliosis after SCI and towards developing potential therapeutic techniques for modifying this process. The central hypothesis is that alteration of the extracellular milieu after SCI can limit the deleterious effects of glial scar formation and enhance functional recovery.

Astrogliosis following SCI has a dual role; one as a mediator of repair and homeostasis and the other as an inhibitor of regeneration. Ideally, therefore, modifying astrogliosis to promote regeneration for therapeutic purposes would require preservation of the beneficial effects of gliosis while reducing its detrimental effects in inhibition of axon outgrowth.

In Chapter 2, we show that injection of a nanoengineered bioactive peptide amphiphile (IKVAV-PA) into the injured cord reduces scar progression without affecting astrocytic hypertrophy. Further, there is regeneration of sensory and motor axons and improvement in locomotor function in these animals, indicating that the extracellular environment can be reengineered to modulate astrogliosis and promote axon regeneration. In Chapter 3, we identify the β 1 integrin receptor subunit as a key target gene upregulated by IKVAV PA. β 1 integrin is not expressed by reactive astrocytes following SCI, which is consistent

with the finding that the PA does not affect the initial reactive hypertrophy. Instead it prevents astroglial commitment by β 1integrin expressing glial progenitors, thereby reducing the number of astrocytes at the lesion site. In Chapter 4, we investigated the role of BMP signaling in astrogliosis using BMP receptor knock out mice. Conditional ablation of BMPR1a led to deficits in the early reactive hypertrophy, increased infiltration by inflammatory cells and worsened locomotor recovery. Conversely, BMPR1b null mice developed normal reactive astrocytes, had significantly smaller lesion volumes and normal locomotor recovery, and had an attenuated glial scar in the chronic stages following injury. Hence BMP signaling regulates multiple phases of astrogliosis, with BMPR1a and BMPR1b receptors exerting opposing effects on reactive astrocytic hypertrophy.

Overall our findings support the hypothesis that targeting specific signaling pathways involved in gliosis can provide a novel therapeutic approach that enhances functional outcomes after SCI.

Acknowledgements

I have several people to thank for all their contributions to this work. I acknowledge my advisor John A. Kessler, for giving me the opportunity to pursue this work, for knowing just the right amount of mentorship I needed and also for allowing me tremendous creative freedom to design my project and its requisite experiments. For all this, I am extremely grateful. Members of the Kessler lab have been wonderful in their support, both professionally as well as in their companionship. My fellow graduate student and close friend, Vicki Tysseling-Mattiace, was a terrific team member (“and sub-unit of the Vicki-Vibhu heterodimer”) in the spinal cord injury team from its inception and her meticulousness and intensity was as key in getting this work done as her sense of humour and constant companionship. Other members of SCI team : Derin Birch, Isabel Chung and Amy Hebert, your help made some very laborious experiments seem not so bad. I shall always remember Derin, now a graduate student at Northwestern, for entertaining caricatures, his elaborate taping of notes to my bench and his origami! Abhishek Mukhopadhyay initiated the animal colonies that I used in my studies; it was always nice to be able to talk to (and commiserate with) someone in Hindi. Chianyu Peng always provided a keen ear and the perfect sounding board for experimental directions and technical suggestions. Other members of the lab, both past and present also deserve mention for their intellectual inputs, technical assistance and camaraderie : Jayshree Samanta (now at NYU), Tammy Mcguire, Jennifer Jarrett, Lixin Kan, Catherine Czeisler and Bridgid Nolan.

My thesis committee members : Warren Tourtellotte, Dane Chetkovich and Jhumku Kohtz gave useful inputs which always made my committee meetings a useful and productive exercise. Prof. Samuel Stupp and his group designed the amphiphile that was used as in a major part of my work. His graduate students Krista Niece and Eugene Pashuck designed and developed reagents for the work and more importantly, took the time to explain aspects about the material to me (someone completely ignorant when it comes to material science!) I'd also like to thank all my friends at Northwestern, in particular, Melissa Mendez, who shared my weakness for munchables and a well mixed martini!

Jonathan Carroll, his friendship through my graduate work as well as his home-cooked meals offered the best comfort through some gloomy times in graduate school! I thank my family for their love and support. My brother Subal Sahni and sister-in-law Mala Mathur, who were my home away from home. Lastly, to my parents Indu Sahni and Vinod C. Sahni, I could never have become the person who I am today without them and nothing I could write in this space could measure up to their irreplaceable role in my life. They have always loved and supported me unconditionally in all my ventures in life (graduate school being no exception), and for all that I am sincerely and eternally grateful.

TABLE OF CONTENTS

COPYRIGHT.....	2
ABSTRACT.....	3
ACKNOWLEDGEMENTS.....	5
TABLE OF CONTENTS.....	7
LIST OF FIGURES.....	9
CHAPTER 1: GENERAL INTRODUCTION.....	12
Stem/Progenitor cells in the developing nervous system.....	12
Regulation of astrocytic development and lineage commitment.....	14
Sequelae following spinal cord injury.....	18
Astrogliosis following CNS injuries: Friend or foe?.....	22
Origins of reactive astrocytes: a role for progenitor cell recruitment.....	24
Use of artificial scaffolds in spinal cord injury repair.....	27
Summary.....	29
 CHAPTER 2: SELF-ASSEMBLING NANOFIBERS INHIBIT GLIAL SCAR FORMATION AND PROMOTE AXON ELONGATION AFTER SPINAL CORD INJURY.....	31
Abstract.....	31
Introduction.....	32
Materials and methods.....	33
Results.....	39
Discussion.....	46

CHAPTER 3: BETA 1 INTEGRIN SIGNALING REGULATES ASTROCYTIC LINEAGE COMMITMENT AND ASTRGLIOSIS FOLLOWING SPINAL CORD INJURY.....	51
Abstract.....	51
Introduction.....	52
Materials and methods.....	55
Results.....	61
Discussion.....	75
CHAPTER 4: BMPR1A AND BMPR1B SIGNALING EXERT OPPOSING EFFECTS ON GLIOSIS AFTER SPINAL CORD INJURY.....	81
Abstract.....	81
Introduction.....	82
Materials and methods.....	84
Results.....	91
Discussion.....	103
CHAPTER 5: CONCLUSIONS.....	110
REFERENCES.....	163

LIST OF FIGURES

Chapter 2, figure 1: Structure of IKVAV PA.....	115
Chapter 2, figure 2: IKVAV PA solution self-assembles <i>in vivo</i>	116
Chapter 2, figure 3: Structure of IKVAV peptide amphiphile (PA).....	117
Chapter 2, figure 4: IKVAV PA promotes functional recovery as analyzed by the BBB scale.....	118
Chapter 2, figure 5: IKVAV sequence in the IKVAV PA is critical for functional recovery after SCI.....	119
Chapter 2, figure 6: Intense gliosis surrounds the area of dense infiltration.....	120
Chapter 2, figure 7: IKVAV PA attenuates astrogliosis <i>in vivo</i> after SCI.	121
Chapter 2, figure 8: Apoptotic cell death is reduced in IKVAV PA-injected animals.	122
Chapter 2, figure 9: IKVAV PA promotes regeneration of motor axons after SCI.....	123
Chapter 2, figure 10: IKVAV PA promotes regeneration of sensory axons after SCI...124	
Chapter 2, figure 11: Montage demonstrating meandering course of a single axon.....	125
Chapter 2, figure 12: Montage illustrating a single axon tracing.....	127
Chapter 3, figure 1: IKVAV sequence is necessary for bioactivity of the IKVAV PA.....	128
Chapter 3, figure 2: The IKVAV PA is a powerful tool for upregulating $\beta 1$ integrin...130	
Chapter 3, figure 3: Detection of endogenous versus transgenically expressed $\beta 1$ integrin.....	132
Chapter 3, figure 4: Cells retain progenitor characteristics and specifically avoid astrocytic commitment in the IKVAV PA.....	133
Chapter 3, figure 5: O4 positive cells were not in cell cycle at 7 days <i>in vitro</i>	135
Chapter 3, figure 6: Altering $\beta 1$ integrin signaling affects Astrocytic lineage commitment.....	136

Chapter 3, figure 7: The $\beta 1$ integrin receptor subunit is expressed on the NG2 positive progenitor population and not on reactive astrocytes after SCI.....	137
Chapter 3, figure 8: Maintenance of progenitor traits in IKVAV PA injected animals..	139
Chapter 3, figure 9: IKVAV PA does not alter inflammatory response after SCI.....	141
Chapter 3, figure 10: NG2 positive progenitor cells undergo cell divisions after spinal cord injury.....	142
Chapter 3, figure 11: NG2 positive progenitor cells can differentiate into astrocytes after spinal cord injury.....	143
Chapter 3, figure 12: IKVAV PA prevents astroglial lineage commitment from glial progenitors cells.....	144
Chapter 4, figure 1: Reactive astrocytes compact inflammatory cells after SCI.....	145
Chapter 4, figure 2: BMP signaling is active during reactive gliosis after spinal cord contusion injury.....	146
Chapter 4, figure 3: BMPR1a is more abundant than BMPR1b in the adult spinal cord.....	147
Chapter 4, figure 4: BMPR1a receptor is expressed on reactive astrocytes and not on inflammatory cells.....	148
Chapter 4, figure 5: Strategy to obtain BMPR1a conditional knock out mice.....	150
Chapter 4, figure 6: BMPR1a CKO astrocytes develop normally.....	151
Chapter 4, figure 7: Normal distribution of neurons, astrocytes and oligodendrocytes in BMPR1a CKO spinal cords.....	152
Chapter 4, figure 8: BMPR1a Conditional knock out mice show defective gliosis and increased inflammatory infiltration after spinal cord injury.....	153
Chapter 4, figure 9: BMPR1a Conditional knock out mice have reduced gliosis and increased lesion volumes in the chronic injured spinal cord and show worsened locomotor recovery.....	155
Chapter 4, figure 10: BMPR1a signaling affects post-transcriptional regulation of GFAP.....	157

Chapter 4, figure 11: BMPR1a signaling is not required for STAT3 activation by BMP4 in neural progenitor cells.....	159
Chapter 4, figure 12: BMPR1b knock out mice have reduced lesion volumes after spinal cord injury.....	160
Chapter 4, figure 13: BMPR1b knock out mice have reduced glial scar and normal functional recovery after spinal cord injury.....	161
Chapter 4, figure 14: BMPR1b KO animals do not show deficits in proliferation in the sub acute phase of spinal cord injury.....	162

Chapter 1

General Introduction

Stem/Progenitor cells in the developing nervous system

The Central Nervous system (CNS) arises from the neural plate, a cytologically homogenous sheet of epithelial cells that forms the dorsal surface of the gastrula-stage embryo, which then rolls up into the neural tube. The diverse cell types that constitute the CNS are produced by mitotic neural stem cells that are present in this developing neuroepithelium. Stem cells can undergo asymmetric divisions that generate two different daughter cells, as well as symmetric divisions that generate two identical daughters. Asymmetric divisions are considered a hallmark of stem cell behavior. They are central to their ability to produce multiple types of differentiated progeny, and to self-renew - ability to make more stem cells. The term “multipotent” describes cells that are capable of generating multiple cell types. To be considered a stem cell in the CNS, a cell must have the potential to differentiate into neurons, astrocytes and oligodendrocytes and to self-renew sufficiently to provide the multitude of cell types in the brain. The term “progenitor” or “precursor” refers to a cell with a more restricted potential than a stem cell (For reviews see(McKay, 1997; Frisen et al., 1998; Alvarez-Buylla et al., 2001; Temple, 2001).

The ventricular (VZ) and subventricular zones (SVZ) represent CNS germinative zones

present during embryonic development that contain multipotent neural progenitor cells (Privat and Leblond, 1972; Lois and Alvarez-Buylla, 1993; Gates et al., 1995). The timing of their differentiation is such that neurogenesis precedes gliogenesis; the former occurring in the embryonic periods while the latter mostly occurs postnatally with astroglialogenesis preceding the bulk of oligodendroglialogenesis. (Frederiksen and McKay, 1988; Skoff, 1990).

As the neural tube develops and is patterned into the sub regions of the nervous system, these cells reside in a well-defined germinal zone and act as progenitor cells for diverse types of neurons and glia. In order to do this, they have to proliferate and differentiate in a strictly controlled manner, and several key molecular mechanisms underlying this proliferation and differentiation have been identified. The control over this process is exerted by two principal mechanisms: intrinsic or extrinsic. In a system based on intrinsic factors, the decision to generate two identical or nonidentical daughter cells is based on molecules operating within the cell, while an extrinsic mechanism relies on signals influencing the cell from its surrounding environment. These mechanisms were initially identified by expanding neural stem/progenitor cells in culture as proliferative neurospheres in the presence of growth factors such as epidermal growth factor (EGF)(Reynolds et al., 1992; Reynolds and Weiss, 1992, 1996) or fibroblast growth factor (FGF)(Murphy et al., 1990; Vescovi et al., 1993; Palmer et al., 1995) amongst several others. Numerous studies have implicated several different growth factors, cytokines, and neurotrophic factors in influencing lineage commitment, cellular differentiation, and survival of CNS neural progenitor cells(Cattaneo and McKay, 1990; Murphy et al., 1990;

Mehler et al., 1993; Ahmed et al., 1995; Gage et al., 1995; Mehler et al., 1995). For the purposes of this work, we shall specifically focus on the mechanisms of astrocytic lineage commitment.

Regulation of Astrocytic development and Lineage commitment

The name astrocyte, or star-shaped cell, was given by Lehossek to a group of non-neuronal cells that have a characteristic stellate morphology and that contain cytoplasmic bundles now known to consist primarily of the intermediate filament protein, glial fibrillary acidic protein (GFAP). Original studies relied upon identification of these cells using electron microscopy (Caley and Maxwell, 1968; Privat, 1975) and tracing their precursors using golgi impregnation (Rakic, 1971; Schmechel and Rakic, 1979) both of which had several technical limitations. To overcome these difficulties, investigators turned to using some markers that could help identify these cells. The most commonly used marker for these cell types, is the intermediate filament protein GFAP which still remains limited in the number of astrocytes that it labels (Walz, 2000). Newer putative markers of the astrocyte phenotype have been identified including aquaporin 4 (Rash et al., 1998), S100 β , and GLAST (Storck et al., 1992), but their patterns of expression do not correspond precisely with the distribution of GFAP. The lack of an unambiguous biochemical marker has complicated the precise definition of astrocyte identity (Gotz and Steindler, 2003; Kimelberg, 2004).

Hence, while fate determination genes that can promote neuronal and oligodendroglial lineages from neural stem cells have been well characterized, the astrocytic lineage development remains poorly understood. The origins of astrocytic development in the embryo, lies in progenitor cells that exhibit glial characteristics called radial glia. While these cells act as neuronal progenitors during embryonic development, they eventually differentiate into astrocytes (Parnavelas and Nadarajah, 2001; Goldman, 2003). It seems apparent, however that even within the macroglial lineage, past a certain point in development, the precursors that give rise to astrocytes and oligodendrocytes largely do not overlap. The most compelling evidence for this comes from work with the basic helix-loop-helix transcription factors Olig1 and 2. While deletion of Olig gene function ablates the bulk of the oligodendrocytes from the adult CNS, the astrocyte populations in these knockout animals remain largely unaffected (Lu et al., 2002; Zhou and Anderson, 2002). Studies have established differences in the ability of dorsal and ventral regions of the neural tube in their ability to give rise to astrocytes and oligodendrocytes, respectively (Pringle et al., 1998). A large number of the factors that influence the development of astrocytes from neural progenitor cells have been established using cell culture techniques in vitro and extending these observations in vivo. Progenitor cell cultures have been established from different parts of the developing nervous system that can differentiate either into astrocytes or oligodendrocytes. In fact, the first such cell to be identified, was isolated from the rat optic nerve and was called an “O2-A” cell, indicating its potential to differentiate either into oligodendrocytes or type-2 astrocytes (Raff et al., 1983a). Though these cells express the oligodendrocytic lineage marker Platelet Derived

Growth factor Receptor alpha (PDGFR α), upon treatment with 10% fetal Calf Serum, or Bone Morphogenetic Proteins (BMPs) or Ciliary Neurotrophic Factor, they can differentiate into astrocytes (Lillien and Raff, 1990; Mabie et al., 1997). Similar progenitors have been isolated from the embryonic nervous system, which have the “tripotential” of differentiating into type1 or type2 astrocytes as well as oligodendroglia and the term “glial-restricted progenitor cells” has been used to describe them (Rao et al., 1998). Treatment with the cytokines described earlier has similar effects on these cells. Primary cultures of astroglia that are prepared from the post natal rodent brain (McCarthy and de Vellis, 1980) have been useful in providing information regarding the transcriptional profiles of these cells as they mature into post mitotic stellate astrocytes. However, it is unclear if these cultures represent just a small progenitor population and the relationship of these cells to mature astrocytes in the adult remains unclear. Recent transcriptome analyses of primary astrocytes could provide some insights into the molecular control of astrocytic lineage commitment (Cahoy et al., 2008).

As described earlier, some extrinsic cues that regulate the development of astrocytes from neural stem cells have been identified. In culture, neural stem cells express GFAP in response to two different classes of cytokines, the leukemia inhibitory factor (LIF) / ciliary neurotrophic factor (CNTF) family (Bonni et al., 1997) and the bone morphogenetic proteins (BMPs) (Gross et al., 1996; Johe et al., 1996). LIF/CNTF signal via the JAK/STAT pathways (Bonni et al., 1997) whereas BMP signals primarily through SMAD pathways (Hall and Miller, 2004). Nevertheless their signaling pathways have points of convergence in the regulation of GFAP, leading to suggestions that these

cytokine families activate astrogliogenesis through the same mechanisms. However, the role of LIF signaling in mediating mature astrocytic fates *in vivo* remains doubtful. LIF, as mentioned above, signals via a glycoprotein gp130/ LIF Receptor LIFR complex that can activate the Janus kinase (JAK) / Signal Transducer and activator of transcription (STAT) pathway to promote astrogliogenesis *in vitro* (Molne et al., 2000; Viti et al., 2003; Chang et al., 2004; Bonaguidi et al., 2005; He et al., 2005). However, these cells even though can express GFAP, they still maintain an immature phenotype and still exhibit progenitor cell characteristics suggesting a role for LIF signaling in neural stem cell renewal (Shimazaki et al., 2001; Pitman et al., 2004; Bonaguidi et al., 2005; Gregg and Weiss, 2005). What complicates matters further is the issue that some GFAP positive cells actually retain stem cell properties and they retain the multipotentiality and hence mere expression of GFAP does not necessarily indicate a mature post mitotic astrocyte. Overexpression of LIF *in vivo* in the adult brain, actually promotes NSC self renewal and prevents their differentiation (Bauer and Patterson, 2006). In contrast, BMP signaling promotes the generation of astrocytes from forebrain stem cells both *in vitro* and *in vivo* and promotes the formation of a GFAP positive cell type that has lost stem/progenitor properties and exhibits the typical stellate morphology of an astrocyte (Bonaguidi et al., 2005). Further, BMP2 treatment of progenitor cells cultured from LIFR null animals induces astrogliogenesis indicating that signaling from this receptor is not necessary for the generation of astrocytes.

Mechanisms that are described above may be reactivated in the adult damaged or diseased central nervous system. We shall examine some of the fundamental pathways

that drive these fate commitment choices and evaluate their roles in the phenomenon of astrogliosis following spinal cord injury. An overview of the cellular events that occur following such injuries is described below.

Sequelae following spinal cord injury

Spinal cord injuries (SCI) are crippling; where patients find themselves paralyzed, confined to a wheelchair and in case of cervical injuries, even with respiratory distress to the point that they become ventilator-dependent. The assault often leads to permanent paralysis and loss of sensation below the site of the injury. Clinically, the result of an incomplete or complete spinal cord lesion is either paraplegia (paralysis of the lower body) or quadriplegia (paralysis of the body from the neck down), depending on whether the injury was sustained in the thoracic/lumbar region or neck region of the spinal column, respectively. The damage to neural tissue at the site of trauma causes loss of neurons and oligodendrocytes locally. The functional deficits arise from both, damage to the local circuitry within the spinal cord as well as the disruption to the long ascending and descending fiber tracts that extend the length of the cord (Schwab, 2002). In addition to this, the scar that forms at the site of injury also contributes to failure of axon regeneration. The injury site is invaded by circulating macrophages, meningeal cells which either directly or indirectly initiate astrocytic scar formation that again contributes to the grave functional outcomes.

In order to dissect out the pathways that operate in the injury responses, different models of spinal cord injuries have been established in rodents. These models need to be reliable, consistent, and reproducible and should replicate some of the important features of human spinal cord injury (SCI). A number of studies have used the transection lesion. Complete transections have been used in a number of bridging studies where people have tried to bridge the gap at the injury site so as to foster a regenerative environment. However, for obvious reasons, the clinical relevance of these studies is limited as they seldom mimic the vast majority of human spinal cord injuries. The contusion lesions do mimic some of basic hallmarks of pathology seen after human SCI. Contusion lesions are characterized by a central region of hemorrhagic necrosis that expands over time due to the activation of secondary injury processes such as apoptotic cell death. Characteristically, at the center of the injury, a spared rim of tissue and axons remains at the periphery (Basso et al., 1996a). This spared rim of axons has also been observed in human SCI, in which even neurologically complete patients exhibit some tissue sparing. What is true of both (rat and human SCI) is that while there is clearly direct damage induced by contusion of the cord such as membrane disruption, vascular damage and hemorrhage, the final pathologic picture is far greater than that identifiable in the first few hours after injury. The spread of damage is thought to be due to the activation of biochemical events leading to frank cellular breakdown and excitotoxic damage. There is increasing evidence that links Ca^{2+} influx to neuronal damage. (Stokes et al., 1983) (Balentine, 1988)

In addition to secondary necrosis, the active process of programmed cell death or apoptosis is also involved in the spread of damage after trauma. Studies in rats have shown that both neurons and glia can die by apoptosis after SCI and that the time-course of these events can spread for weeks after the initial trauma. (Liu et al., 1997). Much of the apoptosis that occurs long after the injury is related to wallerian degeneration; oligodendrocytes undergo apoptosis in the white matter regions containing degenerating axons. Using multiple criteria such as Terminal deoxynucleotidyl transferase (TdT)-mediated deoxyuridine triphosphate–biotin nick end labeling (TUNEL), electron microscopy and DNA fragmentation, Liu et al (Liu et al., 1997) showed that apoptosis in neurons peaked at 8hr following the lesion and by 24 hours post injury, few TUNEL positive neurons, were seen. The pattern of glial death showed two distinct phases. The first phase of death was similar to the profile of neuronal death and was observed to peak by 8 hrs after injury and then declined by 24 hours after the injury. The second phase showed TUNEL positive glia in the white matter tracts around the lesion. These cells colocalized with the oligodendrocytes marker, Rip. In monkeys with SCI, the same pattern is observed, with apoptotic cells located all along the degenerating ascending and descending tracts. (Crowe et al., 1997). These observations have been extended to human SCI as well. (Emery et al., 1998).

In addition to the changes observed in the neural components, there is also a strong immune component to CNS injury.(Blight, 1992; Popovich et al., 1997) This is easy to understand in traumatic injuries where the blood brain barrier is damaged and so the peripheral cells can invade. In addition, however, an important response of resident cells,

microglia, may also contribute to secondary damage through both apoptosis and necrosis. Microglia in the normal brain are in a quiescent state, with short branched processes. Following injury they exhibit various behaviors, including activation, cell division, and migration to the injury. (Kreutzberg, 1996). Shuman et al (Shuman et al., 1997) showed that the pattern of microglial activation follows the pattern of wallerian degeneration and that microglia were closely apposed to apoptotic oligodendrocytes, suggesting that they may be involved in the activation of cell death programs. There is evidence that apoptotic oligodendrocytes activate caspase-3 and that this mechanism of cell death requires signaling by the neurotrophin receptor p75 (Beattie et al., 2002). Furthermore, the actions of p75 are mediated by proNGF. There is evidence that microglia derived nerve growth factor (NGF) causes cell death in the developing retina. (Frade and Barde, 1998) Microglia have also been attributed with the role of producing cytokines that could cause apoptosis in oligodendrocytes. Another interesting point to note is that the activation of microglia in the contused rat spinal cord precedes the bulk of monocyte influx and macrophage activation. (Popovich et al., 1997). Watanabe et al (Watanabe et al., 1999) have reported that there are two distinct phases of microglial activation as well. The first phase peaks at 24 hours post injury while the second occurs between 2-4 weeks later. This correlates with the apoptotic profile of oligodendrocytes. The death of oligodendrocytes contributes to chronic demyelination and dysfunction after partial SCI. In addition, myelin breakdown products (MAG, OMgp) have been known to be potent inhibitors for neurite outgrowth (reviewed in (Filbin, 2003). Therapeutic strategies that could reduce

the incidence of this death would therefore, help to reduce the functional deficit caused by chronic demyelination and also promote repair.

Astrogliosis following CNS injuries: Friend or foe?

Whenever the central nervous system (CNS) is damaged the resident astrocytes respond with a characteristic hypertrophy, a phenomenon called reactive astrocytosis or astrogliosis. One can identify hypertrophic reactive astrocytes by immunocytochemical methods that reveal increases in expression of GFAP as well as other intermediate filament proteins, such as vimentin. In time, more cell types are recruited in this injury response that culminates in the formation of a “glial scar”. The glial scar is an evolving structure, with different cells arriving and participating at different times. Details about progression and formation of the glial scar are discussed subsequently with a focus on progenitor cell recruitment and differentiation in this process.

The glial scar, however, has long been known to pose a problem for neurite outgrowth. Axons cannot regenerate beyond the glial scar, and they take on a dystrophic appearance of stalled growth. Identification of enlarged and entangled reactive astrocytes surrounding dystrophic endballs at the tips of non-regenerating fibers led to the idea that the reactive glia form a physical barrier that is responsible for failed regeneration. Therapies that combat the glial scar (Pekny et al., 1999; Menet et al., 2003; Wilhelmsson et al., 2004) or diminish its inhibitory effect (Bradbury et al., 2002) can be used to support regeneration even in the chronic lesion. There is also increasing evidence that the reason

for failed regeneration is the expression of chondroitin sulfate proteoglycans (CSPGs) which are highly enriched in the scar tissue (Busch and Silver, 2007). Several theories have been proposed to describe the molecular mechanisms by which scar-associated CSPGs inhibit axon regeneration. CSPGs may restrict growth cone access to growth promoting cell adhesion molecules (CAMs) by actively binding to them (Friedlander et al., 1994; Milev et al., 1994; Milev et al., 1996). CSPGs may also initiate growth inhibitory signal cascades through other membrane-bound receptors (Oohira et al., 2000). Enzymatic removal of proteoglycans chondroitin and keratin sulfate GAG side chains decreases CSPG axon growth inhibitory properties *in vitro* (Zuo et al., 1998) and promotes axon growth after traumatic CNS injury *in vivo* (Moon et al., 2001). Chronically injured axons in the spinal cord can regenerate into implanted peripheral nerve grafts after four weeks of stagnation in the lesion environment (Houle, 1991). This suggests that if the environment can be manipulated, these axons will re-grow and that the inhibition from the scar itself is one of the key mediators of inhibition of neurite outgrowth.

However, recent findings have shown that the initial reactive astrogliosis serves beneficial purposes and that loss of reactive astrocytes causes detrimental effects in multiple models of CNS injury (reviewed in (Sofroniew, 2005)). Deficits in reactive astrogliosis after spinal cord injury results in increased infiltration by inflammatory cells, failure of repair of the blood brain barrier and poor functional outcomes (Faulkner et al., 2004; Okada et al., 2006; Herrmann et al., 2008). Hence the reactive astrocytes that first develop in the initial to sub acute stages following the injury play an important role to

limit and restrain the inflammatory response, but this may be at the expense of reduced axonal regrowth. Some of the mechanisms that drive reactive gliosis have begun to be identified. The signaling mechanisms that were described in the earlier sections for their roles in astrocytic lineage commitment and development have been shown to promote reactive hypertrophy in adult astrocytes. The role of the JAK/STAT pathway has been investigated and shown to be critical in this process. Conditional ablation of STAT3 has been shown to reduce reactive gliosis with the consequences that are described above (Okada et al., 2006; Herrmann et al., 2008). Chapter 4 of this thesis describes the role of BMP signaling in this process as well.

Origins of reactive astrocytes: a role for progenitor cell recruitment.

It is evident that there is a multitude of cell types in the lesion area and that the glial scar represents an evolving and therefore heterogeneous population of cells. The first cells to arrive are macrophages from the bloodstream and microglia, as has already been discussed. After 3–5 days, large numbers of oligodendrocyte precursors are recruited from the surrounding tissue, which can also be seen later in the chronic scar tissue. In lesions that spare the dura mater (like contusion injuries), the final structure of the glial scar is predominantly astrocytic. In the initial stages, the predominant reactive astrocytic response to injury is hypertrophy with increased production of intermediate filaments. A tight link exists between macrophage activation and the induction of astrocytic hypertrophy (Fitch et al., 1999). Thus, activated macrophages that invade the lesion very

early on, are important players in reactive gliosis.

As the astrocytic scar develops, there is an increase in the number of astrocytes that participate in its progression. The origin of these astrocytes remains controversial. There is limited glial cell division that occurs, but most of this remains confined mostly to the lesion penumbra, in the area immediately adjacent to the injury site(Faulkner et al., 2004). However, there is some evidence to suggest that the reactive astrocytes in the injured brain arise from pre-existing astrocytes(Buffo et al., 2008).

In 1962, Adrian and Walker(Adrian and Walker, 1962) showed using a pin prick model of SCI, that astrocytes as well as other glial cell populations proliferate in response to the injury as evidenced by incorporation of [³H]-thymidine. Further, there was evidence that nestin+ progenitor cells that abut the central canal also proliferate rapidly following similar injuries and contribute to the glial scar(Frisen et al., 1995). There has been a recent interest in the idea that reactive astrocytes in the injured spinal cord could arise from stem/progenitor populations. The observation that neural stem cells continue to exist in restricted domains or “niches” in the adult CNS spawned this idea. Johansson et al have described that in the adult spinal cord, the ependymal cell represents a multipotent stem cell population(Johansson et al., 1999). They also showed that these cells responded to a stab injury to the spinal cord by proliferating and differentiating into macroglia. More recently, efforts have been made to trace the lineage arising from these cells using inducible cre lines that were crossed to reporter mice. Following prick wounds to the spinal cord, there is evidence that these cells divide to give rise to progeny that lose stem markers such as Sox2, migrate away from the ependymal layer and over the course

of 3-4 weeks, differentiate into astrocytes that contribute to the formation of the glial scar(Meletis et al., 2008).

Another progenitor cell population exists in the white matter. These precursors, are present in the normal adult spinal cord as a continuous meshwork of cells and express the proteoglycan NG2 and the platelet-derived growth factor (PDGF)- receptor alpha on their surface. (reviewed in (Horner et al., 2002). Proliferating NG-2 positive cells have been demonstrated in the contused rat spinal cord, where the numbers of these cells remains elevated as late as 4 weeks post injury. In addition, there is indirect evidence to suggest that they contribute to oligodendrocyte formation around the injured area, though not in the immediate vicinity (i.e. in the scar tissue) (McTigue et al., 2001). The NG2 expressing cell population represents a heterogeneous population of cells that is distinct from the other glial cell lineages in the CNS, and this has led to the term “polydendrocyte” to describe this immature glial cell population(Nishiyama et al., 2002). Though routinely thought of as an immature oligodendrocyte precursor cell, lineage tracing experiments in the normal CNS have shown that during development, the NG2 expressing cells do, in fact, give rise to protoplasmic gray matter astrocytes(Zhu et al., 2008). Horky et al used thymidine analogs as well as retroviral labeling techniques to trace the lineage of these cells in response to a contusion injury in the injured spinal cord(Horky et al., 2006).They find that although most of these cells do go on to express mature oligodendrocytic markers such as Adenomatous Polyposis coli gene product (APC/CC1), a fraction of these cells do express GFAP, hence suggesting that even these cell types can contribute to the glial scar formation. However, in all the instances

described, there was never any evidence of neurogenesis indicating that neuronal phenotypes are not generated following spinal cord injury. Hence it is intriguing to evaluate the mechanisms that drive the differentiation of these stem/progenitor populations in order to devise approaches to manipulate their behavior and affect glial scar formation.

Use of Artificial Scaffolds in Spinal cord injury repair

As mentioned earlier, a groundbreaking discovery in the field involved placing peripheral nerve grafts in a completely transected cord which resulted in the damaged axons growing into the graft suggesting that manipulating the environment could help axon outgrowth(Richardson et al., 1980). This has spawned the idea that one approach toward repairing the damaged spinal cord would be to bridge the cysts and scar tissue to help the injured damaged axons to navigate through an environment non-permissive to neurite outgrowth. A host of cellular grafts ranging from engineered neural stem cells, schwann cells, olfactory ensheathing glia, etc have been transplanted into the cord with limited success (reviewed in (Bunge, 2001)). However, the use of cellular transplants comes with the problem of translating this research into use for human injuries, especially with regards to availability of material and rejection of the grafts by the host tissue.

The use of artificial scaffolds in this regard hence prompts a special interest. The use of polymer-derived scaffolds that were seeded with neural stem cells has been shown to promote functional recovery following spinal cord injury(Teng et al., 2002). Scaffolds

have been described that incorporate bioactive peptides enzymatically into the matrices (Schense et al., 2000), the idea being that the scaffolds are designed to therefore effect cellular responses rather than acting as inert substrates.

The approach that was chosen in this work, used scaffolds that incorporate peptide sequences that are known to be bioactive and form by self assembly from aqueous solutions of peptide amphiphiles (PAs). Unlike polymerization, self-assembly involves the formation of non-covalent bonds between monomers, which though weak, can still hold the monomers together in supramolecular structures. The nanofibers can in turn be customized to present cells with the epitope of choice. The monomers themselves have a net negative charge that forces them to stay apart by electrostatic repulsion. Upon injection into living tissue, the repulsion can be screened by electrolytes in the extracellular environment and the scaffolds can be created in living tissues by simply injecting a liquid (i.e., peptide amphiphile solutions that self assemble *in vivo*) (Hartgerink et al., 2001, 2002). These molecules hence provide a novel approach to redesign the extracellular matrix inside living tissues and since the scaffold is created by injecting a liquid, this avoids damaging the already injured spinal cord. This approach also offers many other advantages over previous scaffold systems. First, since the exposed portion of the scaffold is primarily peptidic, the epitope is likely to be presented in a more natural manner. Also, by using a “one epitope per monomer” approach, higher epitope densities can be reached for potentially amplified biological response.

In one set of experiments, nanofibers were specifically designed to present cells with the IKVAV sequence of laminin, in what shall be described as the IKVAV PA. This

sequence is present on the α chain of laminin and is known to promote neurite outgrowth of cultured neurons (Sephel et al., 1989; Tashiro et al., 1989). Embryonic neural progenitor cells encapsulated in this scaffold differentiated primarily into neurons and avoided astrocytic fates (Silva et al., 2004). This showed that the PA was capable of altering the extracellular milieu and affect cellular responses. Hence, using these artificial scaffolds provides a novel approach to change the hostile environment in the injured spinal cord and allows us to specifically target certain cell types and signaling systems in a biologically meaningful manner.

Summary

There is possibly a role for progenitor cell recruitment in the development of the glial scar following CNS injury. Understanding the mechanisms that drive this process can help us modulate it to foster an environment conducive to recovery without affecting the beneficial effects that it offers. In chapter 2 we show that using a nanoengineered scaffold, namely the IKVAV PA, helps attenuate the glial scar and promotes axon regeneration. Further, the PA produces significant functional recovery following injury. In chapter 3 we show that the underlying mechanism for the effects on astrocytic commitment and astrogliosis by the IKVAV PA are mediated by $\beta 1$ integrin. Also, this signaling maintains progenitors in an undifferentiated state, creating a “stem cell niche”. Further, the IKVAV PA serves as a useful tool for the upregulation of $\beta 1$ integrin. In chapter 4, we have investigated the role of BMP signaling, which is known to play a crucial role in astroglial

development, in astrogliosis following spinal cord injury. Cumulatively, we provide evidence that distinct mechanisms regulate astrocytic hypertrophy versus astrocytic hyperplasia during the formation of the glial scar following spinal cord injury. Targeting specific pathways could hence be used to regulate this process for functional recovery.

Chapter 2

Self-assembling Nanofibers Inhibit Glial Scar Formation and Promote Axon Elongation After Spinal Cord Injury

ABSTRACT

Peptide amphiphile (PA) molecules that self-assemble *in vivo* into supramolecular nanofibers were used as a therapy in a mouse model of spinal cord injury (SCI). Because self-assembly of these molecules is triggered by the ionic strength of the *in vivo* environment, nanoscale structures can be created within the extracellular spaces of the spinal cord by simply injecting a liquid. The molecules are designed to form cylindrical nanofibers that display to cells in the spinal cord the laminin epitope IKVAV at nearly van der Waals density. IKVAV PA nanofibers are known to inhibit glial differentiation of cultured neural stem cells and to promote neurite outgrowth from cultured neurons. In this work *in vivo* treatment with the PA after SCI reduced astrogliosis, reduced cell death, and increased the number of oligodendroglia at the site of injury. Furthermore, the nanofibers promoted regeneration of both descending motor fibers and ascending sensory fibers through the lesion site. Treatment with the PA also resulted in significant behavioral improvement. These observations demonstrate that it is possible to inhibit glial scar formation and to facilitate regeneration after SCI using bioactive three-dimensional nanostructures displaying high densities of neuroactive epitopes on their surfaces.

INTRODUCTION

Spinal cord injury (SCI) often leads to permanent paralysis and loss of sensation below the site of injury because of the inability of damaged axons to regenerate in the adult central nervous system. Various approaches have been utilized to treat SCI with notable but unfortunately limited success(Thuret et al., 2006). We report here on the use of a molecularly designed bioactive matrix without exogenous proteins or cells as a different therapeutic approach for SCI. The matrix is composed of peptide amphiphile (PA) molecules that self-assemble from aqueous solution into cylindrical nanofibers that display bioactive epitopes on their surfaces(Hartgerink et al., 2001, 2002; Silva et al., 2004) (Figure 1). The cylinders have a well defined diameter in the range of 6 to 8 nanometers, and consist of β -sheet assemblies that tend to be parallel to the nanofibers(Jiang et al., 2007). Since each molecule contains an epitope sequence at its hydrophilic terminus, the nanostructures assembled in an aqueous medium are able to display bioactive sequences perpendicular to their long axis at nearly van der Waals density. This intensifies the epitope density compared to laminin by a factor of 10^3 (Silva et al., 2004).

We reported previously on a negatively charged PA incorporating the neuroactive pentapeptide epitope from laminin, isoleucine-lysine-valine-alanine-valine (IKVAV)(Silva et al., 2004). Addition of physiological fluids to dilute aqueous solutions of this PA leads to spontaneous formation of nanofibers *in vitro* and *in vivo*(Silva et al., 2004). In our previous studies the nanofibers containing the IKVAV epitope were found to promote outgrowth of processes from cultured neurons and to suppress astrocytic

differentiation of cultured neural progenitor cells (Silva et al., 2004). The suppression of astrocytic differentiation was not observed when using a simple IKVAV peptide, the protein laminin, or a control PA that did not contain the neuroactive epitope and that instead had the non-bioactive sequence EQS at one terminus (EQS PA) (Silva et al., 2004). Further, the PA promoted copious neurite outgrowth that far exceeded what was observed with either laminin or IKVAV peptide. Thus the biological effects of the IKVAV-PA differ strikingly from those of either laminin or IKVAV peptide. These observations suggested that injection of the bioactive amphiphile after SCI might reduce astrogliosis and possibly promote axon outgrowth.

MATERIALS AND METHODS

Mouse spinal cord injuries, amphiphile injections and animal care

All animal procedures were undertaken in accordance with the PHS Policy on Humane Care and Use of Laboratory Animals. The Institutional Animal Care and Use Committee approved all procedures. Female 129 SvJ mice (10 weeks old; Jackson Labs, USA) were anesthetized using avertin intraperitoneally. After laminectomy at the T10 vertebral segment the spinal cord was compressed dorso-ventrally by the extradural application of a 24 g modified aneurysm clip for 1 min (FEJOTA™ mouse clip). Following SCI, the skin was sutured using AUTOCLIP (9mm, Becton Dickinson). Post-operatively, animals were kept under a heat-lamp to maintain body temperature. A 1.0 cc injection of saline

was given subcutaneously which was repeated daily for the first week following the injury. Bladders were manually emptied twice daily throughout the duration of the study. In the event of discomfort, buprenex (2mg/kg SC, twice daily) was administered. Gentamycin was administered once daily in the event of hematuria (20 mg/kg) subcutaneously for 5 days. Mice that exhibited any hind-limb movement 24 hours after the injury were excluded from the study.

PA (1% aqueous solution) or vehicle was injected 24 hours after SCI using borosilicate glass capillary micropipettes (Sutter Instruments) (OD:100 μ m) coated with Sigmacote (Sigma) to reduce surface tension. The capillaries were loaded onto a Hamilton syringe using a female luer adaptor (WPI) controlled by a Micro4 microsyringe pump controller (WPI). The amphiphile was diluted 1:1 with a 580 μ M solution of glucose just prior to injection and loaded into the capillary. Under avertin anesthesia, the autoclips were removed and the injury site was exposed. The micropipette was inserted to a depth of 750 μ m measured from the dorsal surface of the cord and 2.5 μ l of the diluted amphiphile solution or vehicle was injected at 1 μ l/min. The micropipette was withdrawn at intervals of 250 μ m to leave a trail (ventral to dorsal) of the IKVAV PA in the cord. At the end of injection, the capillary was left in the cord for an additional 5 min, after which the pipette was withdrawn and the wound closed. For all experiments, the experimenters were kept blinded to the identity of the animals.

Animal perfusions and tissue acquisition

Animals were sacrificed using an overdose of Halothane anesthesia and transcardially perfused with 4% paraformaldehyde in phosphate buffered saline (PBS). The spinal cords were dissected and fixed overnight in 30% sucrose in 4% PFA. The spinal cords were then frozen in Tissue-Tek embedding compound and sectioned on a Leica CM3050S cryostat. 20 μ m thick longitudinal sections were taken.

GFAP quantitation

Sections were rinsed with PBS twice and then incubated with anti-GFAP [1:250] (Sigma, mouse monoclonal IgG1) for an hour at room temperature. Following this, sections were rinsed thrice with PBS and incubated with alexa-fluor conjugated anti-mouse IgG1 secondary antibodies [1:500] (Molecular Probes) for 1h at room temperature. Sections were finally rinsed thrice with PBS and then incubated with Hoechst nuclear stain for 10 min at room temperature. Following a final rinse with PBS, they were mounted using Prolong Gold anti fade reagent (Molecular Probes) and imaged using a Zeiss UVLSM-Meta confocal microscope (Carl Zeiss, Inc.). Following immunostaining, we measured the fluorescence intensity of GFAP immunoreactivity to estimate the fold-increase in GFAP levels around the lesion over baseline levels in uninjured parts of the cord. We also compared the GFAP fluorescence intensity to levels in spinal cord of normal uninjured animals. For each animal, sections at equivalent medio-lateral depth were used

for analysis. Since we knew the right-left thickness of each spinal cord, we could pick sections at the equivalent mediolateral depths in different animals very accurately. Further, the mediolateral thickness of the cord was not observed to be different between IKVAV PA-injected and control animals. Confocal scans in the lesioned area were taken immediately adjacent to the area of peak infiltration (Figure 5), where we observed the most intense GFAP immunoreactivity. Each scan was performed using identical laser powers, gain and offset values. These values were set such that the pixels in the images of the lesioned area did not saturate as well as those in uninjured areas weren't too dim (intensity sufficiently above zero). Z stacks of the scans were reconstructed using LSM image browser (Carl Zeiss). Fluorescence quantitation was performed by converting the entire Z-stack into a monochrome (.tif) image and subsequently measuring the intensity of each pixel. Each pixel has a gray scale that ranges from 0 to 255. The total pixel intensity of each stack was integrated using the MetaMorph 2.6 software. Intensity values at the lesioned area for each individual section, were normalized to the baseline values derived from scans taken over uninjured parts of the same section, which we have defined as 1 mm away from the edge of the area of increased GFAP immunoreactivity. We also normalized the intensity of gliosis at the lesion site to the values obtained from an uninjured cord. For each section, four sites (two rostral and two caudal to the lesion epicenter) in the lesioned area and three in the uninjured area (spanning both grey and white matter) were scanned. At least four sections were analyzed for each animal in such a manner. The total intensity values were then averaged for each group. The final fluorescence values were therefore expressed as fold increases over the baseline

(uninjured area) values for individual sections which were then grouped for each animal for comparison between IKVAV PA and vehicle-injected groups.

Apoptotic cell death and oligodendrocyte density quantification

Sections were boiled in 10mM sodium citrate for 20 min and then cooled to room temperature. They were then incubated in blocking solution (PBS containing 10% BSA, 1% Normal Goat Serum (NGS), 0.25% Triton X100) for 1 hour at room temperature. Following this, the sections were incubated in primary antibody solution (PBS with 1% NGS, 0.25 % Triton X100) overnight at 4 degrees. Following three 1x PBS washes on the next day, the sections were incubated with the appropriate secondary antibody (1:500) for an hour at room temperature and then rinsed with PBS and stained with Hoechst nuclear stain as already described above. Antibodies used were anti-APC/mAb CC1 (Calbiochem, 1:200) and anti-cleaved caspase-3 (Cell signalling technologies, 1:200).

Similar to the quantification of GFAP levels, sagittal sections in all animals were taken at the equivalent medio-lateral depths. The lesion was defined as the area marked by dense infiltration, and apoptotic cells were counted both in the epicenter as well as 400 μ m rostral and caudal to it. CC1 positive cells were counted 400 μ m rostral and caudal to the lesion. The area analyzed spanned the entire dorso-ventral thickness of the cord.

Tract tracing and analysis

At 1 day or 9 weeks post injury, mice were anesthetized with Avertin and were injected with mini-ruby-conjugated BDA (Molecular Probes, Eugene OR) using a 10 μ l Hamilton microsyringe fitted with a pulled glass micropipette. For dorsal column labeling, 2 μ l were injected just distal to the L5 dorsal root ganglion. The corticospinal tract was labeled with 3 injections (0.5 μ l each) made at 1.0 mm lateral to the midline at 0.5 mm anterior, 0.5 mm posterior, and 1.0 mm posterior to bregma, and at a depth of 0.5 mm from the cortical surface. Animals were sacrificed 14 days post BDA injection and perfused. Floating 20 μ m sagittal serial sections were each collected and washed 3 times in 1x PBS and 0.1% Triton X-100, incubated overnight at 4° C with avidin and biotinylated horseradish peroxidase (Vectastain ABC Kit Elite, Vector, Burlingame, CA), washed again 3 times in 1x PBS, and then reacted with DAB in 50 mM Tris buffer, pH 7.6, 0.024% hydrogen peroxide, and 0.5% nickel chloride. Every section was collected serially so that individual axons could be traced from section to section. Sections were then transferred to PBS and mounted in serial order on microscope slides using a weak mounting media containing 0.1% gelatine and 10% ethanol in PBS. Tracts were traced using Neurolucida imaging software (MicroBrightField, Inc.) for each axon that was labeled within a 500 μ m distance rostral to the lesion.

RESULTS

A unique feature of the PA is its ability to self-assemble into nanofibers when it is injected into tissue and contacts cations (Silva et al., 2004). To test the *in vivo* properties of the IKVAV PA as well as the therapeutic effects on recovery, we used a clip compression model of SCI that produces a consistent injury in mice where an initial impact is followed by persistent compression analogous to most cases of human SCI (Joshi and Fehlings, 2002a, b). Parameters were chosen to produce a particularly severe injury. Since a PBS buffer would trigger self assembly and make the PA gel before injection, an isotonic glucose solution was used for injections of PA. We first tested the stability of the biodegradable IKVAV PA nanofibers. At 24 hours after SCI, the lesion site was injected with a fluorescent derivative of the IKVAV PA (PA2 in Figure 3). Longitudinal sections of spinal cord show the fluorescent IKVAV PA is present at 2 weeks but by 4 weeks, the IKVAV PA has mostly biodegraded. Therefore, the stability of the IKVAV PA was found to be on the order of weeks (Figure 2).

Functional recovery post SCI

We used the BBB locomotor scale modified for the mouse (Basso et al., 1996b; Joshi and Fehlings, 2002b) to assess behavioral recovery from experimental SCI. For this and all subsequent experiments, the experimenters were kept blinded to the identity of the

animals. At 24 hours after SCI, the lesion site was injected either with IKVAV PA, the non-bioactive EQS PA, or with glucose, and some animals received sham injection. At 9 weeks post SCI, the EQS PA, sham injection, and glucose groups did not differ from one other and all scored significantly less than the IKVAV PA group (Figure 4a). Notably injection of IKVAV peptide alone did not promote functional recovery (Figure 4b), indicating that both the nanostructure of the PA as well as the IKVAV sequence are necessary for the beneficial effects on behavior. The nearly identical scores for the three control groups are also identical to those of animals in prior studies that received a complete transection of the spinal cord (Joshi and Fehlings, 2002b). A glucose control group was therefore used for comparison with IKVAV PA in all of the subsequent experiments in which animals were analyzed anatomically. In the behavioral analysis of the animals used for the anatomic studies, there were no distinguishable differences between the control and IKVAV PA groups until 5 weeks (Figure 4c). However at 5 weeks and thereafter the IKVAV PA-injected group displayed significant behavioral improvement compared to the glucose control. At 9 weeks the mean BBB score for the control group was 7.03 ± 0.8 while the mean score for the IKVAV PA-injected group was 9.2 ± 0.5 ($p < 0.04$). Importantly, this represents significant functional recovery, since a score of 7 implies no functional movement despite an extensive range of movement in all three joints in the hind limb whereas a score of 9 indicates dorsal stepping in which the animal steps on the dorsal side of its foot during locomotion, i.e. the hind-limb movement has a functional use.

We also evaluated the effects of the IKVAV PA in a different mouse strain. Adult CD1 mice were given contusion injuries, injected either with IKVAV PA, EQS PA or sham injected as described previously and evaluated for locomotor recovery. While the groups did not differ significantly at 1 week, by 2 weeks and thereafter the IKVAV PA injected animals performed significantly better than the EQS PA or sham injected animals (Figure 5). What was striking was that at 9 weeks, the average scores in the IKVAV PA injected animals was similar to the scores that were observed in the 129 SVJ animals. This indicates that the underlying mechanisms for the recovery observed extend across mouse strains. Hence the IKVAV sequence of the PA is essential for locomotor recovery and this is true in two separate mouse strains.

Effects of IKVAV PA on astrogliosis

Since the IKVAV PA produced significant long-term functional improvement, it seemed likely that it had altered cellular events, such as glial scar formation and cell death, that prevent recovery from SCI. Astrogliosis following neural injury involves an early hypertrophic (increased cell size) as well as a hyperplastic (increased cell number) response (Fawcett and Asher, 1999; Faulkner et al., 2004). At 4 days after SCI, glial fibrillary acidic protein (GFAP) immunohistochemistry revealed no apparent difference between the treated and control animals (Figure 7 a,d). However at 5 weeks and at 11 weeks after SCI there was an obvious reduction in astrogliosis in the IKVAV PA-injected

group (Figure 7 b-c). To quantify these changes, we measured the intensity of GFAP immunofluorescence in the lesion site normalized to baseline levels in the same cord 1 mm from the lesion (Figure 7 d) and found a significant reduction in the treated group (2.56 ± 0.6 for IKVAV PA; 3.31 ± 0.9 for controls, $p < 0.02$ at 5 weeks and 2.0 ± 0.1 for IKVAV PA; 2.7 ± 0.2 for controls, $p < 0.04$ at 11 weeks). By contrast, there was no difference in GFAP in animals that received non-bioactive PA (EQS) compared to glucose. Results were similar when the GFAP immunofluorescence was normalized to intensity values in normal, uninjured spinal cords (Figure 7 e). Thus injection of the IKVAV PA suppressed progression of astrogliosis at the lesion site but did not alter the initial reactive hypertrophy that may be essential for repairing the blood brain barrier and restoring homeostasis (Faulkner et al., 2004; Okada et al., 2006).

Effects of IKVAV PA on cell death

The waves of apoptotic cell death that occur after SCI are also detrimental to functional recovery (Crowe et al., 1997; Beattie et al., 2002). We quantified cell death late in the second phase of apoptosis using cleaved caspase-3 immunohistochemistry at 10 days post SCI (Liu et al., 1997; Beattie et al., 2002). In IKVAV PA-injected animals, there were significantly fewer cells undergoing apoptosis both in the area of maximal cell infiltration (lesion) (44.7 ± 3.06 for vehicle versus 34.3 ± 2.02 for IKVAV PA $p < 0.008$) (Figure 8 b,d), and also on either side of the lesion (30.8 ± 4.26 for vehicle and 16.3 ± 1.25 for

IKVAV PA, $p < 0.001$) (Figure 8a,d). Since there is typically significant oligodendroglial (OL) death at this stage after injury (Beattie et al., 2002), we used CC1 immunohistochemistry (Beattie et al., 2002) to measure OL density in the same area adjacent to the lesion, where we found a decreased incidence of cell-death after IKVAV PA injection. There was a significant increase in the number of CC1+ cells in the IKVAV PA-injected animals (64.4 ± 4.75 cells per 0.25 mm^2 after vehicle versus 85.8 ± 6.56 after IKVAV PA, $p < 0.025$) suggesting enhanced OL survival (Figure 8 c,e). Thus IKVAV PA injection increased OL cell numbers concurrent with reduced apoptotic cell death and reduction of glial scar formation.

Tract tracing of motor axons

We utilized tract tracing techniques with BDA to determine whether the amphiphile injection could support regeneration of injured motor and sensory axons. Representative traces and pictures of corticospinal tract tracing from an IKVAV PA-injected and a vehicle-injected animal at 11 weeks post injury (Figures 9 a-f,) illustrate the marked difference (Figure 9 h) between the treated and control groups. Almost 80% of all labeled corticospinal axons in the IKVAV PA group entered the lesion compared to about 50% of the fibers in control animals (Figure 9 h). No fibers in the control animals were ever detected as far as 25% of the way across the lesion. By contrast, approximately 50% of the fibers in the treated group penetrated half of the way through the lesion, and about

45% of the fibers penetrated three quarters of the distance. Strikingly, about 35% of all of the labeled corticospinal fibers actually grew through the lesion and entered the spinal cord caudal to the lesion. The fibers took meandering, unusual courses through the lesion site and terminated after growing through the lesion. Nevertheless, to further exclude the possibility of axon sparing, BDA labeling was examined at 2 weeks post injury in a separate group (Figure 9 g). At this time, axons were heavily labeled with BDA, indicating intact integrity of axoplasmic transport, and the number of labeled axons near the rostral end of lesion did not differ between IKVAV PA-injected and control animals or between the 2 week and 11 week groups. At 2 weeks post injury, no fibers in either group were ever observed even 25% of the way through the lesion, demonstrating that spared fibers were not present in any animals. Taken together these findings strongly support the thesis that the bioactive nanofibers promoted regeneration of CST motor fibers.

Tract tracing of sensory axons

Representative traces and pictures of sensory axon tracing from IKVAV PA-injected and vehicle-injected animals at 11 weeks post injury (Figure 10 a-f) illustrate the marked difference between the treated and control groups that received BDA injections. Approximately 60% of labeled axons in the IKVAV PA group entered the lesion compared to only about 20% of the fibers in controls (Figure 10 h). Only rare fibers in

controls grew 25% of the way across the lesion, and no fibers in controls penetrated as far as 50%. By contrast, approximately 35% of the fibers in the treated group penetrated 25% of the way through the lesion, and about 25% of the fibers penetrated 50% of the distance. Importantly, about 10% of the fibers actually grew through the lesion and entered the spinal cord rostral to the lesion. Again to further exclude the possibility of axon sparing, BDA labeling was examined at 2 weeks post injury in a separate group (Figure 10 g). At this time, axons were heavily labeled with BDA, indicating the integrity of axoplasmic transport, and the number of labeled axons near the caudal end of lesion did not differ between IKVAV and control. At 2 weeks post injury, no fibers in either group were ever observed penetrating even as far as 25% of the way through the lesion, demonstrating that spared fibers were not present. In toto these findings support the thesis that the bioactive nanofibers promoted regeneration of sensory fibers.

Illustration of the unusual course and morphology of traced axons

The NeuroLucida drawings in Figures 9 and 10 are two-dimensional reconstructions of a three-dimensional phenomenon and therefore do not completely demonstrate the unusual courses of the axons. To further illustrate this process, montages of sections and focal planes were assembled for a single representative axon from Figure 10 (Figures 11 ,12). These fibers met the rigorous published criteria(Steward et al., 2003) for distinguishing regeneration from sparing of axons. Notably the fibers took meandering, unusual courses

through the injured tissue (Figures 11,12), terminated at varying distances after passing through the lesion site, and displayed unusual morphologies not characteristic of normal axons (Figures 10-12).

DISCUSSION

Although adult central nervous system neurons have the intrinsic capacity to regenerate axons after injury (Richardson et al., 1980), axon elongation and functional recovery after SCI is limited because of an unfavorable extracellular milieu (Silver and Miller, 2004; Thuret et al., 2006). In this study we sought to develop a clinically relevant technique for providing an environment that might foster recovery from injury. We specifically used an injury model that mimics the type of injury seen in the clinic and we implemented therapy with a delay after experimental injury that is relevant to the time elapsed from clinical injury to hospital or spinal stabilization. The efficacy of the IKVAV PA despite the severity of the injury and delay in treatment highlights its unique ability to provide an environment conducive to recovery after SCI.

Cellular actions of the IKVAV PA

In prior studies we investigated PA containing the bioactive sequence, IKVAV, and the non-bioactive sequence EQS for their effects on cultured neural progenitor cells and neurons (Silva et al., 2004). As predicted, the IKVAV PA promoted copious outgrowth

of neurites from cultured neurons (Silva et al., 2004). Unexpectedly, however, the IKVAV PA suppressed astroglial differentiation of cultured neural progenitor cells (Silva et al., 2004). The IKVAV sequence was necessary for the effects of the molecule on progenitor cells and neurons. However the IKVAV PA exerted effects strikingly different than either IKVAV peptide alone or laminin, indicating that the nanostructure of the molecule as well as the IKVAV sequence is necessary for its biological actions (Silva et al., 2004). This may reflect the extraordinary density of epitope presented by the matrix, estimated to be 10^3 greater than that of laminin (Silva et al., 2004). Interestingly, the IKVAV PA did not alter the initial astrocytic hypertrophy after injury indicating that this signaling mechanism does not affect hypertrophy and process extension in astrocytes. In turn this suggests a duality of signaling pathways that regulate astrocytic hypertrophy versus hyperplasia. Although formation of the astroglial scar is a major impediment to axonal regeneration after SCI, astrogliosis following CNS injury also serves beneficial functions, such as repairing the blood brain barrier and reducing infiltration by circulating cells (Bush et al., 1999; Faulkner et al., 2004; Okada et al., 2006), which may be critical for restoring homeostasis. These effects have been attributed to the initial reactive hypertrophy (Bush et al., 1999; Faulkner et al., 2004; Okada et al., 2006) which is unaltered in the IKVAV PA-injected animals. Thus the IKVAV PA appears to allow these beneficial events to occur while nevertheless limiting the progression of gliosis that impedes axon outgrowth.

The IKVAV nanofibers do not alter survival of cultured neural cells, and it is thus unclear why they ameliorated apoptosis in the injured spinal cord. Injection of the PA increased

the number of OLs in the injured spinal cord, and it seems likely that this reflects enhanced survival of OLs which undergo apoptosis after SCI (Schwab and Bartholdi, 1996; Popovich et al., 1997; Dumont et al., 2001). However it is also possible that the IKVAV PA fostered generation of OLs from precursor cells. Regardless of the mechanisms, the increased number of OLs at the site of injury could facilitate remyelination of axons that traverse the lesion (Keirstead and Blakemore, 1999; Keirstead et al., 2005; Karimi-Abdolrezaee et al., 2006).

Tract tracing

Tract tracing demonstrated that both motor and sensory axons were able to traverse the area of injury in the treated spinal cord. These axons originated near the site of injury, took unusual courses through the injury site, extended at a plausible rate (3-11 weeks to traverse the injury site), and displayed unusual morphologies not characteristic of normal axons (Figures 9-12). Importantly, all labeled axons terminated at variable distances after crossing the lesion making the sparing of axons unlikely (Steward et al., 2003), particularly in view of the severity of injury. Thus these axons fulfilled the published criteria for distinguishing spared from regenerated axons (Steward et al., 2003). Further, no axons could be detected traversing the injury site two weeks after the injury, strongly mitigating against the possibility that there were spared axons, although this possibility cannot be totally excluded. The regeneration of these fibers occurred between 2 weeks and 11 weeks post injury, however the stability of the nanofibers in the spinal cord is on

the order of weeks. Therefore this regeneration must have occurred during or after the degradation of the material. We propose two possible explanations for the axonal elongation. First, many of the effects of the PA including the increase in the number of oligodendrocytes, the reduction in cell death, and the initial suppression of astrogliosis occur before degradation of the material. It is thus possible that some of the effects on axon elongation are secondary to these changes. Second, our previous publication demonstrated that the PA promotes an extraordinarily rapid effect on neurite production *in vitro* (Silva et al., 2004), and it is possible that *in vivo* the intracellular responses of neurons to the PA persist beyond the lifetime of detectable material in the spinal cord.

The timing of the degradation of the IKVAV PA may be important for its success in facilitating growth of fibers through the lesion site. Permanent grafts using Schwann cells or other non-biodegradable materials can effectively promote axonal growth into, but not through, the transplanted material or tissue because regenerating axons will not exit the favorable microenvironment of the graft (Bunge, 2001). By contrast degradation of the IKVAV PA after ingrowth of axons may have allowed regenerating axons to continue to grow past the lesion site.

Artificial scaffolds and SCI

Numerous previous studies have utilized a variety of natural (e.g. collagen, agarose, alginates) and synthetic polymers (e.g. poly α -hydroxy acids, polyvinylchloride) for

repair of the damaged spinal cord or brain (Teng et al., 2002; Stokols and Tuszynski, 2004; Jain et al., 2006; Stokols and Tuszynski, 2006). In some instances the scaffolds were coated with laminin or other constituents of the ECM prior to implantation into the nervous system. A unique feature of the PA utilized in this study is its ability to self-assemble into nanofibers after being injected as a liquid into the spinal cord. This material can be injected into an uninjured spinal cord without behavioral sequelae (unpublished observations). Another unique feature that distinguishes it from most prior scaffolds is that a signalling sequence has been incorporated into its backbone to enable it to act in an instructive manner on surrounding cells. This is an important advance since it allows us to use biologically relevant epitopes, like the IKVAV sequence, that elicit responses different from those of the parent molecule. Notably the IKVAV PA caused cellular changes, including reductions in both gliosis and cell death, as far away as 400 μm from the injection site.

Although the IKVAV PA promoted functional improvement, only partial recovery was seen and the relationship between the behavioral improvement and the observed axon regeneration is unclear. Molecular structuring of the molecule or supramolecular structuring of the nanofibers to include other bioactive sequences in addition to IKVAV (Hartgerink et al., 2002) or use in conjunction with other strategies may potentially further enhance its therapeutic efficacy (Thuret et al., 2006). Optimization of other characteristics of the material, such as its half-life in vivo and its mechanical characteristics may also enhance its biological activity.

Chapter 3

Beta 1 integrin signaling regulates astrocytic lineage commitment and astrogliosis following spinal cord injury

ABSTRACT

We have shown that self assembling peptide amphiphiles (PA) that display the IKVAV sequence of laminin, blocked astroglial lineage commitment from neural progenitor cells (NPCs). Further, injection of this material into the injured spinal cord reduced glial scar formation at the site of injury. In this study, we have investigated the mechanism of action of the PA in both these phenomena. We show that a PA with a scrambled IKVAV sequence has no bioactivity in vitro and has no effect on the glial scar, indicating the IKVAV sequence is critical for the bioactivity. The IKVAV sequence is known to interact with β -1 integrin, and NPCs in the IKVAV PA show sustained increases in β -1 integrin expression. They maintained progenitor cell traits and specifically avoided astrocytic lineage commitment but not neuronal or oligodendroglial fates. Overexpression of a dominant negative form of β -1 integrin promoted astrogliogenesis while overexpression of the signaling domain of β -1 integrin alone in NPCs inhibited astrocytic lineage commitment. These observations suggest that IKVAV PA inhibits astrogliogenesis via β -1 integrin signaling. In the injured spinal cord, β 1 integrin is not expressed by reactive astrocytes but is expressed by NG2-expressing glial progenitor cells that populate the lesion site. Injection of IKVAV PA into the injured spinal cord maintained the progenitor cells in an undifferentiated state and limited numbers of

astrocytes. Further, culture of NG2-expressing glial progenitor cells in IKVAV PA blocked astrocytic lineage commitment even in the presence of astrogliogenic factors such as bone morphogenetic protein 4 (BMP4). These observations suggest that $\beta 1$ integrin signaling plays a central role in limiting astrocytic lineage commitment and glial scar progression after SCI. Further, these data demonstrate that it is possible to inhibit glial scar formation using bioactive one-dimensional nanostructures displaying high densities of surface neuroactive epitopes. More generally, such nanoengineered molecules may provide a powerful approach for modulating signaling mechanisms in specific cell types after SCI.

INTRODUCTION

During development, neural progenitor cells (NPCs) undergo several rounds of cell divisions, giving rise to mature cell types in the central nervous system (CNS)(McKay, 1997; Frisen et al., 1998). This process is tightly controlled by cell intrinsic and extrinsic cues. The extracellular matrix (ECM) provides one such cell-extrinsic mechanism that is known to alter NPC behavior. Cues from the ECM molecules are interpreted by the integrin family of cell surface receptors. These consist of heterodimers of α and β subunits that recognize several extracellular matrix(ECM) components(Hynes, 2002). The integrins play multiple roles during the development of the nervous system(Milner and Campbell, 2002). Once integrins are bound to the ECM molecules, it triggers an intracellular signaling cascade, most of which occurs via a small cytoplasmic domain of

the β subunit(Giancotti, 1997) that can cross talk with multiple intracellular signal transduction systems within the cell as well as with the cytoskeleton(Calderwood et al., 2000), thereby altering progenitor cell responses to growth factors(Giancotti and Ruoslahti, 1999) or acting as a scaffolding molecule (Hynes, 1992) .

β 1 integrin signaling has been identified as one of the key regulators in NPCs that responds to cues from the ECM and is in turn responsible for controlling NPC survival and proliferation(Leone et al., 2005). Higher levels of β 1 integrin in cultured progenitor cells correlated with higher capability of self-renewal that was mediated via the MAPK cascade(Campos et al., 2004). However, a major difficulty in these previous studies has been in the difficulty to achieve a sustained increase in β 1 integrin signaling. Given the tight regulation of it's signaling ability, it is difficult to modulate the expression of and signaling from this molecule using conventional gene expression techniques. In order to do so, one needs to modify the ECM as this tightly controls the signaling ability of the integrin expressed on the cell surface.

We have previously described a family of biomaterials that self-assemble from aqueous solution into three dimensional matrices made of well defined supramolecular nanofibers that are designed to present specific bioactive epitopes. This methodology hence allows us to alter the extracellular environment of the cells whereby we can increase the density of neuroactive epitopes that are presented to the cells up to a 1000-fold(Silva et al., 2004). One such epitope that we have described is the Isoleucine-Lysine-Valine-Alanine-Valine (IKVAV) sequence. The IKVAV sequence has been shown to be an important neuroactive site on the laminin A chain that can mimic the effects of laminin-1 on neurite

outgrowth.(Sephel et al., 1989; Tashiro et al., 1989; Nomizu et al., 1995). The effect of IKVAV is believed to be mediated via the $\beta 1$ integrin receptor subunit(Hall et al., 1990). We have previously reported that neural progenitor cells cultured in the IKVAV PA, where the nanofibers can present cells with the IKVAV sequence at very high densities, do not differentiate into astrocytes(Silva et al., 2004). It therefore appeared likely that these effects were being mediated by $\beta 1$ integrin. We show that the IKVAV PA serves to upregulate $\beta 1$ integrin in a sustained manner and this provides a new role for $\beta 1$ integrin signaling in astroglial lineage commitment.

In some regions of the CNS, stem cell niches persist through adulthood (Doetsch et al., 1999; Johansson et al., 1999). Recent findings have shown that progenitor cell populations in the adult CNS can get reactivated following injury(Horky et al., 2006; Meletis et al., 2008), and differentiate into mature cell types(Mothe and Tator, 2005; Barnabe-Heider and Frisen, 2008), giving rise to the idea that mechanisms that control differentiation of NPCs during development, can also regulate this process in adult populations. This becomes an important question in the field of astrogliosis following CNS injuries. The origin of reactive astrocytes in the injured CNS remains unknown. There is evidence that in the injured brain, majority of the astrocytes arise from preexisting astrocytes(Buffo et al., 2008). However, in the injured spinal cord, there is very limited glial cell division(Faulkner et al., 2004). Recent evidence suggests that progenitor cell populations that are recruited to the injury site, both from the white matter(Horky et al., 2006) as well as the ependymal cells(Meletis et al., 2008) are capable of giving rise to astrocytes that contribute to the glial scar. Therefore, insights into

mechanisms that control these processes can be used to design therapeutic techniques that can alter progenitor cell behavior *in vivo*.

We have shown that the injection of the IKVAV PA described earlier, into the injured spinal cord, attenuated glial scar progression but not the initial astrocytic hypertrophy (Tysseling-Mattiace et al., 2008). We asked if $\beta 1$ integrin signaling could also account for these effects. We find that $\beta 1$ integrin is expressed on the NG2 – expressing progenitor population and not on reactive astrocytes in the injured spinal cord. We show that the IKVAV PA acts specifically on these populations to maintain them in an undifferentiated state and prevents their astrocytic commitment. This suggests that $\beta 1$ integrin signaling in the progenitor cells plays a central role in glial scar progression following spinal cord injury (SCI).

MATERIALS AND METHODS

Neurosphere cultures and plating

Neurosphere cultures were derived from 1 day old mouse brains as previously described (Bonaguidi et al., 2008). Neurospheres were derived in DMEM F-12 (Invitrogen) containing antibiotics penicillin- streptomycin as well as serum supplements N2 and B-27 (Gibco), supplemented with 20 ng/ml human recombinant EGF (BD biosciences). Cells were passaged every 4 days and plated at 50,000 cells/ml. Cells were used at passage 2 for the plating experiments.

Plating in the different PAs was as previously described (Silva et al., 2004). Briefly, cells were mixed 1:1 with the PA on glass coverslips such that the final concentration was 5×10^4 cells/ml. The PA was allowed to gel by placing the cells at 37°C for 3 hours before adding media containing 1ng/ml EGF. For controls, cells were plated on PDL-laminin coverslips (BD biosciences) at identical EGF concentrations.

O2A cultures

O2A cells were derived as previously described (McCarthy and de Vellis, 1980). Briefly, post natal day2 brains were demeningized and plated in DMEM containing 10% Fetal Bovine serum. On day9 flasks were rinsed once with sterile 1x PBS and the media was replaced. The next day the flasks were shaken overnight at 37°C for 16 hours. The supernatant was collected and the microglia were removed by plating the cells on Petri dishes for 30 min after which the O2A cells were filtered through a Nitex membrane and plated either on PDL-laminin or in the IKVAV PA at a concentration of 10^5 cells/ml. The media (containing 20ng/ml BMP4 (R&D systems)) was added to the PA conditions as described earlier.

Live/Dead assay

The assay was performed using LIVE/DEAD Viability/Cytotoxicity Kit for mammalian cells (Invitrogen). Cells were incubated in 2µM Calcein and 4µM Ethidium homodimer-1

for 20 min at 37°C and then imaged immediately on a uvLSM510 meta confocal microscope (Zeiss).

Immunocytochemistry

Cells were fixed in 4% Formalin (Sigma) in 1x PBS for 20 minutes at room temperature followed by 3 washes in 1xPBS. The primary antibodies were applied overnight in 1xPBS containing 1% BSA and 0.25% Triton X-100. For labeling with O4, the antibody (Millipore, mouse IgM) was applied on live cells (1:100 in 1xPBS) for 30 min at 37°C, washed 2x with 1xPBS and then fixed as described above. Following 3 washes with 1xPBS, cells were incubated in secondary antibody solutions containing appropriate alexa fluor conjugated secondary antibodies (Molecular Probes, Invitrogen), 1:1000 in 1xPBS. Following another 3 1x PBS washes, nuclei were counterstained with Hoechst nuclear stain (1:5000 in 1xPBS), coverslips were mounted using Prolong Gold antifade reagent (Invitrogen) and imaged on a uvLSM510 meta confocal microscope (Zeiss). The following primary antibodies were used : β III tubulin (Sigma, mouse IgG_{2b}, 1:1000), GFAP (Sigma, mouse IgG₁, 1:1000), Olig2 (Millipore, Rabbit polyclonal, 1:1000), Sox2 (Millipore, rabbit polyclonal 1:500), Nestin (BD biosciences, mouse IgG₁, 1:500), β 1 integrin (Millipore, Rat monoclonal, 1:500).

Retrovirus production and infection.

The $\beta 1$ integrin constructs were cloned into the pCLE-IRES-EGFP retroviral vector and the retrovirus production is as previously described (Bonaguidi et al., 2005). 293 FT cells were transfected with pCLE retroviral and pCMV-VSVG helper plasmids using Lipofectamine 2000 transfection reagent (Invitrogen). The supernatant from the cells was collected on day 2, 4 and 7 post transfection, concentrated, tittered and then $\sim 10^7$ viral particles were used to infect 2.5 million cells for 48 hours in sphere forming media (containing 20ng/ml EGF). Cells were then FACS sorted for GFP and then either used immediately for RNA isolation or plated on PDL-laminin as described above.

For injecting the virus into the spinal cord, the control retrovirus was generated as described above. Under isoflurane anesthesia, 5 μ l of a solution of 10^8 retroviral particles in 1xPBS was then injected 0.5 mm rostral and caudal to the lesion site at a depth of 500 μ m using a borosilicate glass capillary micropipette (Sutter Instruments) (OD:100 μ m) loaded onto a Hamilton syringe using a female luer adaptor (WPI) controlled by a Micro4 microsyringe pump controller (WPI) over a period of 5 minutes.

Thymidine analog labeling

For 5-ethynyl-2'-deoxyuridine (EdU) (Invitrogen) labeling of neurospheres in culture, cells were incubated in neurosphere media containing 10 μ M EdU for 12 h and then processed for EdU detection according to the protocol of the manufacturer (Click-IT Flow Cytometry Assay kit; Invitrogen).

For Bromodeoxyuridine (BrdU) labeling in vivo, mice were injected intraperitoneally with 50 mg/kg BrdU in saline, and then sacrificed 2 hours later. BrdU detection by immunohistochemistry was performed as previously described (Bonaguidi et al, 2007).

RNA extraction and Real time PCR

Total RNA from cultured cells was extracted using RNAqueous micro-kit (Ambion). A total of 0.5 μ g of RNA was used for generating cDNA using the Theroscript reverse transcriptase and oligo-dT primers (Invitrogen), and 2 μ l of cDNA was used per PCR reaction. PCR was performed with the SybrGreen master mix (Applied Biosystems) and Realplex² Mastercycler (Eppendorf) using the following cycling parameters: 95°C, 15 s; 60°C, 60 s for 40 cycles. At the end of the 40 cycles, the melting curves of all the reactions were checked for the presence of a single amplicon.

Mouse spinal cord injuries, amphiphile injections and animal care

Adult (10 week old) CD-1 female mice were obtained from Charles River laboratories.

All animal procedures were undertaken in accordance with the Public Health Service Policy on Humane Care and Use of Laboratory Animals. Mice were anesthetized using Isoflurane inhalation anesthetic (2.5% in 100% oxygen). After laminectomy at the T10 vertebral segment, the spinal cord was compressed dorsoventrally by the extradural application of a 24 g modified aneurysm clip for 1 min (FEJOTA mouse clip). Rest of the procedures of animal care and amphiphile injections were as previously described (Tysseling-Mattiace et al., 2008).

Tissue processing and immunohistochemistry

Mice were euthanized using CO₂ inhalation and then perfused transcardially with cold 1XPBS followed by 4% Paraformaldehyde in 1X PBS. The tissue was dissected and left in the fixative for another 2 hours on ice following which they were dehydrated overnight in 30% sucrose in 1X PBS. Cords were then embedded in Tissue-Tek O.C.T embedding compound (Sakura), frozen on dry ice and stored at -80°C until used.

20µm thick frozen sections were cut on a leica (CM3050S) Cryostat and collected on Superfrost Bond Rite slides (Richard Allen Scientific). Every fifth section was placed on the same slide such that each adjacent section was 80µm away from its neighbor. Four sections were placed on each slide and hence the width of the frozen cord spanned on each slide was 240µm. We roughly averaged about 20 slides per cord. Sections were processed for immunohistochemistry in the same manner as described for the cells. Primary antibodies used were : GFAP (Sigma, mouse IgG1 1:500), CD11b (Serotec, rat IgG, 1:150), β1 integrin (Millipore, rat IgG, 1:500), Olig2 (Millipore, Rabbit polyclonal, 1:1000), Nkx2.2 (Developmental Studies Hybridoma Bank, Iowa, mouse IgM, 1:5), BrdU (Millipore

Fluorescence intensity quantification

These are described in detail in Chapter 4.

RESULTS

The IKVAV sequence is critical for the bioactivity of the IKVAV PA

In order to address the mechanism of action of the PA, we first addressed the necessity of the IKVAV head group for the bio activity of the PA both in vitro and in vivo. For this, we used a PA that had an identical backbone as the IKVAV PA but where the IKVAV sequence itself was scrambled. The scrambled KIAVV PA hence has the same charge and molecular weight as the IKVAV PA, but presents a non-bioactive sequence. Post natal ganglionic eminence progenitor cells were passaged twice and then cultured on either PDL-laminin, the IKVAV PA or KIAVV PA in DMEM containing low EGF (1ng/ml). We assessed the viability of the cells at 24 hours and 7 days post culture. At 24 hours, there were no significant differences between the groups. However, at 7 days, while the levels of viable cells were comparable on PDL-laminin as well as the IKVAV-PA, the majority of the cells in the scrambled PA were dead (Figure 1a,b). While there were still a few clusters of cells that were viable, that expressed the cell cycle marker ki67, these did not stain for any neural markers including β III tubulin, GFAP or nestin (data not shown). This suggested that the cells had lost NPC characteristics and were possibly in the process of dying. This indicates that even though the scrambled PA is not directly toxic to the cells, it is unable to provide a biologically relevant signal and therefore unable to sustain NPC survival. Hence, this indicates that the effects of the

IKVAV PA are not mediated by the peptide backbone of the PA. Nor are they merely a consequence of the 3-D encapsulation of the cells in vitro.

We next asked if the scrambled PA could demonstrate any bioactivity in vivo. We have previously reported that injection of the IKVAV PA into a contused spinal cord resulted in attenuated astrogliosis in the chronic stages of injury (Tysseling-Mattiace et al., 2008). We hence used this assay to test if the scrambled PA could do the same. Adult CD1 female mice were injured as previously described using the clip compression model of spinal cord injury (SCI). 24 hours later, the injury site was injected with either the IKVAV PA, scrambled PA or sham injected. At 3 weeks post SCI, longitudinal spinal cord sections from the three groups were analyzed for gliosis. GFAP immunohistochemistry revealed a robust glial scar in both sham-injected and scrambled PA-injected animals while there was a reduction in astrogliosis in the IKVAV PA injected animals (Figure 1c,d). Quantification of the GFAP intensity at the lesion site showed no difference between the sham and scrambled PA injected groups, but a significant reduction in the IKVAV PA injected animals (Figure 1e, Average GFAP intensity ratios for the groups \pm s.e.m. : Sham injected : 4.25 ± 0.54 , IKVAV PA injected : 2.87 ± 0.27 , Scrambled PA : 5.2 ± 0.5 , $p < 0.01$, 3-way ANOVA). Collectively, these results show that the IKVAV sequence is necessary for the bio activity of the IKVAV PA, both in vitro as well as in vivo.

The IKVAV PA is a tool for upregulating $\beta 1$ integrin

The signaling effects from the IKVAV sequence are mediated, at least in part, by signaling from the $\beta 1$ integrin receptor subunit. We evaluated the presence of different integrin subunits in our cultured progenitor cells and found that they expressed significant levels of $\alpha 5$, $\alpha 6$, α_v and $\beta 1$ integrin and found no significant levels of $\beta 3$ and $\beta 4$ integrins. We therefore examined the levels of $\beta 1$ integrin transcripts in NPCs that had been cultured in the IKVAV PA for 7 days using real time RT-PCR. We found a significant (~3-fold) increase in the $\beta 1$ integrin transcript levels in the cells cultured in the IKVAV PA as compared to the controls that were cultured on PDL-laminin (Figure 2b,c). At the same time, we found no difference in the levels of either $\alpha 5$, $\alpha 6$ or α_v subunits. Immunohistochemistry for $\beta 1$ integrin also confirmed this finding as there was a massive increase in $\beta 1$ integrin staining in cells that were cultured in the IKVAV PA for 7 days (Figure 2a)

To evaluate the significance of the increase in $\beta 1$ integrin levels, we attempted to overexpress $\beta 1$ integrin using retroviral-mediated gene transfer. $\beta 1$ integrin was introduced into the pCLE-IRES EGFP retroviral vector (Gaiano et al., 1999) and NPCs were transduced with either control EGFP or $\beta 1$ integrin-IRES-EGFP expressing retrovirus. Two days later, the cells were sorted for EGFP and then plated on PDL laminin in similar conditions as described previously and the levels of $\beta 1$ integrin were once again examined using real time RT-PCR. Since the overexpressed cDNA lacked the 3'UTR, we could design primers that could detect the endogenous transcript alone as well as ones that detected total $\beta 1$ integrin (figure 3). At 2 days post infection, there was a significant (3 fold) increase in the levels of total $\beta 1$ integrin. However, even at this time,

the levels of endogenous transcript had already decreased by 60% (Figure 2d). At 7 days, we could detect no difference in the levels of $\beta 1$ integrin between the two groups (Figure 2d).

To determine, if the IKVAV PA could sustain the levels of overexpressed $\beta 1$ integrin better than PDL laminin, we cultured NPCs infected with either control EGFP or $\beta 1$ integrin –IRES-EGFP virus, in the IKVAV PA. Again, at 7 days, there was no discernible difference in the levels of $\beta 1$ integrin between the two groups (Figure 2e). Hence, altering the levels of $\beta 1$ integrin using conventional gene overexpression techniques could not sustain the levels that were observed in the IKVAV PA. These data suggest that the levels of $\beta 1$ integrin are regulated by extracellular cues and that the increase in $\beta 1$ integrin transcript levels reflect an alteration in this extracellular milieu, possibly due to the increase in abundance of its ligand. This further highlights the remarkable ability of the IKVAV PA to serve as a tool to upregulate $\beta 1$ integrin.

NPCs maintain progenitor characteristics in the IKVAV PA

Signaling from the $\beta 1$ integrin, subunit has been shown to mediate proliferation and maintenance of the neural stem cell niche. (Campos et al., 2004; Leone et al., 2005) We hence examined the cell cycle status of the NPCs that were cultured in the IKVAV PA, by using the thymidine analog 5-Ethyl-2'-deoxyuridine (EdU). Since were incubated in 10 μ m EdU for 12 hours on day7 in vitro just prior to fixation. Consistent with the increase in $\beta 1$ integrin levels, there was a significant increase in the percentage of EdU

positive cells ($4.5 \pm 2.5\%$ on PDL-laminin versus $31.2 \pm 7.5\%$ in the IKVAV PA) (Figure 4b,c) indicating that the cells had continued to remain in cell cycle in spite of the low EGF concentration that does not typically support stem cell proliferation.

We also evaluated the progenitor markers Sox2 and nestin and found that there was a significant increase in both these markers in the IKVAV PA (Figure 4a,c). While there was no difference in the total percentage of Olig2 positive cells, there was a significant increase in the percentage of Olig2 positive cells that were also EdU positive (Figure 4b,c).

We also evaluated the levels of these markers using real time RT-PCR. Consistent with the immunocytochemistry, there was a modest increase (2-fold, 1 cycle) in the levels of Sox2 and Olig1 (Figure 4e), but no change in the levels of the Platelet Derived Growth Factor Receptor α (PDGFR α) suggesting that the cells remain proliferative and maintain a progenitor cell phenotype. Hence, consistent with the upregulation of $\beta 1$ integrin, the IKVAV PA caused the NPCs to proliferate and maintain progenitor characteristics.

The IKVAV PA specifically blocks astrocytic lineage commitment of NPCs

We have previously reported that embryonic NPCs cultured in the IKVAV PA do not differentiate into astrocytes (Silva et al., 2004). This was also true of the post natal NPCs that are known to be more gliogenic than their embryonic counterparts. (Tysseling-Mattiace et al., 2008). Given that there was an increase in proliferation in the NPCs, we therefore examined all three lineages in the post natal NPC cultures described above and

asked if there was a block in overall lineage commitment or are the effects that were previously described, astrocyte-specific.

We examined the numbers of neurons using β III tubulin, astrocytes using GFAP and oligodendrocytes using O4. Consistent with our earlier observations, we found a significant decrease in the percentage of GFAP positive cells ($31.5 \pm 4.8\%$ on PDL laminin versus $3.3 \pm 1.5\%$ in the IKVAV PA, Figure 4a,c). We found that there was no significant difference in the numbers of β III tubulin-positive or in the numbers of O4-positive cells indicating that the neuronal and oligodendrocytic lineages were not affected by the PA (Figure 4a,c). Our previous studies with the embryonic NPCs had shown that when cultured in the IKVAV PA, they showed a higher degree of neuronal commitment. However, in these studies, we found no significant increase in the percentage of β III tubulin positive cells. This could reflect a change in the developmental potential of these cells since post natal NPCs are known to be more gliogenic than their embryonic counterparts. However, even with the macroglial lineage, we found that there was no effect on the oligodendroglial commitment. We also performed double labeling with O4 and EdU and found that none of the O4 positive cells were EdU positive, both on PDL-laminin as well as in the IKVAV PA. (Figure 5)

We also evaluated the abundance of the transcript levels of β III tubulin, GFAP and Cyclic Nucleotide 3- Phosphodiesterase (CNPase) to examine the three lineages. Real time PCR revealed a huge reduction in the levels of GFAP in cells cultured in the IKVAV PA (Figure 4d, cycle difference from GAPDH : PDL-laminin : 0.91 ; IKVAV PA : 5.35) . However, there was no significant difference in the levels of either β III

tubulin or CNPase (Figure 4d). Hence, the cells that exit cell cycle in the PA can differentiate into neurons as well as oligodendrocytes, but specifically avoid astrocytic commitment.

Modulating $\beta 1$ integrin signaling affects astrocytic lineage commitment from NPCs

Since the IKVAV PA significantly altered the levels of $\beta 1$ integrin we asked if altering the level of $\beta 1$ integrin signaling in NPCs is sufficient to affect their fate choice decisions. As described earlier, mere overexpression of $\beta 1$ integrin using conventional approaches does not achieve the sustained increase in its levels that would be needed to ask this question. We hence used mutant constructs of $\beta 1$ integrin to modulate signaling from this subunit to investigate its role in astrocytic lineage commitment.

The cytoplasmic domain of $\beta 1$ integrin is known to mediate majority of its intracellular signaling (Giancotti, 1997). Mutants of $\beta 1$ integrin that lack this domain alone, have been shown to act as a dominant negative form of the receptor (reviewed in (Hynes, 1992)). Expression of this mutant form of $\beta 1$ integrin in the nervous system has been shown to result in myelination defects (Lee et al., 2006). We misexpressed this form of $\beta 1$ integrin, hereby referred to as $\beta 1\Delta C$, in NPCs using retroviral mediated gene transfer. Conversely, we also misexpressed another mutant form, which lacks the N-terminal domain. This construct was designed with an intact N-terminal signal sequence, and hence can be targeted to the cell membrane, but lacks the remainder of the N-terminus of the protein and therefore can not bind with the alpha subunit thereby abolishing ligand binding as

well. Since the signaling from $\beta 1$ integrin occurs from the cytoplasmic domain we asked, if mere expression of this second form of $\beta 1$ integrin, could allow the requisite signals in NPCs to affect their lineage commitment. We shall hereby refer to this form of $\beta 1$ integrin, as $\beta 1\Delta N$.

NPCs were transduced with either control pCLE, $\beta 1\Delta C$ or $\beta 1\Delta N$ expressing retroviruses in high EGF (20ng/ml). Cells were FACS sorted 48 hours later and then plated on PDL-laminin for 7 days in differentiation conditions (1ng/ml EGF). Astrocytic lineage commitment was determined by GFAP immunocytochemistry (figure 6a). Quantification of the same revealed, that there was a significant increase in the percentage of GFAP positive cells in the $\beta 1\Delta C$ condition as compared to control pCLE. Hence, a reduction in $\beta 1$ integrin signaling, caused an increase in astrocytic commitment (Figure 6b). Conversely there was a 30% reduction in the number of GFAP positive cells in the NPCs transduced with $\beta 1\Delta N$. Hence in its ability to affect astrocytic lineage commitment, the $\beta 1\Delta N$ form behaves like an active form of $\beta 1$ integrin, mimicking the effect of the IKVAV PA. We therefore examined if this decrease in GFAP was also associated with an increase in proliferation. Control pCLE as well as $\beta 1\Delta N$ infected cells were pulsed for 12 hours with EdU on day 7 and then evaluated for the number of proliferating cells. We found that there was a doubling in the percentage of EdU positive cells in the $\beta 1\Delta N$ condition (Figure 6c); a trend similar to the one seen in the IKVAV PA. These results show that $\beta 1$ integrin signaling in NPCs negatively regulates astrocytic lineage commitment.

The $\beta 1$ integrin receptor subunit is expressed on progenitor cells and not reactive astrocytes

We next asked if the effects of the PA on astrogliosis were also mediated by $\beta 1$ integrin. Since there is no direct evidence for the role of $\beta 1$ integrin signaling in injury responses, we began by examining the expression pattern of this receptor subunit in the injured spinal cord. Immunohistochemistry at 4 days post injury, revealed that $\beta 1$ integrin expression was present on the cell population that expressed the Chondroitin Sulphate Proteoglycan NG2 (Figure 7a). NG2⁺ macrophages, however, identifiable by their aberrant amoeboid morphologies (McTigue et al., 2001), did not express $\beta 1$ integrin (Figure 7a). In addition, double labeling with GFAP revealed no overlap with $\beta 1$ integrin (Figure 7b). Hence, reactive astrocytes do not express $\beta 1$ integrin. This was consistent with our in vitro findings where increased levels of $\beta 1$ integrin in the NPCs resulted in reduction in astrocytic lineage commitment. This also explains our initial finding that the initial reactive astrocytic hypertrophy was unaffected by the IKVAV PA (Tysseling-Mattiace et al., 2008). This also raised the intriguing possibility that $\beta 1$ integrin was expressed on the progenitor population that populates the injured spinal cord.

We next performed double labeling for progenitor markers Olig2 and Nkx2.2. NG2 expressing progenitor cells during development, require intact Olig gene function (Ligon et al., 2006). Progenitor cells expressing NG2 along with these transcription factors have been known to be activated following demyelinating lesions (Talbot et al., 2005). Further, progenitor cells arising from the Olig2 lineage can give rise to astrocytes in the

injured CNS(Dimou et al., 2008). At 4 days post injury, we found that there were a significant number of Olig2, Nkx2.2 double positive cells in the area immediately adjacent to the lesion site and that a subset of these cells expressed β 1 integrin (Figure 7c,d). In summary, β 1 integrin is not expressed on reactive astrocytes, but is expressed on the progenitor cells that are recruited to the lesion site following spinal cord injury.

IKVAV PA affects the progenitor population after SCI

We evaluated the progenitors that were present at the injury site at 4 days post injury in sham and IKVAV PA injected animals. We counted the number of Olig2 and Nkx2.2 positive cells in the area adjacent to the lesion site in a precisely defined 0.5mm^2 area. Quantification of the cells revealed a significant increase in the total numbers of Olig2 positive cells (Figure 8 a,c sham : 53.5 ± 6.54 , IKVAV PA : 73.16 ± 5.14 , $p < 0.034$ by student's t test). Interestingly there was an increase in the numbers of Olig2 only positive cells, (Figure 8 a,c) but no significant difference in the numbers of Nkx2.2 only or Nkx2.2,Olig2 double positive cells. Since Olig2 lies upstream of Nkx2.2 in the OPC lineage, this again suggests that the progenitor cells remained less committed in the IKVAV PA injected animals, but that their progression in the lineage is not affected. Hence the IKVAV PA directly affects the progenitor cell population after SCI.

We also evaluated the cell cycle status of the cells at this time point after injury using the thymidine analog Bromo-deoxyuridine (BrdU). Sham and IKVAV PA injected animals were injected once intraperitoneally with 50mg/kg BrdU and then sacrificed two hours

later. This strategy should specifically label cells in the spinal cord that are currently in S-phase and avoids labeling the macrophages that remain proliferative while in circulation but exit from cell cycle upon entering the parenchyma(Horky et al., 2006). BrdU positive cells were counted in the same areas where we saw an increase in the numbers of Olig2 positive cells. There was a significant increase in the number of BrdU+ cells in the IKVAV PA injected animals. (Figure 8 b,d average counts per 0.5mm^2 : Sham : 9.12 ± 2.68 ; IKVAV PA: 26.33 ± 5.6)

IKVAV PA does not affect inflammatory response after SCI

Since NG2 is also expressed by the macrophages that invade the lesion site in the acute stages of the injury(McTigue et al., 2001), we evaluated the inflammatory response in the IKVAV PA injected animals. We examined these cells using CD11b immunohistochemistry at 3 weeks, at a time point when there is a noticeable reduction in the glial scar. There was no discernible difference in the number of CD11b positive cells at this stage between sham and IKVAV PA injected animals (Figure 9c). Quantification of CD11b fluorescence intensity showed no difference between the two groups (Figure 9d).

We also measured the lesion area by measuring the area of cells that were compacted by the glial scar in the two groups. Quantification of this showed that there was no difference between sham and IKVAV PA injected animals (Figure 9a,b). Hence the IKVAV PA does not affect the inflammatory response and wound closure following SCI.

In toto, these findings indicate that the IKVAV PA specifically targets the progenitor cell population after SCI.

NG2 positive dividing cells give rise to astrocytes in the injured spinal cord.

We tested whether the dividing progenitor cell population in our injury model can give rise to astrocytes that participate in the formation of the glial scar. In order to label the proliferating cell population, we injected the pCLE-IRES-EGFP expressing retrovirus(Gaiano et al., 1999) into the injured mouse spinal cord, 0.5mm rostral and caudal to the lesion site, 24 hours after the injury. Mice were sacrificed either 48 hours or 2 weeks post injection and analyzed for GFP expression. In contrast to labeling with thymidine analogs, which also label cells undergoing DNA repair, only cells that undergo M-phase are labeled by the retrovirus. Further, there shouldn't be any dilution of the GFP signal with multiple cell divisions allowing a clearer analysis of the progeny of the proliferating cells. Similar approaches have allowed for labeling of progenitor populations in the contused mouse spinal cord(Horky et al., 2006).

At 48 hours after the injection of the retrovirus, we found high percentage of labeling in the meninges, both rostral as well as caudal to the lesion site (Figure 10 a). However, we did find GFP positive cells in the parenchyma as well. These cells also expressed the progenitor marker NG2 (Figure 10 a,b). However, at this stage we did not find any co-labeling between GFP positive cells and GFAP (Figure 10 b,c) . However, at 2 weeks post injury, double labeling in 3 different animals revealed cells that were GFP positive

and localized in the glial scar(Figure 11). Double labeling and careful confocal microscopy analysis revealed that ~13% of GFP+ cells also expressed GFAP (Figure 11 b,c). Hence, the NG2 positive progenitor cells, are capable of differentiating into astrocytes, and hence can contribute to the formation of the glial scar.

IKVAV PA blocks glial lineage commitment from OPCs

The progenitor cells that are recruited to the lesion site in the injured spinal cord differ from the NPCs described earlier, in that their differentiation potential is restricted; they differentiate into glia but not neurons(Horky et al., 2006; Meletis et al., 2008). We have shown that NG2 expressing progenitor cells in our injury model can differentiate into astrocytes. Consistent with this, the levels of several pro-astrogliogenic factors, such as Leukemia Inhibitory Factor (LIF) and Bone Morphogenetic Proteins (BMPs) are known to be upregulated in the injured spinal cord suggesting a possible role for these factors in driving astrocytic commitment from the progenitor cells in the injured spinal cord. Further, BMP4 treatment of adult progenitors blocks oligodendrocytic and favors astrocytic lineage commitment(Cheng et al., 2007) in vitro. Given the effects of the IKVAV PA on astrocytic commitment from multipotent progenitor cells, we next asked if it could block astrocytic commitment from these glial precursor cells which in turn could explain the effect of the IKVAV PA on the glial scar progression in vivo.

We tested this hypothesis by culturing O2A cells in the IKVAV PA. This bipotent glial progenitor population was first described from the rat optic nerve and can differentiate

into both oligodendrocytes and type-2 astrocytes(Raff et al., 1983b). It has since been derived from multiple regions of the nervous system. Culturing O2A cells in the presence of serum(Raff et al., 1983a) or other factors such as BMPs(Mabie et al., 1997) promotes astrocytic differentiation from these cells.

O2A cells were derived from postnatal mouse brains and were plated on either control, PDL-laminin or in the IKVAV PA in the presence of 20ng/ml BMP4. At 3 days post culture, there were a significant number of astrocytes that were observed on PDL-laminin coverslips as identified by GFAP immunocytochemistry (Figure 12 a,b : $28 \pm 3\%$). In contrast, there were almost no GFAP positive cells that were observed in the IKVAV PA (Figure 12 a,b : 1.8 ± 0.1). This is striking since BMP4 is known to be strongly pro-astroglial. Staining for $\beta 1$ integrin in these cultures revealed a similar increase in its levels on cells cultured in the IKVAV PA, as we have described earlier in the multipotent progenitor cells (Figure 12 c,d). On very rare occasions, we found cells in the IKVAV PA that stained for Myelin Basic Protein (MBP). Double labeling revealed that these cells also expressed $\beta 1$ integrin (Figure 12 e,f). This is consistent with our earlier observation where the commitment to the oligodendrocytic lineage is not blocked by the IKVAV PA. This also suggests that $\beta 1$ integrin signaling is active on mature cell types in this lineage as well. These data highlight the remarkable ability of the IKVAV PA to block astrocytic commitment, not only from uncommitted neural stem cells, but also from a more committed glial progenitor population. This also suggests that the IKVAV PA might operate in a similar manner in the injured spinal cord where it blocks astrocytic commitment from the progenitor population thereby attenuating glial scar progression.

DISCUSSION

The extracellular matrix (ECM) has long been known to direct a wide range of cellular processes in several different systems. The cues from the ECM are recognized by the integrin family of cell surface receptors which translate these cues into intracellular signaling cascades. Signaling from the $\beta 1$ integrin subunit has been known to control stem/progenitor cell maintenance and differentiation in multiple systems (Jensen et al., 1999; Shinohara et al., 1999; Zhu et al., 1999; Xu et al., 2001) including the nervous system (Campos et al., 2004). Here we provide evidence that the IKVAV PA, a self assembling scaffold, can alter the extracellular milieu of cells which in turn affects signaling via the $\beta 1$ integrin receptor subunit and affect progenitor cell proliferation and differentiation both in vitro and in vivo. This further provides evidence that manipulating progenitor cell responses after injury provides a possible approach for attenuating the glial scar and allowing functional recovery after spinal cord injury.

The IKVAV PA upregulates $\beta 1$ integrin

We have shown that the cells cultured in the IKVAV PA specifically upregulate $\beta 1$ integrin and that there is no significant change in the levels of the other integrin subunits. Further, this sustained increase is not achievable by conventional overexpression techniques. What was striking was that even upon overexpression of $\beta 1$ integrin in cells that were cultured in the PA, there was no difference observed between control and $\beta 1$

integrin transduced cells. This indicates that there is active crosstalk between the extracellular milieu and transcript levels of $\beta 1$ integrin and that the final level of $\beta 1$ integrin in progenitor cells is decided by the extracellular milieu. Consistent with this is also the fact that the fold change that we observed in the levels of the transcript in the IKVAV PA were always ~ 1.3 - 1.4 cycles higher than the levels on PDL-laminin. (Note the small standard deviation in the graph in figure 2b). The increase in the abundance of the transcript presumably in this case, reflects the high abundance of the epitope IKVAV. Campos et al have shown that the location of $\beta 1$ integrin⁺, nestin⁺ expressing progenitors both in the embryonic as well as in the early postnatal brain, coincides with the expression of its ligand, namely laminin $\alpha 2$. As the levels of laminin $\alpha 2$ decrease in the post natal brain compared to the embryonic ventricular zone, so does the expression of $\beta 1$ integrin. This further suggests that the expression of $\beta 1$ integrin is controlled by the cues from the ECM and that the levels of the ligand control the expression of the receptor.

The IKVAV PA maintains a stem/progenitor cell niche

$\beta 1$ integrin has now been shown to be required for maintenance of the neural stem cell niche (Campos et al., 2004; Leone et al., 2005). Consistent with this finding, we find that the increased levels of $\beta 1$ integrin in cells cultured in the IKVAV PA is associated with an increase in proliferation and increase in the levels of progenitor markers such as nestin and Sox2. However, we did not find any difference in the levels of neurons (β III tubulin) and oligodendrocytes (O4) suggesting that the high levels of $\beta 1$ integrin promote

asymmetric cell divisions that help maintain the stem cell niche but allow for differentiation as well. However, it is also possible that the increase in the numbers of Sox2 positive cells merely reflects a selected population that was destined for an astrocytic fate, that is specifically being blocked by the IKVAV PA, hence maintaining them as stem/progenitors.

Further, upon injection into the spinal cord, the IKVAV PA specifically acted on the progenitor cell population and increased markers of immature stem/progenitor cells, as evidenced by the increase in the numbers of Olig2 positive cells, but did not affect their progression along the lineage, as indicated by the equal numbers of Nkx2.2 in sham and IKVAV PA injected animals. Further, BrdU analysis revealed that a greater number of cells remained in cell cycle in the IKVAV PA injected animals. These observations are again consistent with the *in vitro* findings where in the NPCs, there was an increase in the numbers of EdU and Sox2 positive cells.

Further, this increase in the number of proliferative Olig2 positive cells could also explain the increase in the number of APC/CC1 positive cells in the IKVAV PA injected animals 10 days post SCI. While we do observe a decrease in the incidence of apoptotic cells at this time point as detected by activated caspase-3, we did not find any difference in the number of CC1, cleaved caspase double positive cells between IKVAV PA-injected and control animals (unpublished observations). The increase in the numbers of OPCs reported here could reconcile these observations and suggest that the increased numbers of oligodendroglia that were observed could be due to an increase in their progenitor numbers rather than a direct anti-apoptotic/protective effect of the PA on

oligodendroglia. However, given the reduced incidence of activated caspase3 that we had observed, it is also possible that the IKVAV PA supports the survival of the Olig2+progenitor cells.

Increasing β 1 integrin signaling specifically blocks astrocytic lineage commitment

Previous studies that have evaluated the role of β 1 integrin in neural progenitor cells that we have referenced earlier, have only evaluated the loss of function effects by analyzing the effects of ablating β 1 integrin using conditional knock out mice. Using the IKVAV PA, we have a useful tool that can specifically upregulate the levels of β 1 integrin which hence allowed us to evaluate a “gain-of-function” effect. Interestingly, this specifically blocked astrocytic lineage commitment in these cells without affecting oligodendrocytic or neuronal lineage commitment. This was even true of glial progenitor cells that did not differentiate into astrocytes even in the presence of BMP4. This further suggests that this effect is independent of the effect of proliferation since these cells have limited proliferative potential.

Modulating levels of β 1 integrin signaling again showed that increased β 1 integrin signaling reduces while decreased β 1 integrin signaling increases astrocytic lineage commitment. Consistent with these findings, immunohistochemistry in the injured spinal cord revealed no overlap between GFAP and β 1 integrin. Hence this finding indicates a novel role for β 1 integrin signaling in astrocytic lineage commitment.

β 1 integrin signaling affects glial scar progression but not reactive astrocytic hypertrophy

The expression pattern of β 1 integrin in the injured spinal cord explains why the IKVAV PA did not affect the initial reactive hypertrophy of astrocytes (Tysseling-Mattiace et al., 2008). This was crucial since reactive astrocytes have now been shown to be critical mediators of homeostasis after injury. They have been shown to be responsible for repair of the blood brain barrier and limiting the infiltration of inflammatory cells into the parenchyma (Faulkner et al., 2004; Okada et al., 2006). We had previously shown that injection of the IKVAV PA did not affect this initial process, even though at this stage it does, in fact, affect the β 1 integrin-expressing progenitor cells in the same area. Consistent with this, we now show that there is no effect on the inflammatory cells or in the lesion area in the IKVAV PA indicating that the repair mechanisms attributed to the reactive astrocytes are unaffected by the PA. These findings implicate β 1 integrin signaling as an attractive candidate that can be modulated in vivo to regulate progenitor cell commitment to attenuate astrogliosis, without affecting the reactive hypertrophy.

In summary, this work highlights novel roles for β 1 integrin signaling in astrocytic lineage commitment and glial scar formation. Further studies to tease out the downstream pathways from this receptor can help design targets that can better modulate progenitor cell behavior in the injured nervous system. We find that the IKVAV PA is a useful tool that can increase β 1 integrin signaling and thereby affect cellular responses in the injured

nervous system. Investigation of other neuroactive epitopes in a similar manner can be a possible approach for manipulating other signaling mechanisms to investigate their roles in the cellular processes described here.

Chapter 4

BMPR1a and BMPR1b Signaling Exert Opposing Effects on Gliosis after Spinal Cord Injury

ABSTRACT

Formation of a glial scar after spinal cord injury (SCI) is a major impediment to regeneration. Since bone morphogenetic proteins (BMPs) regulate the generation of astrocytes in the developing nervous system, we investigated the role of BMP signaling in gliosis in a contusion model of mouse SCI. We found that BMP4 and BMP7 transcripts are upregulated after injury, and that BMP signaling is active in reactive astrocytes. We therefore sought to determine which BMP receptor (BMPR) subtype(s) mediates effects of BMP signaling on gliosis. Astroglial gliosis following spinal cord injury involves an early hypertrophic response that is beneficial and a subsequent hyperplastic response that leads to formation of a dense scar. We find that BMPR1a and BMPR1b receptor signaling exert opposing effects on these events. Conditional ablation of BMPR1a from GFAP-expressing cells leads to defects in the early reactive hypertrophy after SCI, increased infiltration by inflammatory cells, and worsened locomotor recovery. BMPR1b null mice conversely develop normal reactive astrocytes and have significantly smaller lesion volumes. Further, they have an attenuated glial scar in the chronic stages following injury, indicating that BMPR1b signaling regulates the later astrocytic hyperplasia and resultant glial scar progression. These findings indicate that BMP

signaling regulates multiple stages of gliosis and that these effects are receptor subtype specific, with BMPR1a and BMPR1b receptors exerting opposing effects on the initial reactive hypertrophy and subsequent hyperplasia. Targeting specific BMPR subunits for therapeutic purposes may thus provide an approach for manipulating gliosis and enhancing functional outcomes after SCI.

INTRODUCTION

Formation of a glial scar following spinal cord injury (SCI) acts as both a physical and a molecular barrier to axonal regeneration (Fawcett and Asher, 1999; Silver and Miller, 2004). However astrogliosis also plays a crucial role in restoring homeostasis following SCI by facilitating repair of the blood brain barrier and limiting infiltration of inflammatory cells into the parenchyma (Faulkner et al., 2004, Sofroniew, 2005, Okada et al., 2006; Herrmann et al., 2008). Transgenic ablation of reactive astrocytes following SCI in mice increased infiltration of inflammatory cells and worsened long-term functional recovery (Faulkner et al., 2004). Conditional ablation of STAT3 similarly resulted in increased infiltration by inflammatory cells and worsened functional outcomes, indicating that STAT signaling is involved in the beneficial effects of gliosis (Okada et al., 2006; Herrmann et al., 2008). Gliosis following spinal cord injury involves an early hypertrophic response and a subsequent hyperplastic response (Fawcett and Asher, 1999; Barnabe-Heider and Frisen, 2008). The beneficial effects attributed to astrogliosis are largely associated with the earlier, mainly hypertrophic response whereas

the later hyperplastic response and increase in the number of astrocytes at the lesion site leads to formation of a dense scar. Finding a means of inhibiting the later detrimental effects without hindering the earlier beneficial effects offers a potential means of facilitating axonal regeneration.

The bone morphogenetic proteins (BMPs) are members of the TGF β superfamily of growth factors. BMP signaling promotes astrocytic lineage commitment in vitro both by subventricular zone progenitor cells (Gross et al., 1996) and by glial restricted progenitor cells (Mabie et al, 1997; Cheng et al., 2007). Transgenic overexpression of BMP4 in the developing brain leads to a significant increase in the number of astrocytes (Gomes et al, 2003). Conversely, disruption of BMP signaling in vivo negatively affects astrogliogenesis (See et al., 2007). Levels of BMP2/4 and other family members increase following spinal cord injury (Setoguchi et al., 2001; Chen et al., 2005). Several groups have studied the effects of globally inhibiting BMP signaling after SCI with mixed results ((Setoguchi et al., 2004);(Enzmann et al., 2005);(Matsuura et al., 2008)). Enzmann et al (2005) report that transplantation into the injured spinal cord of cells engineered to secrete noggin, an antagonist of BMP signaling, resulted in expanded lesion volumes and poor functional recovery. Other authors (Setoguchi T et al, 2004; Matsuura I et al, 2008) report that inhibition of BMP signaling enhances axonal outgrowth and locomotor recovery after SCI. These observations suggest that BMP signaling may be involved in both the beneficial and the detrimental phases of gliosis.

BMPs exert their biological effects by binding to type I (BMPRIa and BMPRIb) and type II (BMPRII) receptor subunits that are organized with minor modifications of the

prototypical TGF β subclass of serine-threonine kinase receptors (ten Dijke, P et al, 1994; Koenig et al, 1994;(Nohno et al., 1995);(Rosenzweig et al., 1995); (Liu et al., 1995)). The type Ia and type Ib receptors may mediate different biological responses in the nervous system ((Yamauchi et al., 2008);(Brederlau et al., 2004);(Gulacsi and Lillien, 2003), 2003;(Panchision et al., 2001); Samanta et al, 2007). This suggests that the different type I receptors might serve different roles during astrogliosis following SCI, a hypothesis tested by this study. We find that BMPR1a signaling mediates the early beneficial phases of astrocytic hypertrophy after SCI whereas BMPR1b is involved in the later stages of astrocytic hyperplasia.

MATERIALS AND METHODS

Transgenic Mouse lines

The GFAP-cre (line 73.12) mice were maintained in C57BL/6J and BMPR1a-fx mice were maintained in a mixed 129SvJ:C57BL/6 background. The generation of GFAP-cre mice(Garcia et al., 2004), BMPR1a +/- (constitutive null mice)(Mishina et al., 1995) and BMPR1a-fx mice(Mishina et al., 2002) and their genotyping has been described previously. We mated GFAP-Cre mice with heterozygous BMPR1a-null mutant (BMPR1a^{+/-}) mice to obtain GFAP-Cre, BMPR1a^{+/-} mice, which were then mated with homozygous floxed-BMPR1a (BMPR1a^{fx/fx}) mice to obtain four separate genotypes: GFAP-Cre, BMPR1a^{fx/-}, GFAP-Cre, BMPR1a^{fx/+}, BMPR1a^{fx/+}, and BMPR1a^{fx/-} with the last two genotypes being WT for the Cre transgene (see Figure 5). GFAP- Cre, BMPR1a^{fx/-} mice have conditional ablation of the BMPR1a receptor specifically in GFAP-expressing cells, and are referred to

as BMPR1a CKO mice. GFAP Cre mice were crossed to Rosa26 reporter mice (The Jackson Laboratory, Bar Harbor, ME) to generate GFAP Cre, R26R mice.

The BMPR1b receptor knock out mice have been described previously (Yi et al., 2000). We mated heterozygotes to derive BMPR1b $+/+$ (WT), $+/-$ and $-/-$ (BMPR1b KO) mice.

Mouse spinal cord injuries and animal care

All animal procedures were undertaken in accordance with the Public Health Service Policy on Humane Care and Use of Laboratory Animals. Female 129 SvJ mice (10 weeks of age; The Jackson Laboratory, Bar Harbor, ME), and 2 month old WT and KO mice were anesthetized using Isoflurane inhalation anesthetic (2.5% in 100% oxygen). After laminectomy at the T10 vertebral segment, the spinal cord was compressed dorsoventrally by the extradural application of a 24 g modified aneurysm clip for 1 min (FEJOTA mouse clip). After SCI, the skin was sutured using AUTOCLIP (9 mm; BD Biosciences, San Jose, CA). Postoperatively, animals were kept on a heating pad to maintain body temperature. Bladders were manually emptied twice daily throughout the duration of the study. In the event of discomfort, buprenex (2 mg/kg, s.c., twice daily) was administered. Gentamycin was administered once daily in the event of hematuria (20 mg/kg) subcutaneously for 5 d. Mice that exhibited any hindlimb movement 24 h after the injury were excluded from the study.

Astrocyte cultures

Primary astrocyte cultures were derived from brains of postnatal animals as previously described (McCarthy and de Vellis, 1980). Briefly, the brains were demeningized, triturated and plated on tissue culture flasks with air tight lids (BD Biosciences) in DMEM

(invitrogen) supplemented with 10% fetal calf serum (Hyclone). Media was replaced on the second day and every four days thereafter. After overnight shaking on the 10th day, the cells were passaged onto fresh tissue culture flasks. Purity of the cultures was assessed by immunostaining for GFAP and we found that >95% of the cells were GFAP positive. For evaluating the effects of BMP4 treatment, the cultures were passaged and then plated in serum containing media for 1 day following which, the media was replaced with serum free media : DMEM + N2 serum supplement (invitrogen) + Penicillin-Streptomycin-L-Glutamine (invitrogen), for 7 days. Following this, the astrocytes were left either in serum free medium or serum free medium + 20ng/ml BMP4 (R&D biosystems) for the time periods described in the text.

Protein extraction and Western blot analysis

For protein samples from the spinal cord, mice were euthanized as previously described and perfused with 1X PBS. Samples from injured cords were taken from the injured segment as well as one half vertebral segment rostral and caudal to the lesion site. Tissue samples were collected in T-PER protein extraction buffer (Pierce) supplemented with 1X HALT Protease inhibitor cocktail (ThermoScientific), and homogenized on ice using a tissue homogenizer,(Polytron PT3000, Brinkmann). Samples were spun at 4°C for 5 min and then flash frozen and stored at -80°C until used.

For samples from cultured neurospheres and astrocyte monolayers, the cells were harvested in 1XPBS and pelleted and then homogenized in M-PER protein extraction reagent (Pierce) as described above.

For western analysis, samples were boiled for 5 minutes in strong denaturing conditions (1%SDS with 4% beta mercaptoethanol in 40mM Tris) and loaded on SDS-PAGE

following which they were transblotted onto PVDF membranes at 4°C for 1 hour. Membranes were blocked in TBST (Tris-buffered saline with 0.05% Tween-20) with 5% BSA for 1 hour at room temperature following which they were incubated in blocking solution + appropriate primary antibodies overnight at 4°C. On day2 membranes were washed 3x with TBST and then incubated with appropriate HRP-conjugated secondary antibodies (Santa Cruz, 1:5000 in TBST), washed 3x again with TBST and developed using Supersignal West Pico reagent (Thermo scientific). The primary antibodies used were GFAP (Rabbit polyclonal , DAKO; 1:5000), Phospho STAT3 (Tyr 705) and Total STAT3 (Rabbit polyclonal Cell signaling, 1:1000), phospho SMAD 1,5,8 (Cell signaling, 1:1000), GAPDH (mouse IgG, Chemicon; 1:5000).

Tissue Processing and Immunohistochemistry

Mice were euthanized using CO₂ inhalation and then perfused transcardially with cold 1XPBS followed by 4% Paraformaldehyde in 1X PBS. The tissue was dissected and left in the fixative for another 2 hours on ice following which they were dehydrated overnight in 30% sucrose in 1X PBS. Cords were then embedded in Tissue-Tek O.C.T embedding compound (Sakura), frozen on dry ice and stored at -80°C until used.

20µm thick frozen sections were cut on a leica (CM3050S) Cryostat and collected on Superfrost Bond Rite slides (Richard Allen Scientific). Every fifth section was placed on the same slide such that each adjacent section was 80µm away from its neighbor. Four sections were placed on each slide and hence the width of the frozen cord spanned on each slide was 240µm. We roughly averaged about 20 slides per cord. Sections were stained with the primary antibodies diluted in 1XPBS +1%BSA+0.25%Triton X-100, overnight at 4°C. On the next day, sections were washed 3X for 5 minutes in 1X PBS at room temperature and

then incubated in alexa fluor conjugated secondary antibody (molecular probes, Invitrogen, 1:500 in 1xPBS) for 1 hr at room temperature followed by 3 washes in 1XPBS and then counterstained with Hoechst nuclear stain (1:500 in 1X PBS) for 15 min at room temperature and then mounted using Prolong Gold antifade reagent (Invitrogen). For detection of thymidine analogs, the sections were first boiled in 10mM sodium citrate for 10 minutes and allowed to cool to room temperature for 30 minutes, following which the DNA was denatured using 2N Hydrochloric acid application for 45 minutes at room temperature. Sections were rinsed with PBS and then processed subsequently as described above.

Primary antibodies used were: GFAP (Sigma, mouse IgG1, 1:500), Cd11b (Serotec, rat IgG, 1:150), beta galactosidase (abcam, chk IgY 1:200), BMPR1a (Orbigen, Rabbit polyclonal 1:200), phospho SMAD 1/5/8 (Cell signaling, Rabbit polyclonal 1:100), NeuN (mouse IgG1, 1:500), APC/CC1 (Serotec, mouse IgG2b, 1:200), BrdU (Millipore, mouse IgG2a, 1:1000), CldU (Accurate Chemical and Scientific, rat monoclonal anti-BrdU, 1:250;), and IdU (mouse IgG1 anti-BrdU, 1:500; BD Biosciences)

Fluorescence Intensity quantification

The thickness of the cord was determined by counting the total number of longitudinal sections that contained the lesion for each animal. The midline of the cord was then defined by taking the central most section and then two more sections for each animal were picked 200 μ m left and right of the midline section. Sections from WT and KO groups were processed simultaneously. A control uninjured cord was processed in a similar manner and the center of this cord was used to provide the baseline for normalizing the fluorescence intensity values. Following immunostaining for GFAP, the sections were imaged on a Zeiss uvLSM510 confocal microscope. The glial scar was imaged in the area adjacent to the

infiltration site where the highest staining was observed in all cords. Imaging was done using a 20X objective which covered both grey and white matter, and separate scans were taken both rostral and caudal to the lesion. Each section was scanned with identical laser power, amplifier gain and offset values. All sections were imaged in one sitting to avoid problems of fading. Each confocal Z-stack was converted to monochrome tiff images and then the intensity value for each plane of the Z-stack was measured using Metmorph 2.6 software. All the values in the stack were integrated for the total intensity of the entire stack and the process was repeated for each stack at the end of which we had integrated pixel values for each Z-stack from all the sections. These values were individually normalized to the intensity values obtained from scans of uninjured spinal cords and then the intensity values were averaged across the WT and KO groups.

For CD11b intensity measurements, we used 40X objectives to scan the area in the grey matter immediately adjacent to the lesion and then in an area 300 μ m away from the lesion. The fluorescence intensity for the Z-stacks was measured as previously described. Since we couldn't normalize these values to an uninjured cord, the intensity values for each stack are represented in the intensity units that were produced by the software. These values were then averaged between the groups.

Lesion area measurements

Sections were picked as described in the previous section and then imaged with a 10X objective on a Axiovision epifluorescence microscope. The lesion area was defined as the region of dense nuclear staining that was GFAP negative and was flanked by GFAP positive reactive astrocytes. The area was then averaged for each animal and then the areas from all the animals were grouped for comparison.

RNA extraction and real-time RT-PCR

Total RNA was collected from spinal cords or cultured astrocytes using the RNAqueous-4PCR kit (Ambion). A total of 0.5 μ g of RNA was used for generating cDNA using the Thermoscript reverse transcriptase and oligo-dT primers (Invitrogen). Real time PCR was performed with the SybrGreen master mix (Applied Biosystems) and Realplex² Mastercycler (Eppendorf) using the following cycling parameters: 95°C, 15 s; 60°C, 60 s for 40 cycles. 2 μ l of cDNA was used per PCR reaction.

BBB scoring

Functional assessments were performed at weekly intervals extending upto 5 weeks post injury during the active phase of the murine sleep/wake cycle. The mice were assessed for functional recovery by using the modified Basso, Beattie, and Bresnahan hindlimb (BBB) locomotor test for mice (Joshi and Fehlings, 2002b), using two independent observers. The observers who scored the mice were blinded to their identity. Mice that exhibited any hindlimb movement at 24 hours post injury were excluded from this study altogether.

Thymidine analog administration

The thymidine analogs (Sigma) were administered intraperitoneally at the following dosages: Bromodeoxyuridine (BrdU) : 50 mg/kg, 5-chloro-2'-deoxyuridine (CldU) : 42.5 mg/kg. The analogs were diluted in saline for administration.

RESULTS

Astrogliosis follows an initial hypertrophic and subsequent hyperplastic response

Adult 129 SVJ female mice were injured using a clip compression model, where the initial assault is followed by a persistent compression, a phenomenon that mimics what is often seen in cases of human spinal cord injury (SCI) (Joshi and Fehlings, 2002a, b). We used a severe (24 g clip compression) injury that results in locomotor deficits that are identical to those observed with a complete transection of the cord (Joshi and Fehlings, 2002 a, b). The inflammatory response and gliosis following SCI were evaluated by immunostaining for CD11b and glial fibrillary acidic protein (GFAP) respectively. At 4 days following SCI, when the reactive hypertrophy is just beginning to occur, there is an increase in infiltration by CD11b positive inflammatory cells into the parenchyma (figure 1). The core of the lesion at this time is largely devoid of cells and is mostly comprised of cellular debris and degenerating and necrotic nuclei. By 4 weeks after SCI, however, the CD11b positive cells have been largely compacted by reactive astrocytes towards the lesion epicenter and are intermingled with a dense glial scar. The core of the lesion is thus no longer acellular.

GFAP immunohistochemistry revealed that in the initial stages following the injury the lesion site was populated by characteristic reactive astrocytes, that have been well described in the literature (Baldwin and Scheff, 1996), with distinctly hypertrophic cellular processes (Figure 2a). This response predominated at 4 and 7 days post injury. At 5 weeks post injury, however, there was a significant increase in the number of reactive astrocytes at the injury site. We measured the transcript levels of GFAP at different time points after the injury, using quantitative RT-PCR. Consistent with the increased staining, there was a significant increase in GFAP transcript levels in the injured spinal cord compared to uninjured controls. At 4 days post SCI, there was a 2.5 fold increase in GFAP transcript levels, which increased to nearly 4 fold by 7 days and which persisted in later stages after the injury. (Figure 2b)

BMP signaling is upregulated after spinal cord injury

Since BMP signaling promotes astroglial lineage commitment during development. (Gross et al., 1996; Mabie et al., 1997; Gomes et al., 2003), we hypothesized that BMP signaling may play an important role in the upregulation of GFAP observed after SCI. Quantitative RT-PCR demonstrated that BMP4 transcript levels were significantly increased at 4 and 7 days (~2.5 fold) following SCI and even further increased (~4-fold) at 2 weeks post injury. BMP7 transcript levels increased modestly at 2 and 4 days (~1.6 fold), but returned to baseline levels by 7 days following injury (Figure 2c). There were no significant changes in transcript levels for BMP2 (data not shown). These

observations suggested that BMP signaling, particularly by BMP4, might play a significant role in the injury response.

BMP signaling phosphorylates Smad 1/5/8 which complexes with SMAD 4, translocates to the nucleus and mediates the transcriptional effects of BMP signaling (Heldin et al., 1997). The intracellular localization of phospho-SMAD 1,5,8 was therefore examined as a measure of activity of this canonical BMP signaling pathway. At 4 days after the injury, nuclear phospho SMAD 1,5,8 (pSMAD) staining was present in reactive astrocytes (Figure 2d). However, nuclear staining was also observed in some cells that were not GFAP positive, suggesting that astrocytes are not the only cell type responding via this pathway. Since some astrocytes re-enter cell cycle following injury (Baldwin and Scheff, 1996), we examined the cell cycle status of the cells with nuclear localization of pSMAD. Mice were injected with the thymidine analog, BrdU (50mg/kg) and sacrificed 1 hour later. The cells that displayed strong nuclear signals for pSMAD were BrdU negative (Figure 2d), suggesting that BMP signaling is active in non-dividing GFAP positive reactive astrocytes after SCI.

Reactive astrocytes and not inflammatory cells express the BMPRIa receptor

BMPs exert their biological effects by binding to type I (BMPRIa and BMPRIb) and type II (BMPRII) receptor subunits that are organized with minor modifications of the prototypical TGF β subclass of serine-threonine kinase receptors (Koenig et al., 1994; ten Dijke et al., 1994; Ebendal et al., 1998). BMP receptors are abundantly expressed in the

nervous system from early embryogenesis throughout adult life (Zhang et al, 1998). However we found that BMPR1a transcripts are more abundant than BMPR1b transcripts in the uninjured adult spinal cord (figure 3). There were no significant changes in the levels of BMPR1b mRNA following SCI, but BMPR1a transcript levels were increased ~2 fold at 4 days and 7 days post injury (Figure 4a) before returning to baseline at 2 weeks post injury. This increase occurred at a time when reactive hypertrophy is the predominant astrocytic response suggesting that signaling from BMPR1a may participate in this process. In fact, double label immunohistochemistry at 4 days post SCI revealed that BMPR1a and GFAP were co-expressed by reactive astrocytes. By contrast, no co-localization was observed with CD11b indicating that BMPR1a is not expressed by macrophages/microglia that populate the injury site (Figure 4b). Since BMPR1a is activated by BMP4 (Mishina, 2003), this suggests that this receptor mediates the effects of the increase in BMP4 after SCI.

Conditional ablation of the BMPR1a receptor

BMPR1a null embryos die at gastrulation (Mishina et al., 1995). We therefore used the GFAP Cre line 73.12 (Garcia et al., 2004) to conditionally ablate the BMPR1a receptor in astrocytes to help define the role of the receptor in astroglial hypertrophy and reactive gliosis. This Cre line is expressed only in mature astrocytes in the adult spinal cord and is not expressed in neurons or oligodendrocytes or in neurons projecting to the spinal cord (Herrmann et al., 2008). We confirmed this expression pattern by mating these

animals with ROSA26 lacZ reporter mice and examining expression of β -galactosidase. In the adult spinal cord, reporter expression overlapped almost entirely with GFAP (Figure 4c). Conditional null mutation of BMPR1a was accomplished by mating GFAP Cre; BMPR1a +/- double transgenic mice with mice homozygous for the BMPR1a floxed allele (fx/fx) (figure 5). In the floxed mice, the second exon of the receptor is flanked by LoxP sites, and excision of this exon results in a receptor that lacks the ligand binding domain which is critical for receptor activation and signaling (Mishina et al., 2002). The resulting mice that were GFAP Cre, BMPR1a fx/- are hereafter referred to as BMPR1a CKO mice. The fx/+ mice (without the Cre) were used as wild type littermate controls. Adult BMPR1a CKO mice appeared phenotypically normal and had no gross developmental abnormalities. Further there were no changes in the in the number of GFAP immunoreactive cells in the spinal cords of BMPR1a CKO mice (figure 7), and astrocytes cultured from the brains of postnatal day 2 BMPR1a CKO animals expressed GFAP and displayed normal morphologies (figure 6). We confirmed the excision of the floxed allele in the adult spinal cord using real time RT-PCR with primers that detect exon2 of the receptor (Samanta et al., 2007) and found that there was a >90% reduction (~ 4 cycle; figure 4e). Similarly there was a comparable reduction in receptor transcript levels in astrocyte monolayers derived from BMPR1a CKO mice (~5 cycles; figure 6). These observations confirm that astrocytes in BMPR1a CKO mice are largely null for functional receptor. These findings further indicate that a large fraction of the BMPR1a receptor is expressed on GFAP expressing cells in the injured spinal cord.

Reduced astrocytic hypertrophy and increased inflammatory cell infiltration in BMPR1a null mice.

To evaluate the role of BMPR1a in gliosis, two-month-old female WT and BMPR1a CKO mice were injured using clip compression as described earlier. GFAP immunocytochemistry of the spinal cords of injured WT mice at 1 week post injury showed characteristic reactive astrocytes with enlarged soma and elaborate processes. By contrast, the BMPR1a CKO mice had smaller astrocytes with far fewer processes (Figure 8 a,b). Quantification of the GFAP immunofluorescence intensity showed a significant reduction in the KO mice (GFAP ratios: WT: 2.66 ± 0.12 s.e.m., BMPR1a CKO: 1.62 ± 0.14 s.e.m.; $p < 0.0001$, Student's unpaired t test Fig. 8d).

Since the initial reactive hypertrophy has been implicated in limitation of the extent of infiltration of inflammatory cells, we used CD11b immunocytochemistry to determine whether ablation of the receptor altered this process. In injured WT animals, the majority of the CD11b immunoreactive inflammatory cells were compacted immediately adjacent to the lesion (Figure 8 b,c) whereas no such compaction of these cells was observed in the BMPR1a CKO animals (Figure 8 b,c). Most of the CD11b staining in injured WT animals were concentrated within $300\mu\text{m}$ of the lesion, with significantly lower staining in the region spanning $300\text{-}600\mu\text{m}$ from the lesion. By contrast, in the BMPR1a KO mice there was no difference in staining intensity observed between the region $0\text{-}300\mu\text{m}$ and $300\text{-}600\mu\text{m}$ from the lesion (Figure 8e). The intensity of CD11b staining $300 - 600\mu\text{m}$ from the lesion was significantly higher in the BMPR1a CKO mice (Figure 3e, $p < 0.0039$,

Student's unpaired t test). Since the BMPR1a receptor is not expressed by Cd11b positive cells (Figure 4b) and is largely restricted to GFAP-immunoreactive cells in the spinal cord, the increase in infiltration of inflammatory cells is an indirect effect reflecting the defect in reactive gliosis. Thus ablation of BMPR1a caused defective astrocytic hypertrophy with a consequent failure at limiting inflammatory cell infiltration.

We next looked at gliosis in the chronic stages of the injury. Quantification of GFAP immunofluorescence at 5 weeks post SCI revealed a persistent but smaller reduction in the BMPR1a CKO mice (Figure 9 a,b). By 5 weeks the difference between WT and BMPR1a CKO mice was no longer significant (GFAP ratios: WT: 2.44 ± 0.23 ; BMPR1a CKO: 1.9 ± 0.16 , $p < 0.062$, student's unpaired t test). This suggests that in the chronic stages following injury, the defect in gliosis is ameliorated by other mechanisms. However the lesion area, defined as the core area that is flanked by GFAP positive astrocytes, was still significantly larger in the BMPR1a CKO mice indicating a larger lesion volume (Figure 9a,c). This is consistent with the increase in infiltration that was present at 1 week post injury and suggests that BMPR1a signaling exerts an overall beneficial effect after SCI.

BMPR1a knock out mice show deficits in locomotor recovery after severe contusion injury

The BBB locomotor scale modified for the mouse (Basso et al., 1996b; Joshi and Fehlings, 2002b) was used to assess behavioral recovery at weekly intervals for up to 5

weeks after the SCI. BMPR1a CKO mice showed impaired locomotor recovery compared to the WT littermates as early as 1 week after SCI, and this difference persisted through 5 weeks post injury (Figure 9d, average BBB scores at 5 weeks in WT: 5.89 ± 0.4 versus BMPR1aCKO: 4.0 ± 0.7 , $p < 0.05$, Student's t test). These observations suggest that BMPR1a signaling in astrocytes facilitates functional recovery following spinal cord injury.

Defects in astrogliosis reflect a post-transcriptional effect on GFAP in the BMPR1a knock out mice

Given the significantly reduced astrogliosis in the BMPR1a CKO mice at 1 week post injury, we examined the levels of GFAP protein in the injured spinal cord at 6 days post SCI control and KO mice. Consistent with the immunohistochemistry, we found a significant reduction in the levels of GFAP protein in BMPR1a CKO mice (Figure 10 a,b). We also examined the transcript levels of BMP4 and BMP7 and found no significant difference between the groups at this time, suggesting that the defects in gliosis did not reflect a difference in the abundance of the ligands for the receptor (Figure 10c). Interestingly, however, we found that transcript levels of GFAP were significantly higher in the BMPR1a CKO mice (Figure 10d). This was in direct contrast to the decrease in levels of GFAP protein both by western and immunohistochemical analyses.

We next asked if this increase in GFAP transcript levels was due to compensatory mechanisms that were being activated due to the deficient BMP signaling. BMP signaling

has been known to directly increase GFAP transcript levels (Samanta and Kessler, 2004). Hence, it was possible that the BMPR1a CKO astrocytes were unable to do so and that other pathways such as the JAK/STAT pathway (discussed in the next section) were responsible for the higher levels of GFAP transcripts in the injured BMPR1a CKO spinal cords. We therefore investigated if astrocytes in the BMPR1a CKO mice could respond to BMP signaling by increasing GFAP transcription. Astrocyte cultures derived from WT, GFAP Cre BMPR1a *fx/+* (Heterozygotes) and GFAP Cre, BMPR1a *fx/-* (BMPR1a CKO) pups were plated in serum free media for 7 days and then either left in serum free conditions or treated with 20ng/ml BMP4 for 3 days. We compared the transcript levels of GFAP in serum free and BMP4 treated conditions and found that there was an increase in the levels of GFAP transcript in response to BMP4 treatment in both WT and BMPR1a CKO astrocytes (Figure 10 e,f). Interestingly, the fold increase was actually higher in the heterozygotes and CKO astrocytes as compared to the WT (Figure 10 e). Hence, the transcriptional upregulation of GFAP, in response to BMP, remains intact in the BMPR1a CKO astrocytes. This indicates that the reduction in GFAP protein in the BMPR1aCKO mice reflects a post-transcriptional effect and not a block on GFAP transcription. While this doesn't rule out the contribution of other signaling mechanisms toward the increased GFAP transcript levels, it suggests that this might also represent a dysregulation of GFAP transcriptional control in the BMPR1a CKO astrocytes.

BMPR1a regulates astrogliosis via a STAT3 independent pathway.

The defect in gliosis with increased inflammatory cell infiltration after SCI in BMPR1a CKO mice is similar to what has been reported after SCI in mice with conditional null mutation of STAT3 (Okada et al., 2006; Herrmann et al., 2008). BMP signaling interacts with STAT3 signaling in several systems (Kawamura et al., 2000; Hjertner et al., 2001; Ying et al., 2003). Further, BMP4 treatment of cultured neural progenitor cells facilitates activation (phosphorylation) of STAT3 and may be involved in the effects of BMP signaling on expression of GFAP (Rajan et al., 2003; Fukuda et al., 2007). We therefore evaluated the phosphorylation status of STAT3 in injured spinal cords from BMPR1a CKO and wild type mice. STAT3 activation remained intact in the BMPR1a CKO mice; in fact, BMPR1a CKO mice had slightly elevated levels of phosphorylated STAT3 (Figure 10 g,h). We also examined the effects of BMP4 treatment on STAT phosphorylation in neural stem cells cultured from brains of postnatal day 2 BMPR1a CKO and WT animals. The increase in phospho-STAT3 after treatment with BMP4 was intact in BMPR1a CKO neurospheres (figure 11) despite a significant reduction in levels of BMPR1a. These observations suggest that activation of STAT3 by BMP4 does not require the BMPR1a receptor and that the reduction in gliosis in BMPR1a CKO mice occurs via a STAT3 independent pathway.

Accelerated wound closure and attenuated gliosis in BMPR1b knock out mice.

BMPR1b is expressed in the adult spinal cord although it is less abundant than BMPR1a (figure 3). BMPR1b null (BMPR1bKO) mice are viable, survive to adulthood, and have no apparent phenotype in the nervous system (Yi et al., 2000). We therefore obtained BMPR1bKO mice by mating heterozygotes and used WT littermates (+/+) as controls. Adult two-month-old female mice were injured and evaluated at different time intervals after injury. At 1 week post injury, there was no discernible abnormality in the astrocytic response in the BMPR1b KO mice (Figure 12 a). Quantification of GFAP immunofluorescence at this time revealed no difference between BMPR1b KO and control mice (Figure 12 b). Remarkably, however, the lesion area that was compacted by these reactive astrocytes was significantly smaller in the KO animals when compared to controls (Figure 12 a). Quantification of the GFAP negative area showed a lesion area that was only 1/4th that of the WT controls. (Lesion area averages: WT: $977140.45 \pm 78550 \mu\text{m}^2$, BMPR1bKO: $253384 \pm 27205 \mu\text{m}^2$, $p < 10^{-6}$ Student's unpaired t test). At this time reactive astrocytes in WT animals had begun to compact CD11b immunoreactive cells towards the lesion but the lesion core itself was still largely acellular with the majority of the CD11b positive cells intermingled with GFAP positive astrocytes at the lesion's edge (Figure 12 a, and also compare with WT BMPR1a animals in Figure 8a). By contrast, in BMPR1b KO mice the GFAP negative area flanked by the reactive astrocytes was not devoid of cells, and the lesion core showed dense staining for CD11b. Thus there was not only a smaller lesion area in BMPR1b KO mice, but CD11b cells were compacted further than in WT animals. At 5 weeks there were no significant

differences between WT and BMPR1b KO mice in the size of the GFAP negative area (Figure 13 a,d). However in BMPR1b KO mice there were fewer astrocytes in the parenchyma adjacent to the lesion although there was still a wall of reactive astrocytes flanking the lesion core (Figure 13 a,b). Further, quantitation of the intensity of GFAP immunofluorescence revealed a significant decrease in the BMPR1b KO mice. (Figure 13 c) (Average intensity ratios: WT: 2.69 ± 0.15 s.e.m., BMPR1b KO: 2.12 ± 0.18 s.e.m., $p < 0.02$ by student's unpaired t test). This suggests that BMPR1b signaling is involved in the increase in the number of astrocytes at the lesion site and in progression of the glial scar. The decreased gliosis in BMPR1b KO mice at 5 weeks could reflect either decreased astrocytic proliferation or diminished recruitment of astrocytes to the region of the glial scar. To define possible effects on proliferation, mice were injected with the thymidine analog CldU once daily from day7 to day14, and labeling was examined at 5 weeks post SCI. There was no difference in CldU counts between WT and KO mice in the area of gliosis (figure 14), suggesting that the reduction in gliosis may reflect a reduction in recruitment of astrocytes to the glial scar and/or reduced differentiation of progenitor cells into the astrocytic phenotype. In toto, these observations indicate that BMPR1a and BMPR1b signaling exert directly opposing effects on astrocytic hypertrophy and hyperplasia, as well as on infiltration of inflammatory cells

BMPR1b null mice show normal locomotor recovery after severe contusion injury

BBB scoring for BMPR1b KO and WT mice did not differ in the first two weeks following the injury. Thereafter the scores for BMPR1b KO trended higher (Figure 14,e) but still did not differ significantly from scores for WT animals. Thus while loss of BMPR1a signaling impaired locomotor recovery, null mutation of BMPR1b did not alter recovery.

DISCUSSION

The formation of an astroglial scar following SCI is a major impediment to axonal regeneration and functional recovery (Fawcett and Asher, 1999; Silver and Miller, 2004). Since BMP signaling plays a fundamental role in the generation of astrocytes (Gross et al 1996; Mabie et al, 1997; Gomes et al, 2003) several groups have studied the effects of globally inhibiting BMP signaling after SCI with mixed results (Setoguchi T et al, 2004; Enzmann GU et al, 2005; Matsuura I et al, 2008). Astrogliosis following CNS injury has both beneficial as well as detrimental effects (for review see (Barnabe-Heider and Frisen, 2008), and global inhibition of BMP signaling does not specifically target the detrimental aspects of gliosis. We show here that BMPR1a signaling promotes reactive gliosis and wound closure following SCI whereas BMPR1b signaling not only inhibits these processes but also increases formation of the glial scar. These observations suggest that specific inhibition of BMPR1b signaling may provide a therapeutic approach for

attenuating gliosis without altering the beneficial effects of BMP signaling on wound closure and limitation of the area of inflammation after SCI.

BMPR1a and BMPR1b signaling may not serve identical biological roles

BMPs exert their biological effects by binding to type I (BMPR1a, BMPR1b) and type II (BMPRII) receptor subunits that are organized with minor modifications of the prototypical TGF β subclass of serine-threonine kinase receptors (ten Dijke, P et al, 1994; Koenig et al, 1994; Nohno et al, 1995; Rosenzweig et al, 1995; Liu et al, 1995). Both BMPR1a and BMPR1b are expressed in the nervous system from early embryogenesis throughout adult life although BMPR1a is the predominant type I receptor in the adult nervous system including the spinal cord (Zhang et al, 1998; supplementary figure 2). The two type I receptors may serve overlapping functions in many organ systems including brain (Qin et al., 2006), but there are also distinct differences in their actions. For example, in the developing spinal cord both type I BMPRs can specify the fate of commissural neurons, but axon guidance of these neurons is mediated only by BMPR1b (Yamauchi et al, 2008). Importantly, BMPR1a signaling in astrocytes regulates the expression of VEGF for proper cerebrovascular angiogenesis and has a role in the formation of the blood–brain-barrier (Araya et al., 2008). Some studies have suggested that BMPR1b signaling is responsible for BMP-mediated exit from cell cycle and terminal differentiation of neural stem cells (Panchision et al, 2001; Brederlau et al, 2004; Gulacsi and Lillien, 2003). Thus BMPR1a and BMPR1b cannot be viewed as being

biologically interchangeable under all circumstances. Differences in the functions of BMPR1a and BMPR1b can also reflect differences in the spatiotemporal distribution of the receptors. Although we find that both receptors are expressed by virtually all astrocytes, it is possible that there are subpopulations of astrocytes that preferentially express more of one of the receptor subtypes and that respond differently to BMP signaling because of other phenotypic differences. In any case, our findings demonstrate that the two different type I receptors serve strikingly different roles in the injured spinal cord.

BMPR1a promotes reactive gliosis and wound closure following spinal cord injury

We find that the levels of the BMPR1a receptor are increased after SCI and that the receptor is predominantly expressed by reactive astrocytes. Ablation of BMPR1a in astrocytes led to poor reactive gliosis with increased infiltration by inflammatory cells. This is consistent with other studies where disruption of reactive astrocytes in the initial stages of injury caused similar results (Faulkner et al., 2004). BMPR1a signaling in astrocytes has a role in the formation of the blood–brain-barrier (Araya et al, 2008), and the increased infiltration of inflammatory cells and expanded size of the lesion after ablation of BMPR1a may reflect delayed closure of the ruptured blood-brain-barrier. STAT3 is a critical regulator of this process (Okada et al., 2006; Herrmann et al., 2008), but the levels of activated STAT3 in the BMPR1a CKO mice after SCI were normal or slightly higher. Since the defects in astrogliosis in the BMPR1a CKO mice occurred in

the presence of activated STAT3, the downstream effectors of BMPR1a signaling are distinct from this pathway. It is important to note that the lesion area in BMPR1a CKO mice remained higher even in the chronic stages of the injury, suggesting that BMPR1a signaling plays an indispensable role in reactive astrocytes for the purposes of wound closure.

BMPR1b negatively regulates wound closure following spinal cord injury and is involved in glial scar progression.

In contrast to BMPR1a, BMPR1b transcript levels did not change significantly during the injury response. However, BMPR1b KO mice showed significantly reduced lesion areas at 1 week post injury. This is diametrically opposite to the phenotype that was observed in BMPR1a CKO mice suggesting that the two receptors exert opposing effects, either directly or indirectly, on wound closure. The reduction in the lesion area, however, appeared transient, since no difference was observed between WT and KO animals at 5 weeks post injury. This could reflect a difference in the ability of astrocytes to limit cell infiltration in the acute versus chronic stages of the injury. Infiltration by inflammatory cells in the injured spinal cord occurs in several waves with a peak of infiltration that occurs initially after the injury and one that occurs several weeks after the assault (Kigerl et al., 2006). The second phase is believed to be a mediator of secondary pathogenesis and can affect wound healing (Trivedi et al., 2006). Astrocytes in the BMPR1b KO mice are better able to condense the initial infiltrating cells, but in the chronic stages this

ability may be lost as more cells find their way to the lesion. While there was no difference in GFAP immunoreactivity observed in the BMPR1b KO animals at 1 week post injury during the phase of astrocytic hypertrophy, there was an attenuation of the glial scar at 5 weeks after the injury. This suggests that BMPR1b signaling regulates astrocytic hyperplasia and glial scar progression but not the initial hypertrophy. In turn this suggests that these two distinct phases of gliosis are regulated by different mechanisms. Similarly injection of a self-assembling peptide amphiphile into the injured spinal cord does not alter the initial astrocytic hypertrophy after injury but reduces astrocytic hyperplasia and glial scar formation (Tysseling-Mattiace et al, 2008). These observations indicating the duality of signaling pathways that regulate astrocytic hypertrophy versus hyperplasia suggest that it may be possible therapeutically to reduce gliosis without affecting the initial hypertrophic response or wound healing. It is possible that some of the later effects on gliosis in the BMPR1b KO are secondary to earlier effects that limit inflammatory cell infiltration. Infiltrating leukocytes are known to produce mediators that can increase gliosis (Yong et al., 1991; Balasingam et al., 1994), and disruption of signaling mechanisms that perturb this response in astrocytes reduces gliosis (Goldshmit et al., 2004). Thus the effects of ablation of BMPR1b on the chronic phases of gliosis could secondarily reflect the reduced cell infiltration and smaller lesion area in the more acute stages of the injury.

Astrocytic BMPR1a and not BMPR1b signaling is essential for functional recovery after spinal cord injury

BMPR1a CKO mice showed poor locomotor recovery. The lower BBB scores in these mice occurred at the initial stages following injury and persisted in the chronic stages as well. This is consistent with prior findings that disruption of reactive astrogliosis caused worsened functional outcomes (Okada et al., 2006). However, in this study, a severe injury model was used that results in locomotor deficits indistinguishable from those seen after complete transection of the spinal cord (Joshi and Fehlings, 2002a, b). Thus the modicum of behavioral recovery that is normally noted after severe SCI appears to depend upon the crucial role that reactive astrocytes play in the re-establishment of homeostasis, in the absence of which, behavioral recovery was adversely affected. In contrast to the BMPR1a CKO mice, BMPR1b KO mice showed no functional deficits and exhibited normal locomotor recovery. However we did not find significantly improved locomotor performance in the BMPR1b KO mice despite the accelerated wound closure in these animals. This contrasts the finding that ablation of Socs3, which results in similar anatomical findings of accelerated wound closure, is associated with improved BBB scores (Okada et al., 2006). This could reflect a difference in the severity of the injuries that were used in these two studies since the injury model that was applied in the current study was more severe than the one used by Okada et al. It is also possible that Socs3 signaling is indirectly involved in other components of functional recovery that are unaffected by BMPR1b signaling.

In summary, these findings indicate that BMP signaling regulates multiple stages of gliosis and that these effects are receptor subtype specific, with BMPR1a and BMPR1b receptors exerting opposing effects on the initial reactive hypertrophy and subsequent hyperplasia. Specific inhibition of BMPR1b signaling for therapeutic purposes may provide an approach for manipulating gliosis and enhancing functional outcomes after SCI. These findings may also influence cell transplantation strategies where stem/progenitor cells are transplanted into the injured spinal cord with the goal of lineage specific commitment and cell replacement.

Chapter 5

CONCLUSIONS

The theme of this work was that understanding principles of development can help elucidate mechanisms that are activated in pathological processes with the ultimate goal of manipulating these mechanisms to design better therapeutic outcomes. The formation of the glial scar has been largely attributed for the failure of regeneration of axons following traumatic injury to the central nervous system. This work focused specifically on the problem of astrogliosis following spinal cord injury. The idea was to investigate the mechanisms that operate in the development of astrocytes and evaluating their possible role in the development of astrogliosis.

The glial scar serves both as a physical as well as molecular barrier for neurite outgrowth. Several treatment paradigms have been targeted toward reducing gliosis as a means to promote axon elongation. However, recent findings have suggested that astrogliosis after traumatic injuries serves an important role in repair of the blood brain barrier, limiting macrophage/microglial infiltration, thereby playing a crucial role in restoring homeostasis following the assault. Hence, astrogliosis following SCI has a dual role; one as a mediator of repair and homeostasis and the other as an inhibitor of regeneration. Ideally, therefore, modifying astrogliosis to promote regeneration for therapeutic purposes would require preservation of the beneficial effects of gliosis while reducing its detrimental effects in inhibition of axon outgrowth.

Astrogliosis following spinal cord injury follows an early hypertrophic (increased cell size) and a subsequent hyperplastic (increased cell number) response where there is a definite increase in the number of reactive astrocytes that develop around the lesion site. The beneficial effects that have been attributed to astrogliosis have been largely associated with the earlier, mainly hypertrophic response. Our hypothesis was that the mechanisms that mediate the two phases in the astrocytic scar formation are also distinct. If this were true, it should be possible to affect the latter stage of gliosis but not the former. Through our work, we have found evidence that this is possible. We have identified signaling pathways that mediate these distinct phases of astrogliosis and showed that it is possible to abrogate glial scar progression without affecting astrocytic hypertrophy.

In the first part of this work, we showed that using a nanoengineered bioactive peptide amphiphile (PA) that can be injected into the injured spinal cord to create an artificial scaffold, it is possible to reduce the glial scar progression without affecting astrocytic hypertrophy. The PA was engineered to present cells with the IKVAV epitope of laminin at extremely high densities (10^3 fold higher than laminin). Mice injected with the IKVAV PA showed reduced gliosis in the chronic stages compared to controls. Further, in these animals, there was regeneration of both sensory and motor axons, indicating that it is

possible to reengineer the extra cellular matrix to specifically modulate astrogliosis and therefore create an environment conducive to axon regeneration.

In the second part of this work, we investigated the mechanism by which the IKVAV PA exerts its effects both *in vitro* and *in vivo*. We identified the beta 1 integrin receptor subunit as a key target gene that is specifically upregulated by the IKVAV PA. This was especially compelling given that conventional gene overexpression techniques fail to alter levels of $\beta 1$ integrin in the sustained manner observed in the IKVAV PA. Changing levels of $\beta 1$ integrin involved changing the extracellular milieu of the cells; a phenomenon that we achieved using the IKVAV PA. Hence the IKVAV PA becomes an attractive tool for upregulating $\beta 1$ integrin, something that to date has been impossible to accomplish and consequently has implications far beyond the nervous system, for a variety of cell types where signaling from this receptor subunit is active. We find that this upregulation in neural progenitor cells in the PA recapitulates a neural stem cell niche that these cells reside in *in vivo*, whereby they maintain progenitor characteristics. Further, this specifically inhibits their astroglial commitment while not affecting commitment to the neuronal or oligodendroglial lineage. Following spinal cord injury, *in vivo*, we found that $\beta 1$ integrin is not expressed by reactive astrocytes. Instead we showed that $\beta 1$ integrin is expressed on the NG2 positive progenitor cell population that invades the injury site and these cells again respond to the IKVAV PA by retaining progenitor characteristics, similar to the results *in vitro*. We provide evidence that the

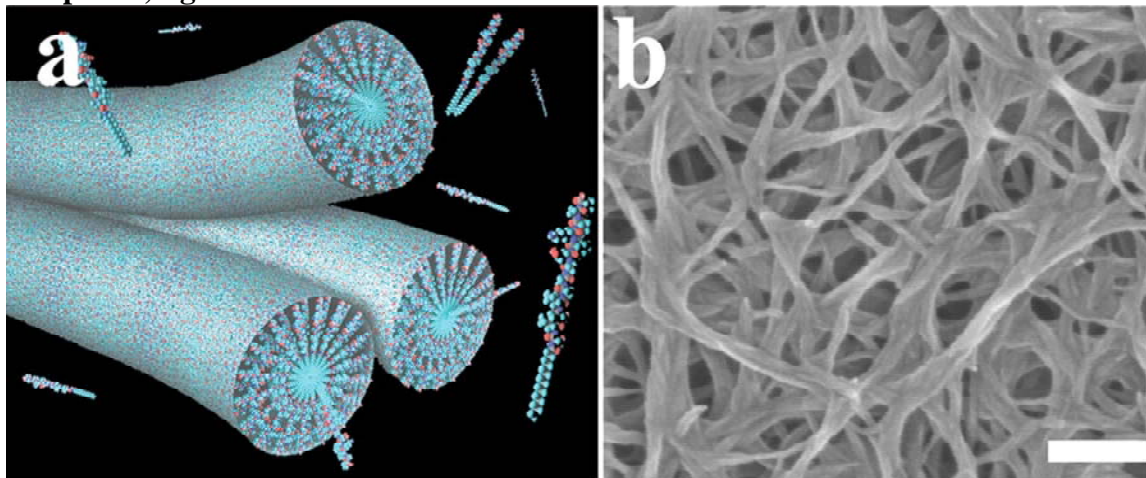
IKVAV PA prevents astroglial commitment from these glial restricted progenitors in vitro, even in the presence of strong astrogligenic factors such as BMP4. These findings provide a novel role for $\beta 1$ integrin signaling in glial scar formation, and implicate it as an attractive candidate that can be targeted to attenuate glial scar progression without affecting reactive hypertrophy.

In the third part of this work, we investigated the role of BMP signaling as a potential regulator of astrogliosis. We showed that levels of BMPs are increased in the injured spinal cord and that BMP signaling is active in reactive astrocytes. The effects of BMP signaling on distinct phases of gliosis is evidenced by the differing phenotypes that were observed in BMP Receptor knock out mice. Conditional ablation of the BMPR1a receptor from GFAP expressing cells led to deficits in the early reactive hypertrophy, increased infiltration by inflammatory cells and worsened locomotor recovery. Conversely, BMPR1b knock out mice developed normal reactive astrocytes, had significantly smaller lesion volumes and normal locomotor recovery. Further, they had an attenuated glial scar in the chronic stages following injury. Hence BMP signaling regulates multiple phases of astrogliosis and these effects are receptor subtype specific, with BMPR1a and BMPR1b receptors exerting opposing effects on reactive astrocytic hypertrophy. This also is the first instance, to our knowledge where the two BMP type 1 receptors exert such opposing effects in a system. This provides new insights into the

biology of BMP signaling and hence now allows for further investigation into the distinct molecular effectors downstream of these two receptors that mediate these distinct responses.

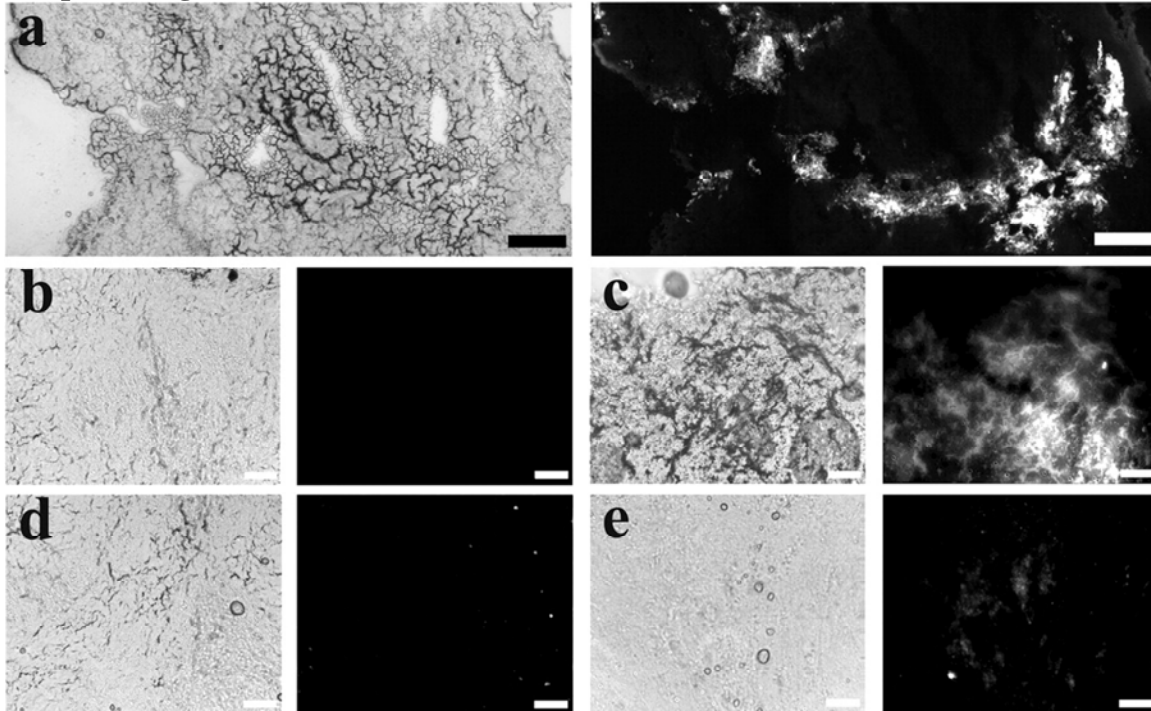
In summary, we have found that signaling events that mediate reactive astrocytic hypertrophy versus astrocytic hyperplasia are distinct. β 1 integrin signaling regulates the latter stage alone and can be manipulated for providing a better environment for axon regeneration. The use of the IKVAV PA already provides evidence for this therapeutic approach. BMP signaling affects both phases, but its effects on the two phases are mediated by separate receptor subtypes. BMPR1a is more important in the initial reactive hypertrophy while BMPR1b plays a role in glial scar progression. Hence targeting these specific signaling pathways can provide novel therapeutic approaches to enhance functional outcomes after CNS injuries.

Chapter 2, figure 1



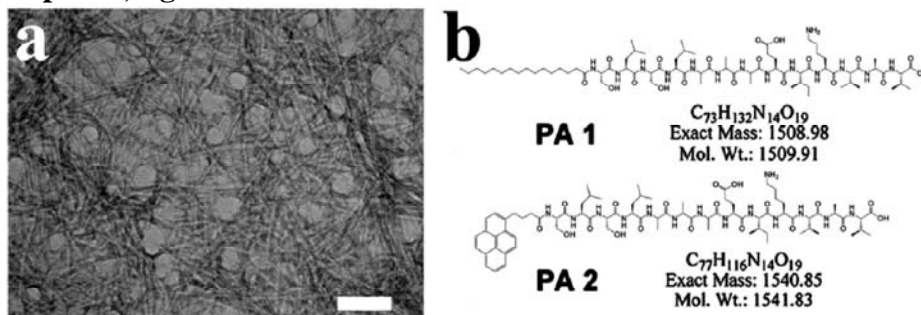
Structure of IKVAV PA. *a*, Schematic representation showing individual PA molecules assembled into a bundle of nanofibers interwoven to produce the IKVAV PA. *b*, Scanning electron micrograph image shows the network of nanofibers *in vitro*. Scale bar, 200 nm.

Chapter 2, figure 2



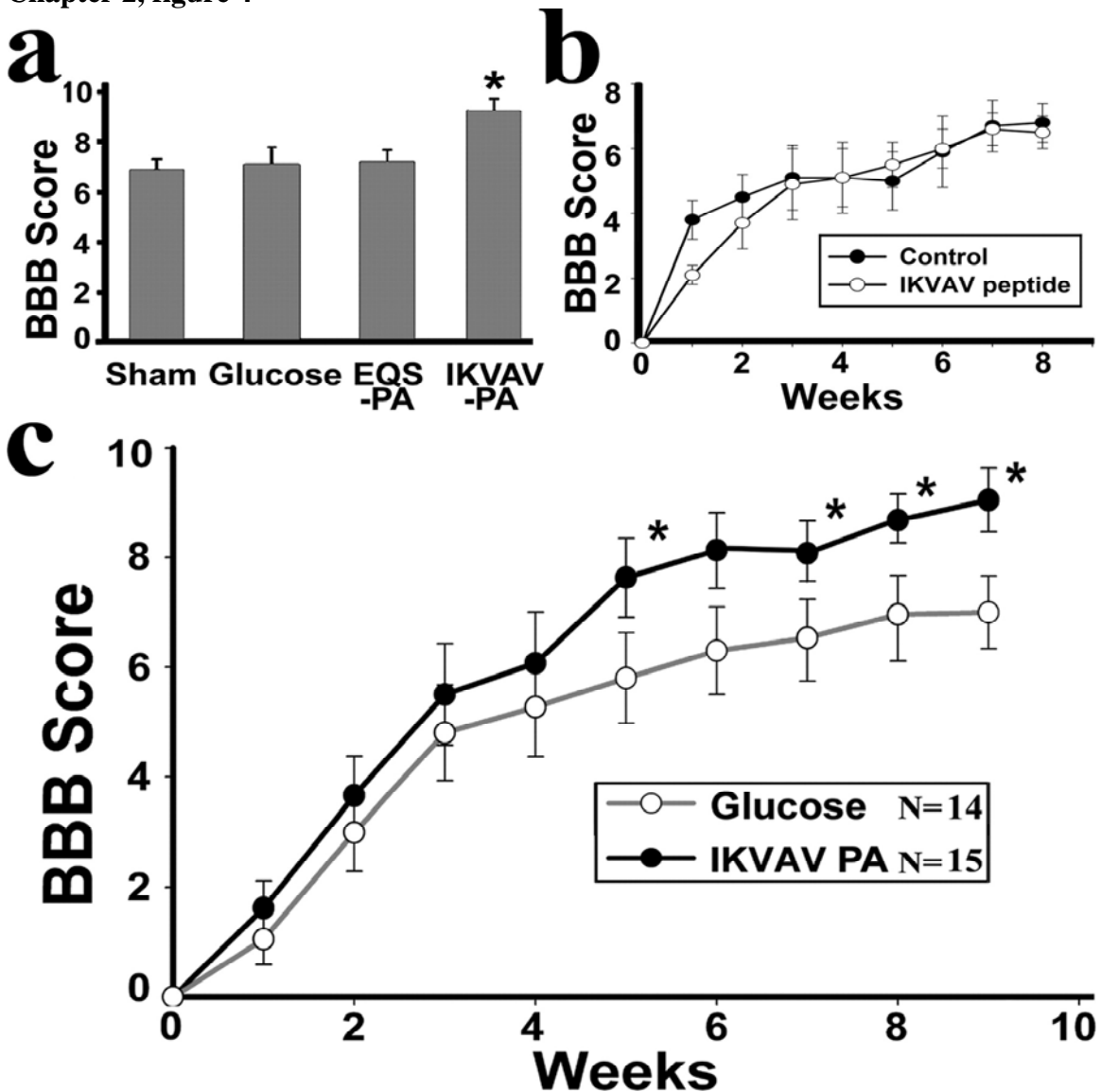
IKVAV PA solution self-assembles *in vivo*. *a*, Phase (left) and fluorescent (right) images showing the fluorescent IKVAV PA in the injured spinal cord 24 h after injection (dorsal, left; rostral, top). *b–e*, Longitudinal sections of spinal cord showing the fluorescent IKVAV PA is present at 2 weeks after injection only in IKVAV PA-injected animals (*c*) versus control (uninjected; *b*), but by 4 weeks, the IKVAV PA has mostly biodegraded, as seen in the IKVAV PA-injected animals (*e*) compared with uninjected animals (*d*). Scale bars: *a*, 100 μm , *b–e*, 50 μm .

Chapter 2, figure 3



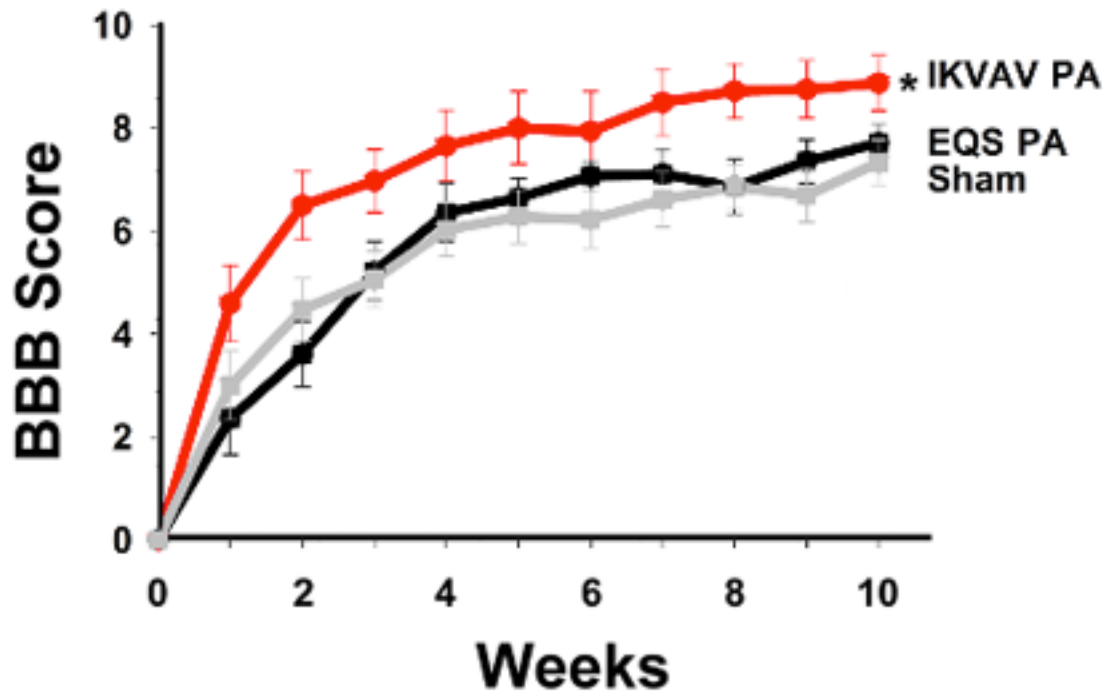
Structure of IKVAV peptide amphiphile (PA) **a**, Transmission electron microscope images showing the network of nanofibers. Scale bar: 100 nm. **b**, The chemical structure of the PAs used in these studies. The peptide sequence, SLSLAAAEIKVAV, is terminated at the N-terminus with a palmitoyl tail (PA1) or a pyrenebutyl tail in the fluorescent version (PA2).

Chapter 2, figure 4



IKVAV PA promotes functional recovery as analyzed by the BBB scale. *a*, Graph shows mean mouse BBB locomotor scores at 9 weeks after SCI for animals receiving injections of glucose, EQS PA, IKVAV PA, or sham injection. The IKVAV PA group differed from all others at $p < 0.045$. $n = 7$. *b*, IKVAV peptide was injected at the same manner as the IKVAV PA. There were no significant differences in the BBB scores of animals injected with IKVAV peptide compared with sham controls. *c*, The graph shows mean mouse BBB locomotor scores between IKVAV PA and glucose injections after SCI. The IKVAV ($n = 15$) and glucose ($n = 14$) groups differ from each other at $p < 0.04$ by ANOVA with repeated measures. *Tukey's HSD *post hoc t* tests showed that scores differed at $p < 0.045$ at every time point 5 weeks after SCI and thereafter.

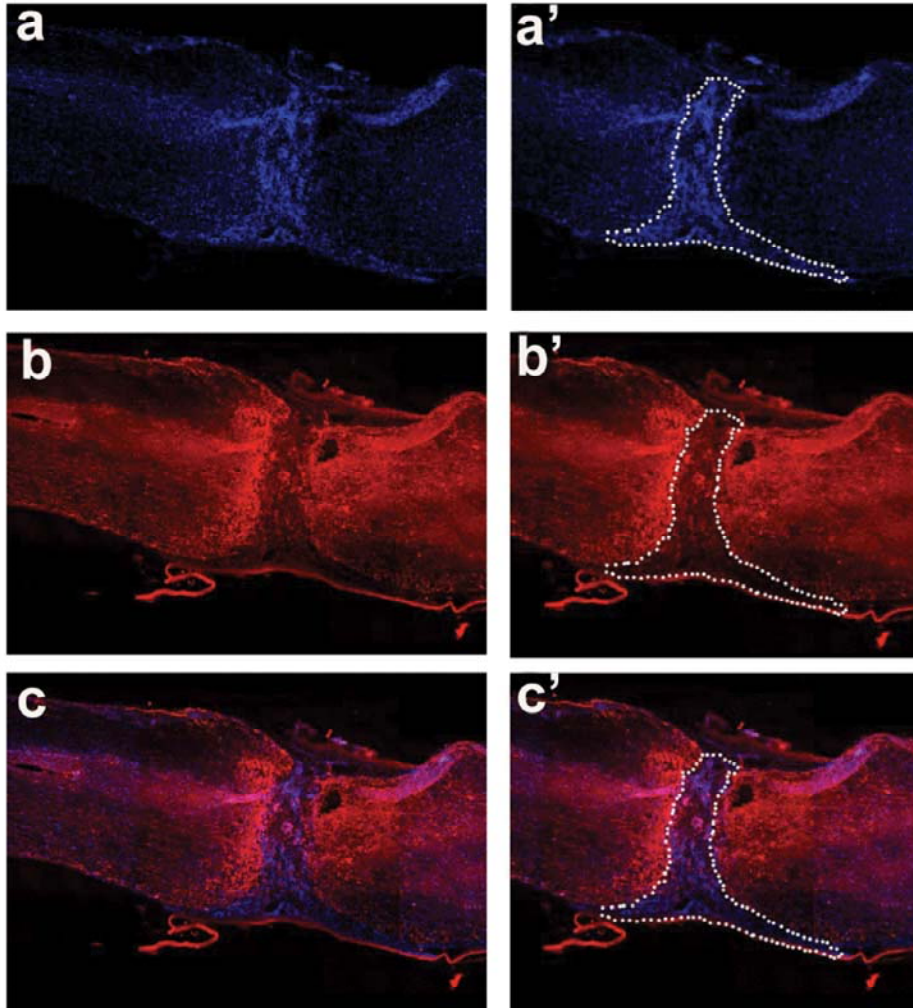
Chapter 2, figure 5



IKVAV sequence in the IKVAV PA is critical for functional recovery after SCI.

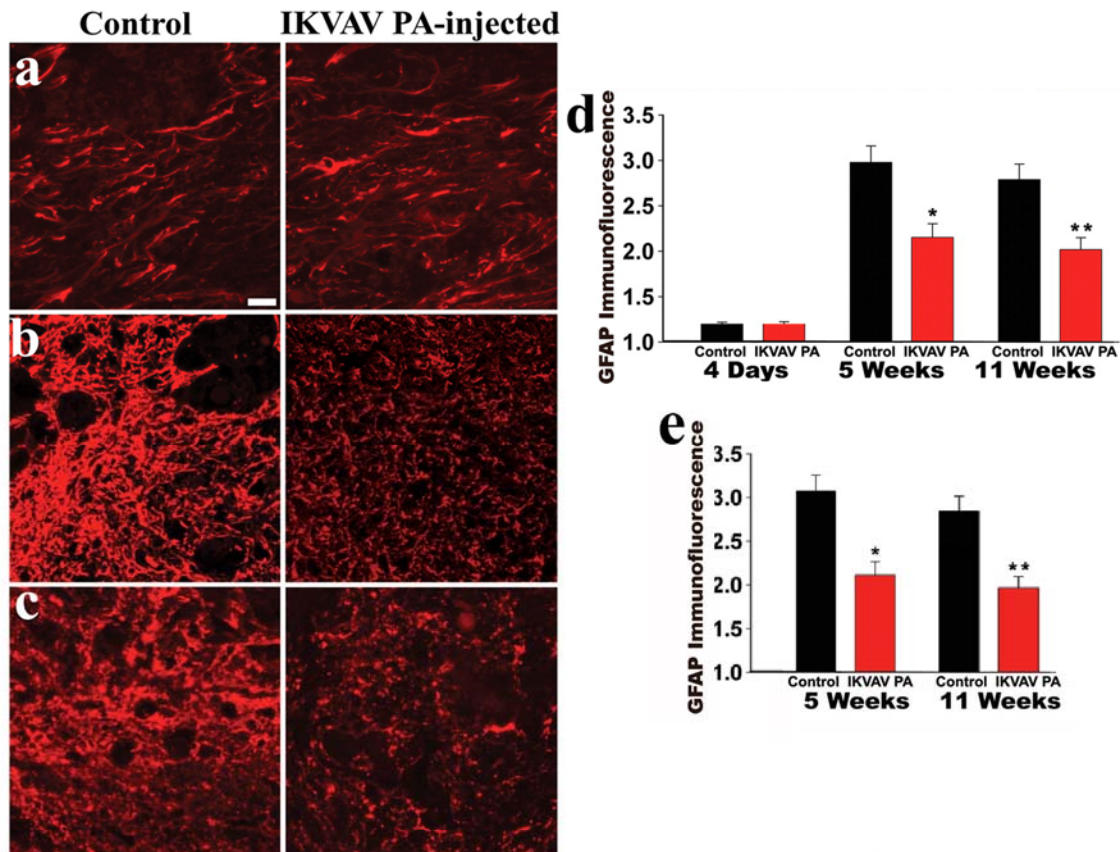
Graph showing mean mouse BBB locomotor scores after severe compression SCI. The IKVAV (n=16), EQS (n=14), and Sham (n=17) groups differ from each other at $p < 0.01$ by ANOVA with repeated measures. Tukey Kramer post hoc t tests showed no difference between sham and EQS PA-injected controls, however, the IKVAV PA-injected group differed from the other groups ($p < 0.05$).

Chapter 2, figure 6



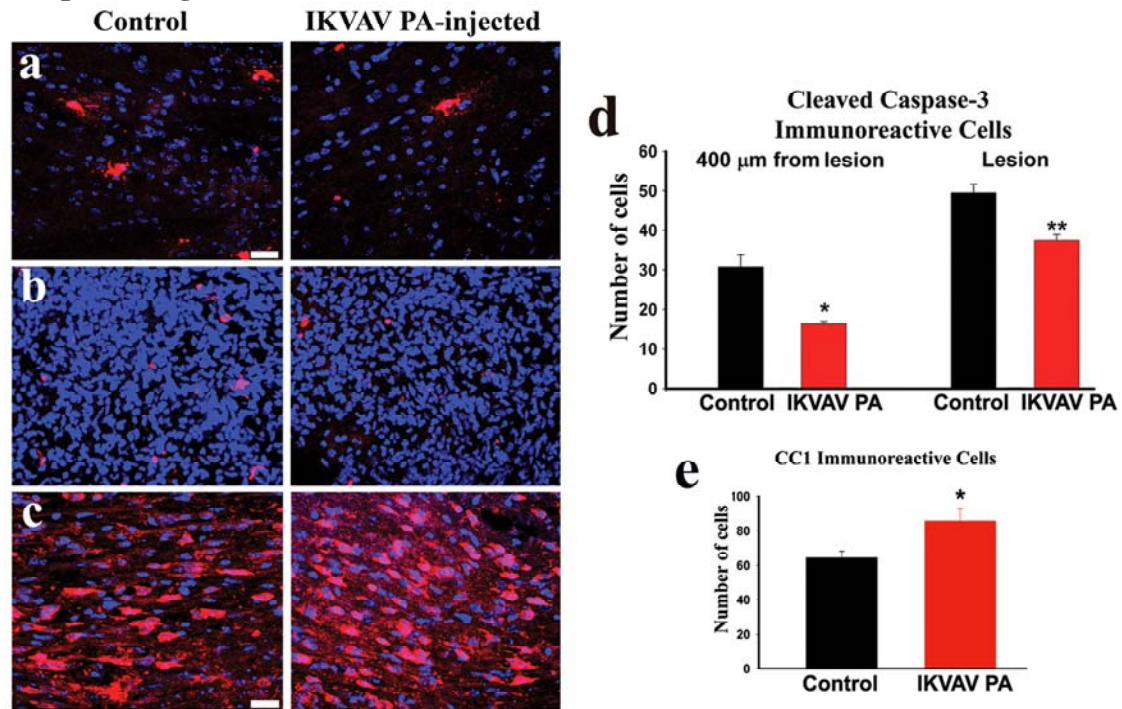
Intense Gliosis surrounds the area of dense infiltration. Low magnification image of an injured spinal cord 11 weeks post injury stained for GFAP in red (b) and Hoechst nuclear stain in blue (a). The merged picture is shown in c. On the right the same images have a dotted line indicating the centre of the lesion where infiltrating cells (note the high nuclear density in this region) have been compacted by the surrounding astrocytes. We have defined this area to be the “lesion area”. Note that this area is largely unstained for GFAP and that the peak GFAP immunofluorescence is immediately adjacent to this area. The intensity of GFAP was quantified in the area of peak intensity as described in Methods.

Chapter 2, figure 7



IKVAV PA attenuates astrogliosis *in vivo* after SCI. *a–c*, Representative confocal Z-stacks of injured areas stained with GFAP in control and IKVAV PA-injected animals. The lesion is defined as the area marked by dense infiltration (Okada et al., 2006). The two groups do not differ at 4 d (*a*), but at 5 weeks (*b*) and 11 weeks (*c*), there is significantly less glial scarring in the IKVAV PA-injected animals. *d*, GFAP immunofluorescence levels (expressed as fold increases over uninjured areas) in the IKVAV PA-injected animals are significantly reduced compared with control animals at 5 and 11 weeks (* $p < 0.02$, ** $p < 0.04$ by *t* test). *e*, GFAP immunofluorescence levels in the IKVAV PA-injected and control animals were normalized to normal, uninjured spinal cord. The levels in the IKVAV group are significantly reduced compared to control (* $p < 0.015$, ** $p < 0.03$ by *t* test). Scale bar, 20 μm .

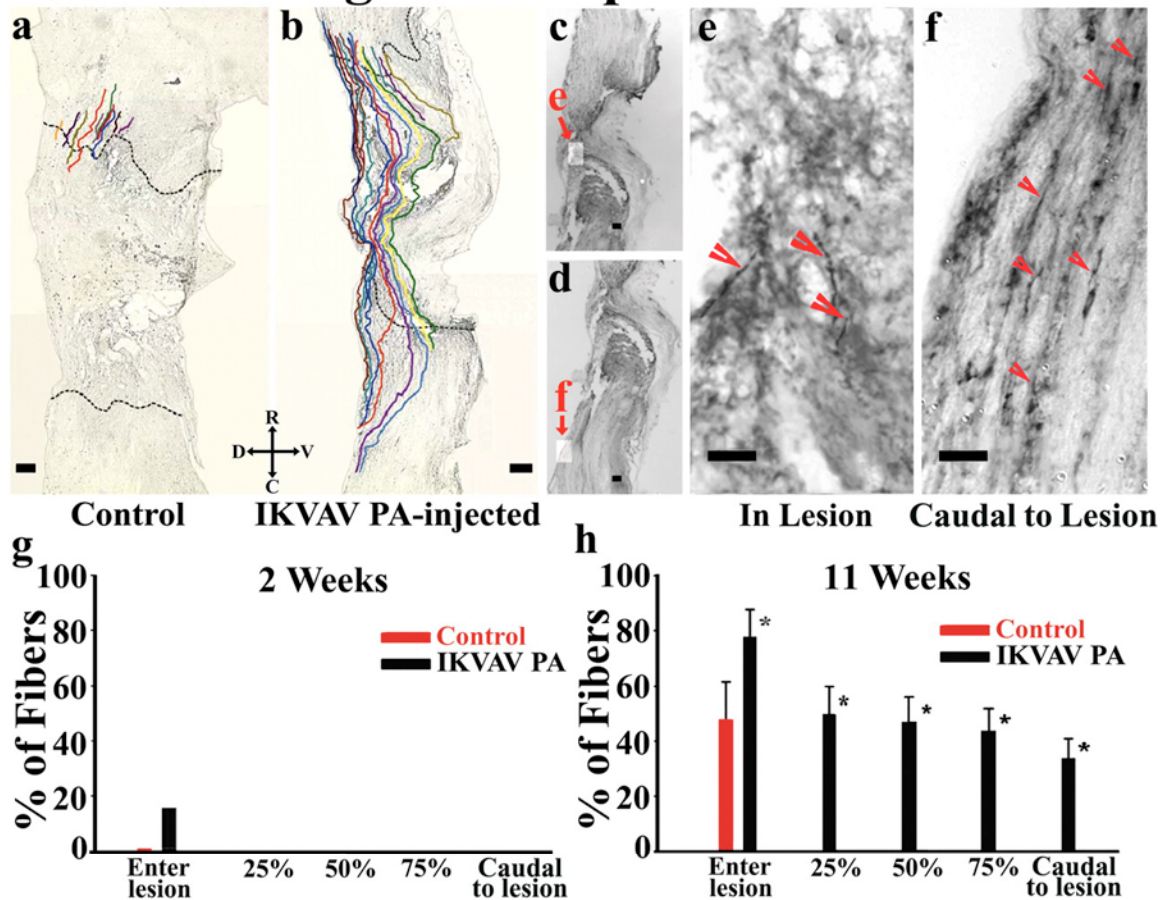
Chapter 2, figure 8



Apoptotic cell death is reduced in IKVAV PA-injected animals. *a, b*, Collapsed confocal Z-stacks of 20- μm -thick spinal cord sections (red, activated caspase-3; blue, Hoechst nuclear stain). The IKVAV PA-injected animals had fewer cleaved caspase-3-positive cells in every 20- μm -thick section in the lesion (defined as the area marked by dense infiltration; *b, d*; ** $p < 0.008$ by *t* test) and as far as 400 μm rostral and caudal to the lesion (*a, d*; * $p < 0.001$ by *t* test). *c*, Confocal Z-stacks of 20- μm -thick sections within 400 μm of the lesion (red, CC1; blue, Hoechst) reveals an increased density of OLs in the IKVAV PA-injected animals. *e*. Quantification of the oligodendroglial density described in (*c*) (* $p < 0.025$) Scale bar, 20 μm .

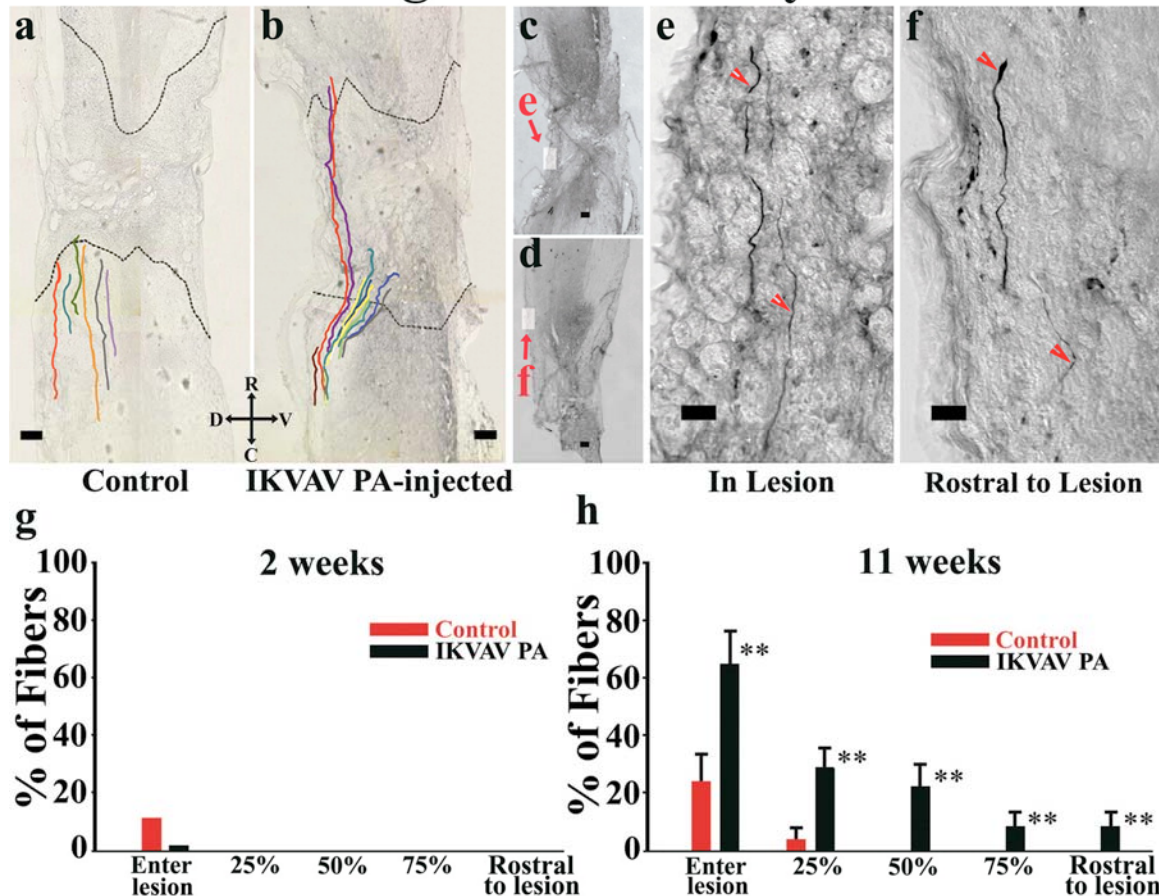
Chapter 2, figure 9

Descending Corticospinal Motor Axons



IKVAV PA promotes regeneration of motor axons after SCI. *a, b*, Representative NeuroLucida tracings of BDA-labeled descending motor fibers within a distance of 500 μm rostral of the lesion in vehicle-injected (*a*) and IKVAV PA-injected (*b*) animals. The dotted lines demarcate the borders of the lesion. *c-f*, Bright-field images of BDA-labeled tracts in lesion (*c, e*) and caudal to lesion (*d, f*) used for NeuroLucida tracings in an IKVAV PA-injected spinal cord (*a, b*). *g, h*, Bar graphs show the extent to which labeled corticospinal axons penetrated the lesion. *The groups representing three control and three IKVAV PA mice and the tracing of 130 individual axons differ from each other at $p < 0.03$ by the Wilcoxon rank test. R, Rostral; C, caudal; D, dorsal; V, ventral. Scale bars: *a-d*, 100 μm ; *e-f*, 25 μm .

Chapter 2, figure 10

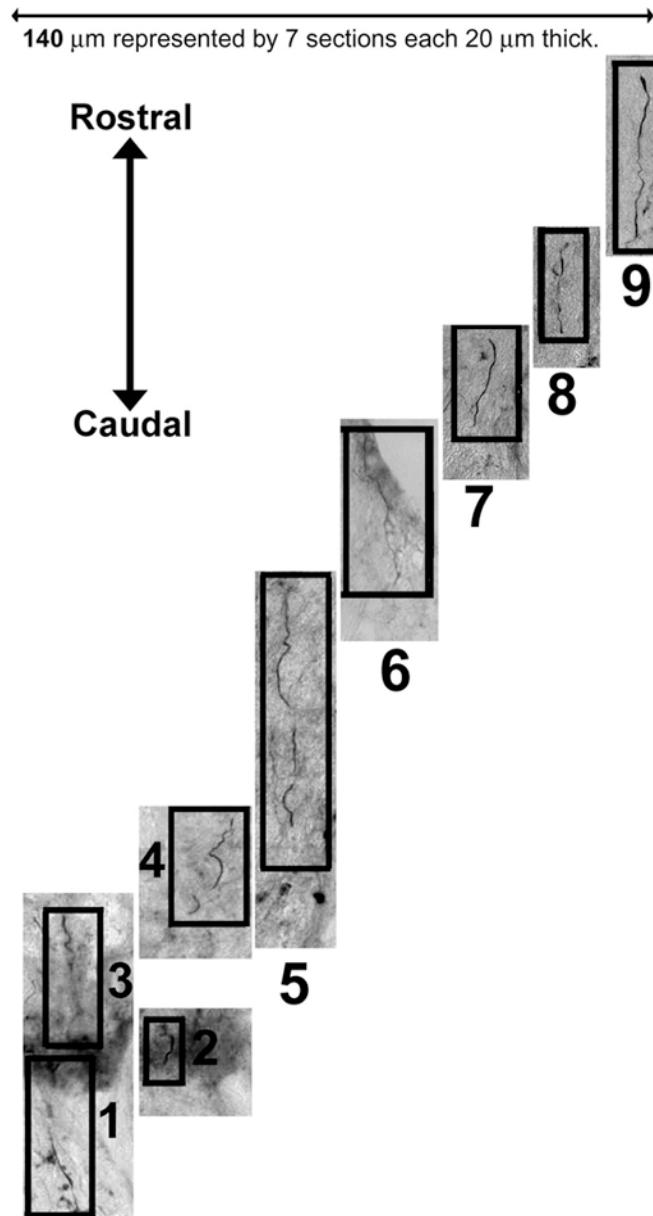
Ascending Dorsal Sensory Axons

IKVAV PA promotes regeneration of sensory axons after SCI. *a, b*, Representative Neurolucida tracings of BDA-labeled ascending sensory fibers within a distance of 500 μm of the lesion epicenter in vehicle-injected (*a*) and IKVAV PA-injected (*b*) animals. The dotted lines demarcate the borders of the lesion. *c-f*, Bright-field images of BDA-labeled tracts in lesion (*c, e*) and rostral to lesion (*d, f*) used for Neurolucida tracings in an IKVAV PA-injected spinal cord (*a, b*). The top arrowhead points to an axon tip that morphologically resembles a growth cone. *g, h*, Bar graphs showing the extent to which labeled dorsal column axons entered and grew through the lesion. **The groups (representing 4 control and 4 IKVAV PA mice and the tracing of 185 individual axons) differ from each other at $p < 0.05$ by the Wilcoxon rank test. R, Rostral; C, caudal; D, dorsal; V, ventral. Scale bars: *a-d*, 100 μm ; *e-f*, 25 μm .

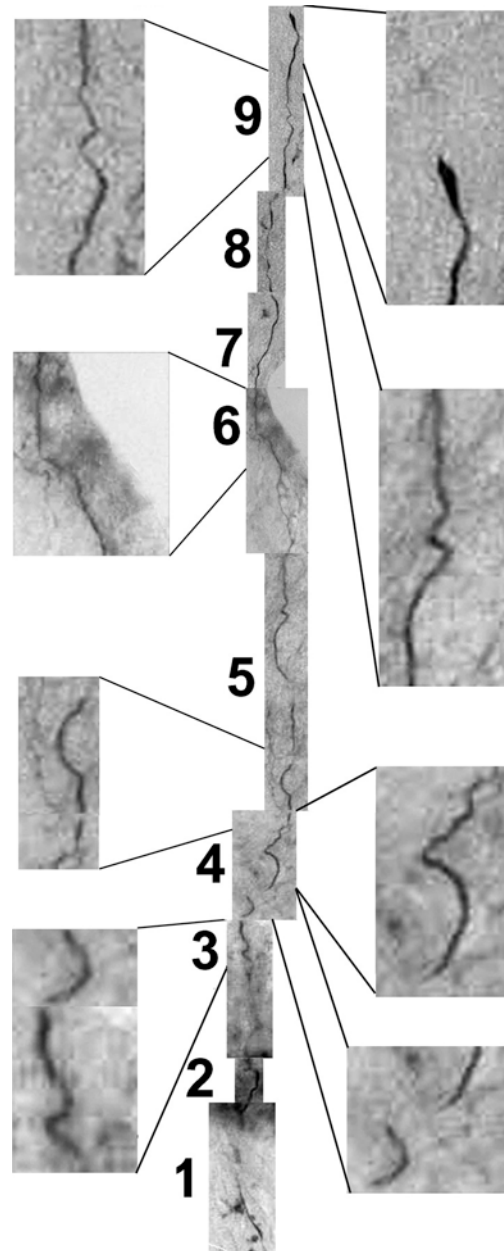
Chapter 2, figure 11

Montage demonstrating meandering course of a single axon. Montage of spinal cord sections illustrates the third dimension of axon regeneration. The Neurolucida drawings in Figures 10 & 11 are two-dimensional reconstructions of a three-dimensional phenomenon, and they therefore do not fully demonstrate the very unusual courses and morphologies of axons passing through the lesioned area. To further demonstrate the type of path taken by axons in the IKVAV PA-treated lesions, seven bright-field sections containing a representative axon from figure 11 were assembled. These seven sections represent only a small part of the total of 94 sections for this spinal cord. Note the meandering, unusual course of the fiber through the injured tissue and that it migrates out of and back into individual sections and across different sections. Also note that the fiber terminates rostral to the lesion after passing through the lesion site. The numbers label the individual images of the combined montage in Figure 13.

Chapter 2, figure 11



Chapter 2, figure 12

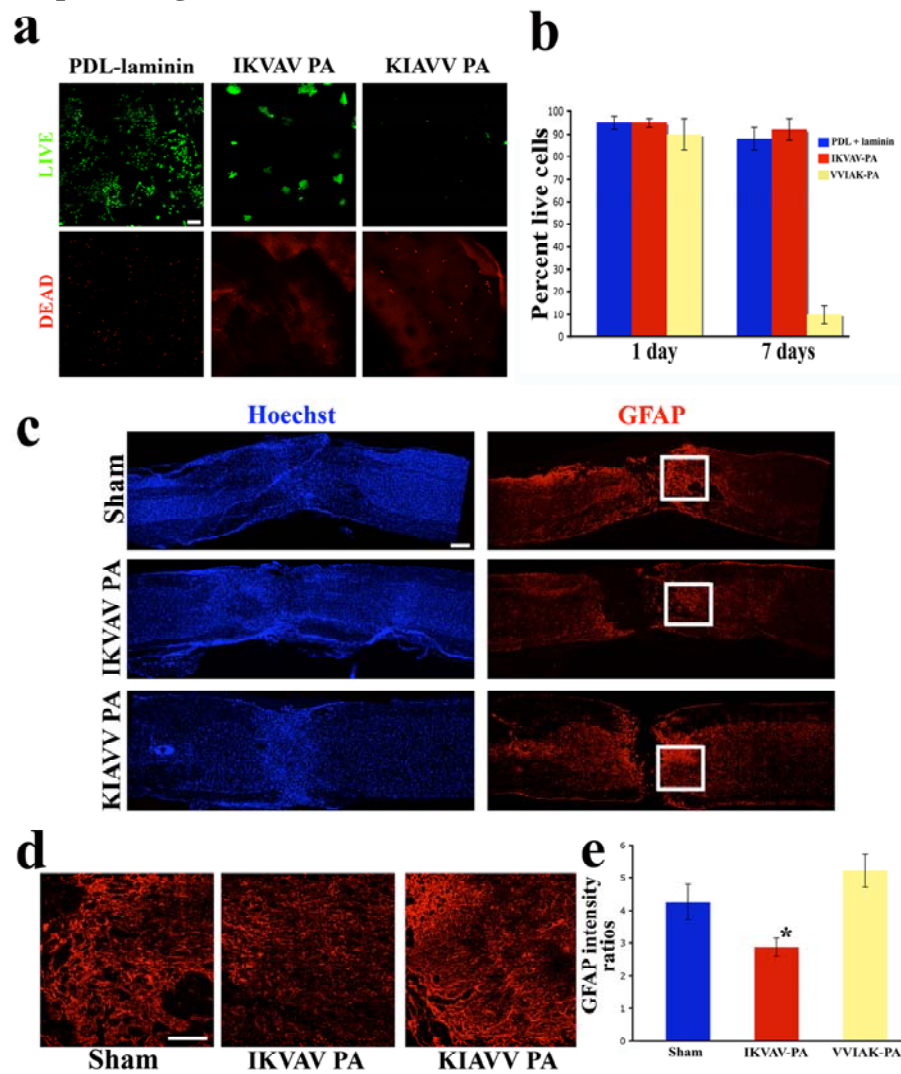


Montage illustrating a single axon tracing. Combined montage flattens the representative axon to two dimensions to demonstrate the unusual morphology of the axon as it passes through the lesion. The NeuroLucida tracings in figures 10 & 11 follow individual axons in three dimensions by tracing them from section to section and displaying their courses in a usable two-dimensional form. The drawing does not reflect the unusual morphologies of the axons. To demonstrate this, separate sections of Figure 12 were aligned in a montage to display the course of a single axon as it starts at the caudal end of the lesion, passes through the lesion, and terminates rostral to the lesion. Note the unusual course and morphology, and that the axon terminates in normal tissue rostral to the lesion.

Chapter 3, figure 1

IKVAV sequence is necessary for bioactivity of the IKVAV PA **a.** Neural Progenitor cells were cultured either on PDL-laminin, IKVAV PA or the scrambled non-bioactive KIAVV PA for 7 days and assessed for cell viability. Live cells are marked (green) while dead cells are (red). **b.** Quantification of cell viability in the groups described above at 24 hours and 7 days in culture. Note that the viability levels are comparable in all 3 groups at 24 hours, but by 7 days, while the levels are similar between cells cultured on PDL laminin and in the IKVAV PA, but are significantly lower in the scrambled KIAVV PA. **c.** Low magnification (10X) images of IKVAV PA, KIAVV PA or sham injected spinal cords 3 weeks post SCI. Sections are stained with Hoechst nuclear stain (blue) and GFAP (red). Scale bar: 200 μ m. **d.** Representative confocal Z-stacks taken at higher magnification (20X) of the areas boxed in (c) showing reduced gliosis in the IKVAV PA injected animals. Scale bar: 100 μ m. **e.** Quantification of the GFAP immunofluorescence shown in (d). Fluorescence intensity is expressed as fold increases over uninjured control spinal cords. The intensity values are significantly lower in the IKVAV PA injected animals while there is no difference between the sham and scrambled KIAVV PA injected groups. (n=3 animals per group, *p<0.01 by ANOVA single factor)

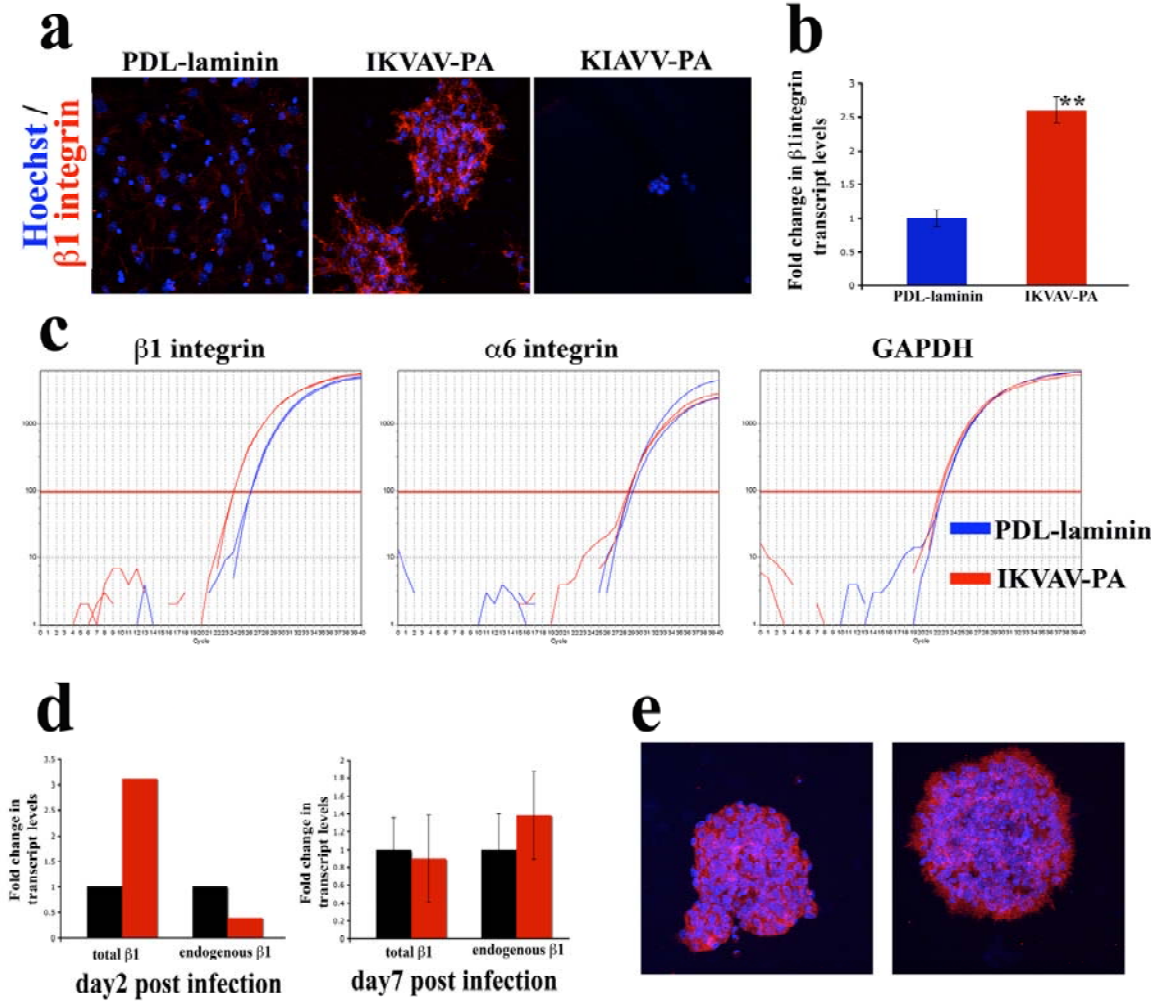
Chapter 3, figure 1



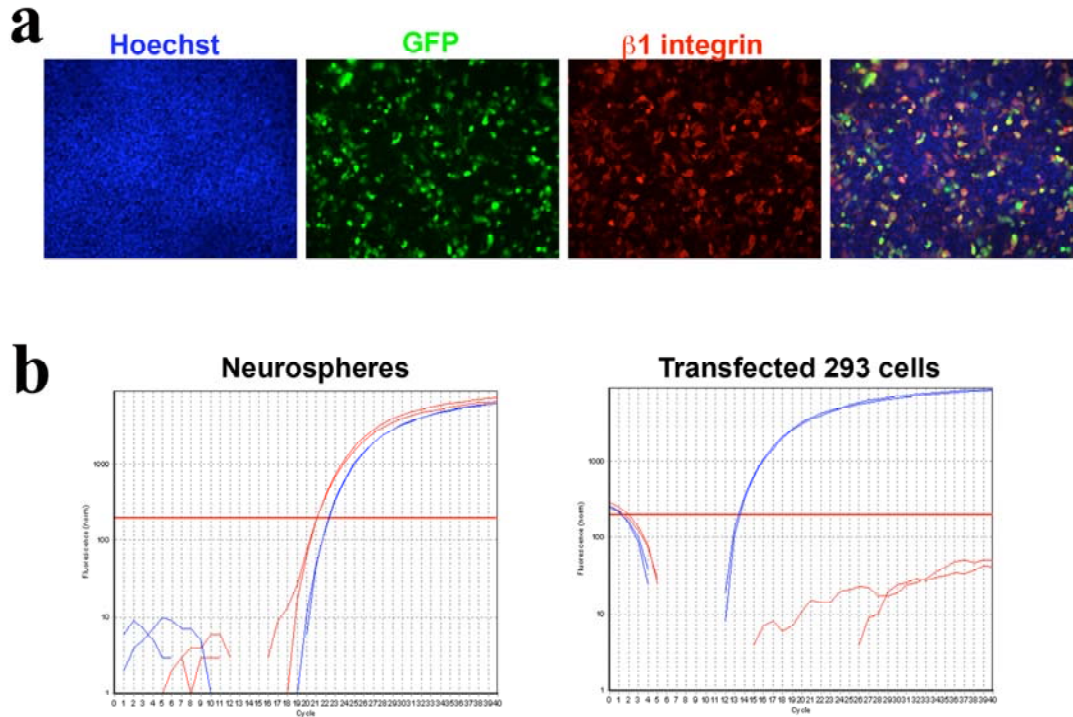
Chapter 3, figure 2

The IKVAV PA is a powerful tool for upregulating $\beta 1$ integrin **a.** NPCs cultured for 7 days stained for $\beta 1$ integrin (red) and Hoechst nuclear stain (blue). Note the increased staining for $\beta 1$ integrin in the IKVAV PA over the other two conditions. **b.** Fold increase in the transcript levels of $\beta 1$ integrin in the IKVAV PA versus PDL laminin. Plot represents an average of 3 different sets of cells that were cultured in the two substrates \pm standard deviations. (** $p < 0.0007$ by student's unpaired t test) **c.** Real time PCR amplification plots for the conditions in (b) showing that the $\beta 1$ integrin transcript is abundantly expressed as compared to levels of GAPDH. Note that there is no significant difference in the levels of $\alpha 6$ integrin. **d.** Transcript levels (detected by real time PCR) of endogenous versus total $\beta 1$ integrin in NPCs that were infected with either a control or $\beta 1$ integrin overexpressing retrovirus and cultured on PDL-laminin. There is a significant increase in the total $\beta 1$ integrin levels at 2 days post infection that disappears by 7 days. Graphs represent levels normalized to the ones from control virus-infected cells from 3 rounds of infection. **e.** NPCs described in (d) were cultured in the IKVAV PA for 7 days and stained for $\beta 1$ integrin (red) and Hoechst nuclear stain (blue). Note that there is no significant difference in the levels of $\beta 1$ integrin in either condition. (Scale bars in a,e : $20\mu\text{m}$)

Chapter 3, figure 2



Chapter 3, figure 3

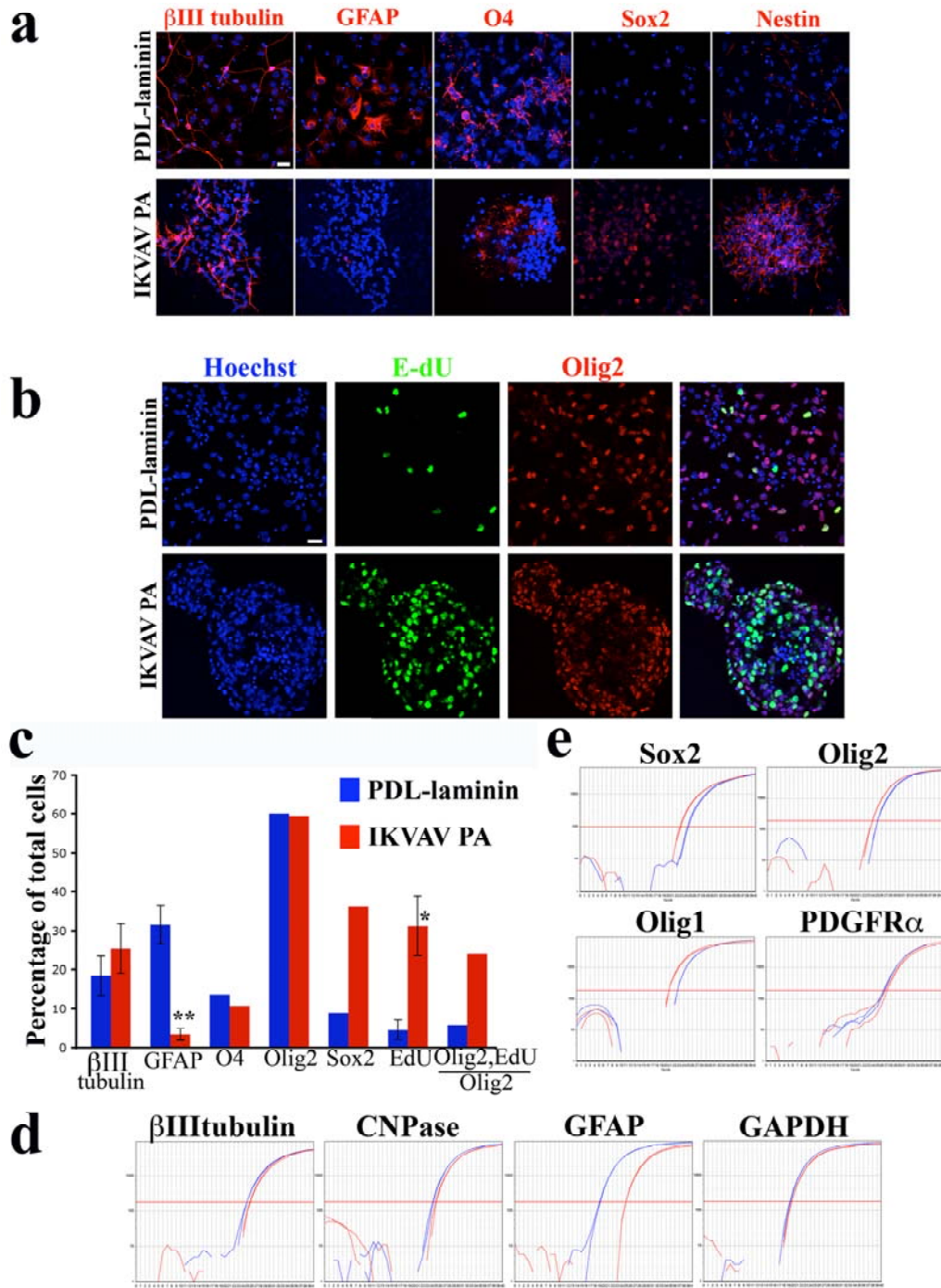
**Detection of endogenous versus transgenically expressed $\beta 1$ integrin**

a. 293 cells transfected with pCLE- $\beta 1$ integrin-IRES GFP expressing plasmid. Green (GFP) , red ($\beta 1$ integrin). **b.** Real time RT-PCR amplification plots for $\beta 1$ integrin obtained from post natal neurospheres or 293 cells transfected with $\beta 1$ integrin. The amplicon was detected either by primers targeted in the 3' UTR and designed to detect endogenous $\beta 1$ integrin (red traces) or by primers targeted to the coding sequence that can detect both endogenous as well as over expressed $\beta 1$ integrin (blue traces).

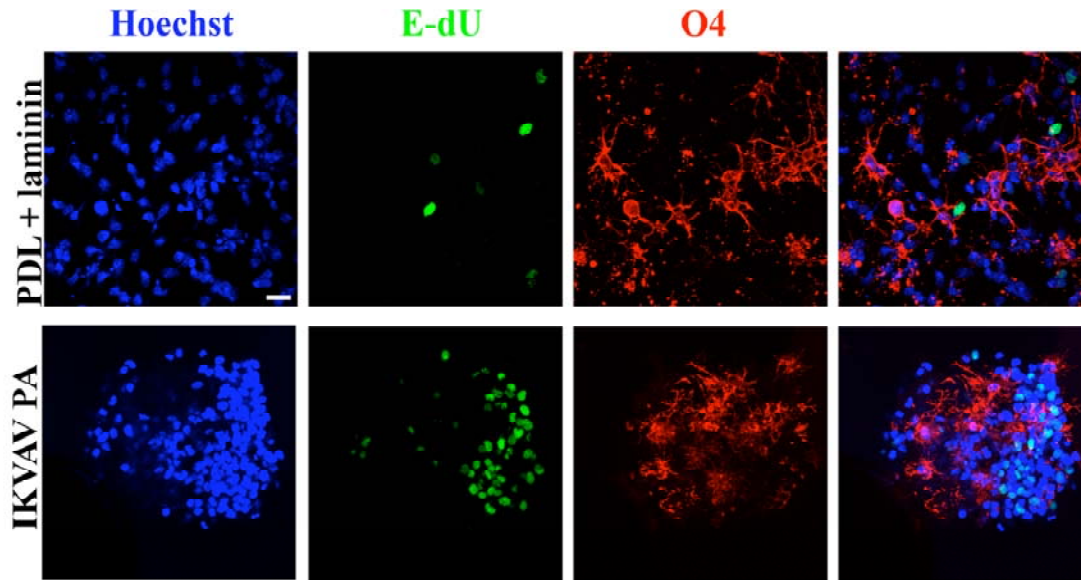
Chapter 3, figure 4**Cells retain progenitor characteristics and specifically avoid astrocytic commitment in the IKVAV PA**

a. Neural progenitor cells cultured either on PDL-laminin coverslips (Top row) or in the IKVAV PA (bottom row) for 7 days and stained with Hoechst nuclear stain (blue) and the marker (red). Note the absence of GFAP staining in the IKVAV PA and the concomitant increase in the progenitor markers Sox2 and Nestin. **b.** The cultures described in (a) stained with Olig2 (red), the thymidine analog EdU (green) and Hoechst nuclear stain (blue). Note that there is an increase in the number of EdU positive cells in the IKVAV PA and also the number of Olig2, EdU double positive cells in the IKVAV PA. (Scale bars in a,b : 20 μ m) **c.** Quantification of the percentage of cells in the conditions described in (a), (b). Bars represent average counts \pm s.e.m. (*, $p < 0.017$, ** $p < 0.005$ by Student's unpaired t test) **d.** Real time PCR amplification plots for transcript levels of β III tubulin, GFAP and CNPase in cells cultured in the IKVAV PA (red traces) versus PDL laminin controls (blue trace) . Note the large reduction specifically in the levels of GFAP transcripts in the IKVAV PA. **e.** Real time PCR plots as in d showing modest increases in the levels of progenitor markers Olig1, Olig2 and Sox2 in the cells cultured in the IKVAV PA.

Chapter 3, figure 4

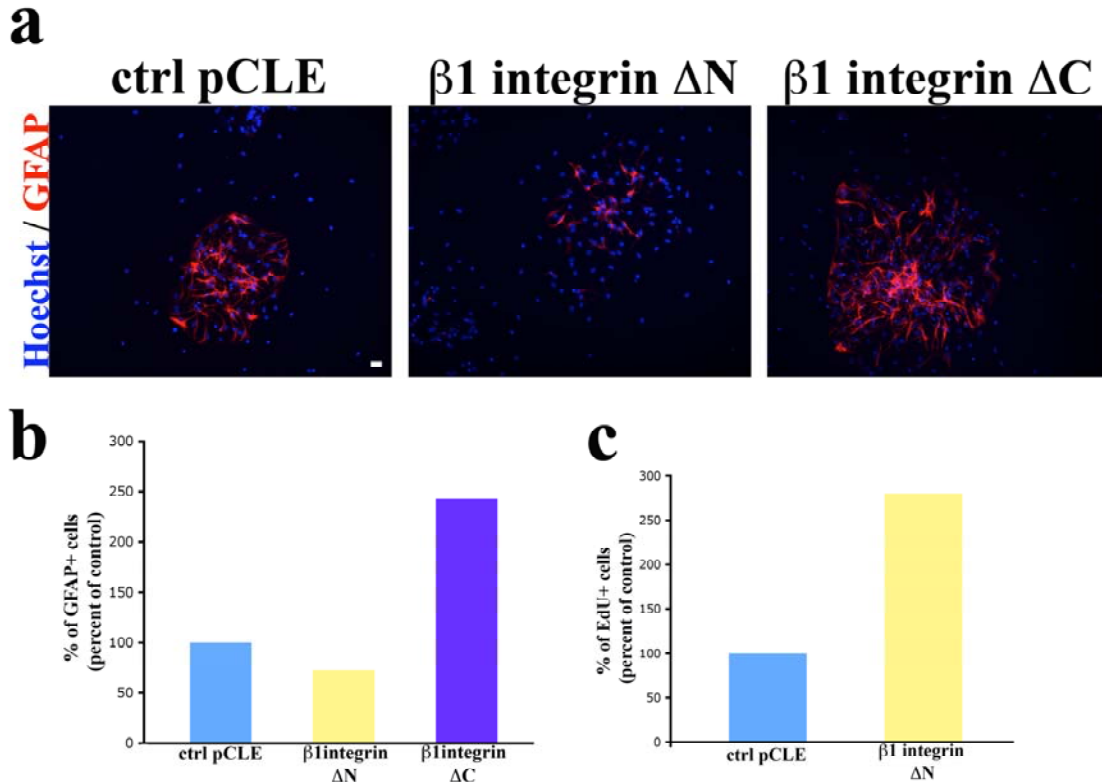


Chapter3, figure 5

**O4 positive cells were not in cell cycle at 7 days in vitro.**

Neural Progenitor cells were cultured for 7 days on either PDL laminin or in the IKVAV PA and pulsed for 12 hours with the thymidine analog, EdU (see text for details). Cultures are stained for O4 (red) and E-dU (green). Note that in either condition, O4 positive cells are EdU negative suggesting they have exited cell cycle. Scale bar : 20 μ m.

Chapter 3, figure 6



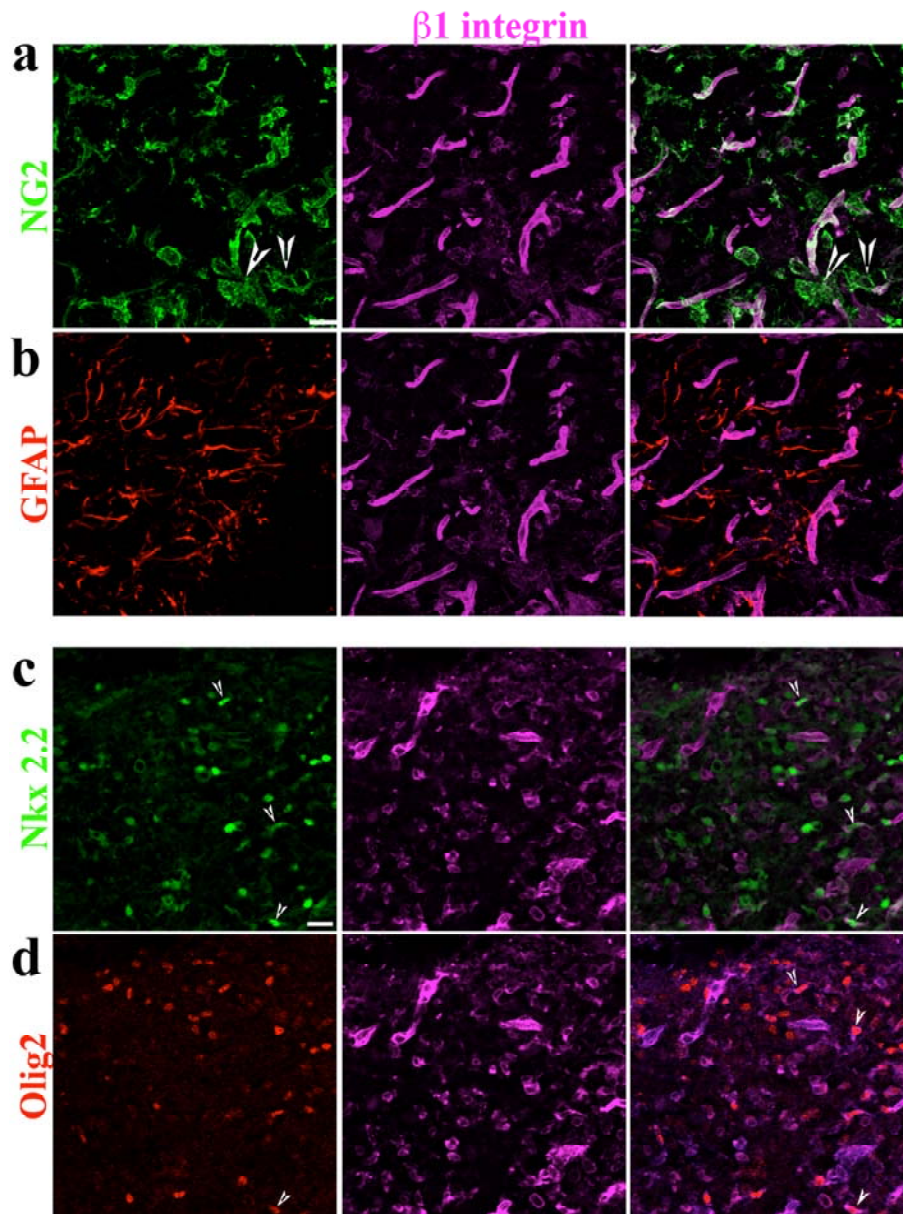
Altering $\beta 1$ integrin signaling affects Astrocytic lineage commitment

a. NPCs were infected with retroviruses expressing GFP alone (ctrl pCLE), $\beta 1$ integrin lacking the cytoplasmic domain ($\beta 1$ integrin ΔC) or $\beta 1$ integrin lacking the N-terminal domain ($\beta 1$ integrin ΔN) (See text for details). Cells were sorted for GFP two days after infection, cultured for 7 days on PDL-laminin and stained for GFAP (red) and Hoechst nuclear stain (blue). Scale bar: 20 μ m. **b.** Quantification of GFAP + cells in the conditions described in (a). Numbers are represented as a percentage over those observed in the control virus condition. **c.** Quantification of E-dU + cells in the conditions described in (a). The thymidine analog was applied in the last 12 hours before fixation. Numbers are represented as a percentage over those observed in the control virus condition.

Chapter 3, figure 7**The $\beta 1$ integrin receptor subunit is expressed on the NG2 positive progenitor population and not on reactive astrocytes after SCI**

Representative confocal Z-stacks of injured areas, 4 days post spinal cord injury stained with $\beta 1$ integrin (pink) and Hoechst nuclear stain (blue). Triple immunostaining was done with NG2 (green) in **(a)**, GFAP (red) in **(b)**, Nkx2.2 (green) in **(c)** and Olig2 (red) in **(d)**. The $\beta 1$ integrin receptor sub unit staining is seen on NG2 expressing cells with spindle shaped morphology indicating that they are the progenitor cell population that are known to invade the lesion site after injury. Note that cells with aberrant morphologies (macrophages) do not exhibit any staining (arrowheads in a). GFAP expressing reactive astrocytes (red) do not express $\beta 1$ integrin (pink) . A subset of the progenitor cells that are Nkx2.2 or Olig2 positive express $\beta 1$ integrin (arrowheads in c,d). Scale bar : 20 μ m.

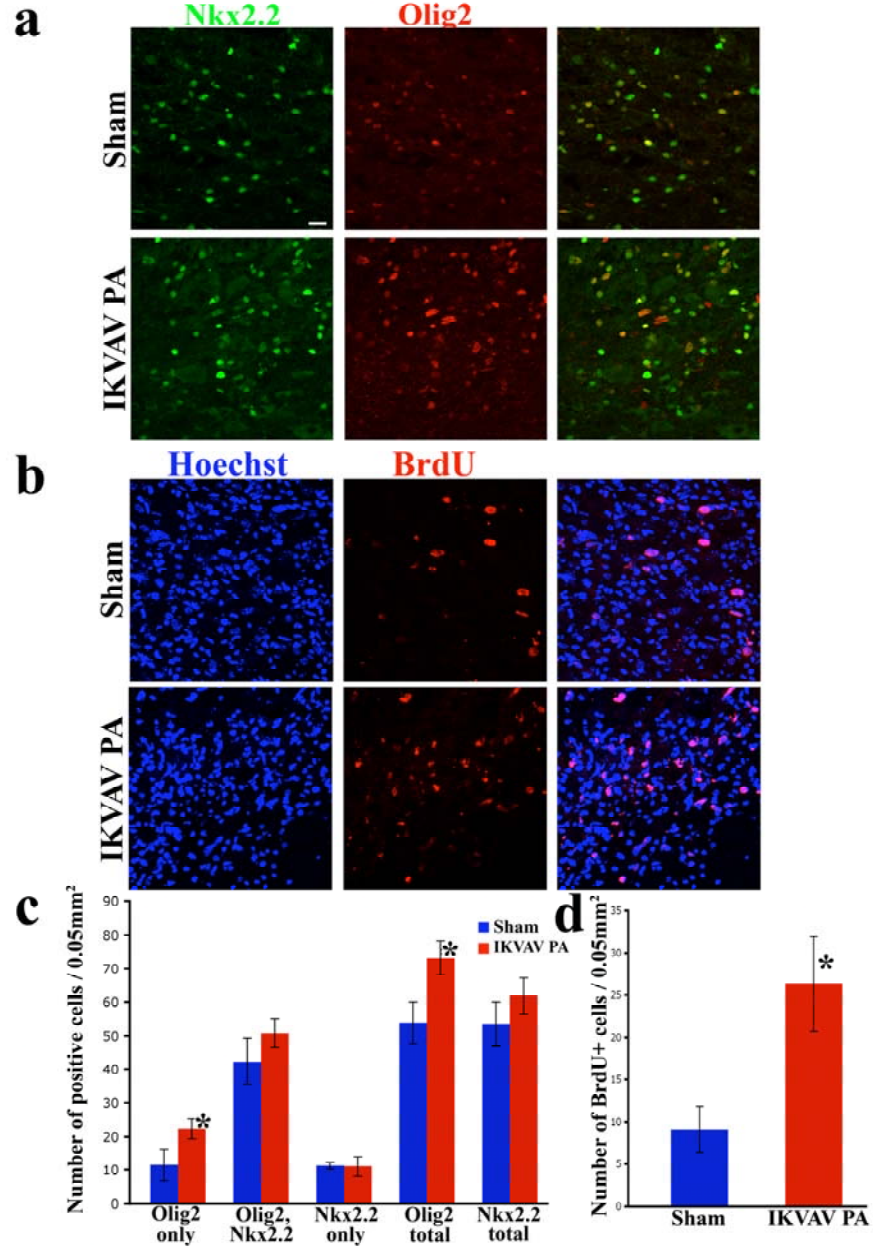
Chapter 3, figure 7



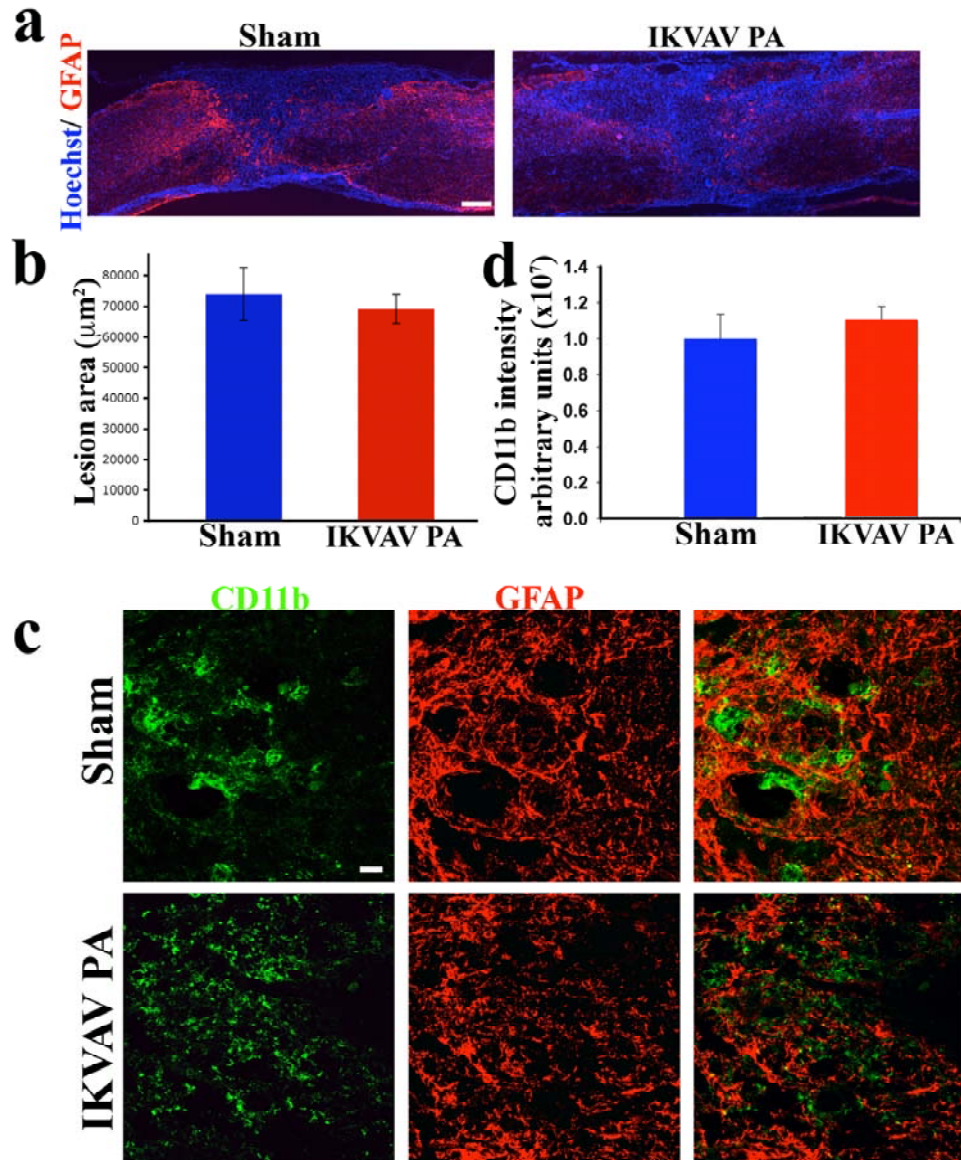
Chapter 3, figure 8

Maintenance of progenitor traits in IKVAV PA injected animals **a.** Representative images of spinal cord areas adjacent to the lesion site in sham and IKVAV PA injected animals at 4 days post SCI, stained for Nkx2.2 (green) and Olig2 (red). **b.** Representative images of spinal cord areas adjacent to the lesion site stained for BrdU (red) and Hoechst nuclear stain (blue) in sham and IKVAV PA injected animals at 4 days post SCI. (Scale bar in a,b: 20 μ m) **c.** Quantification of the cells counted in the 0.5 mm² areas shown in (a). Note the increase in the number of total Olig2 positive cells in the IKVAV PA injected animals. Bars represent average counts \pm s.e.m. (*p<0.08, ** p<0.03 by student's unpaired t test) **d.** Quantification of BrdU positive cells in the areas shown in (b). Bars represent average counts \pm s.e.m. (*p<0.03 by Student's unpaired t test)

Chapter 3, figure 8

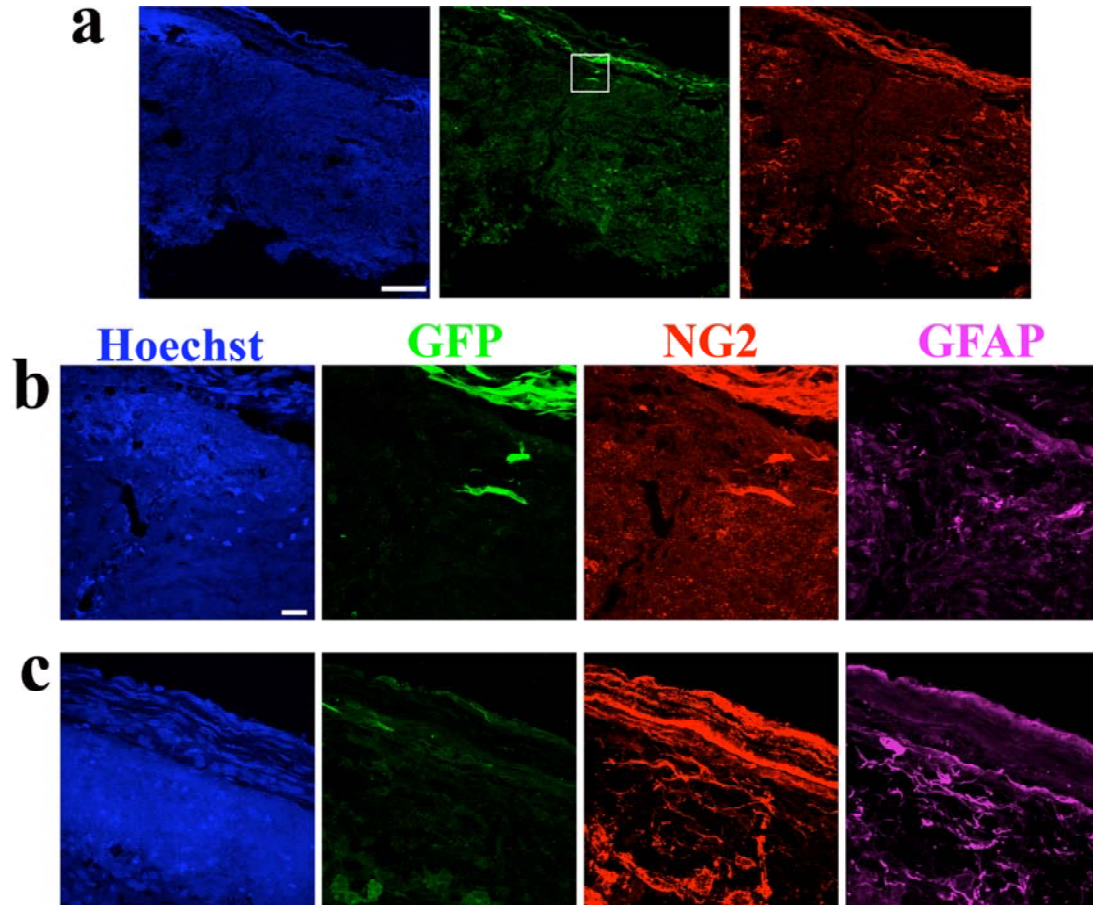


Chapter3, figure 9

**IKVAV PA does not alter inflammatory response after SCI**

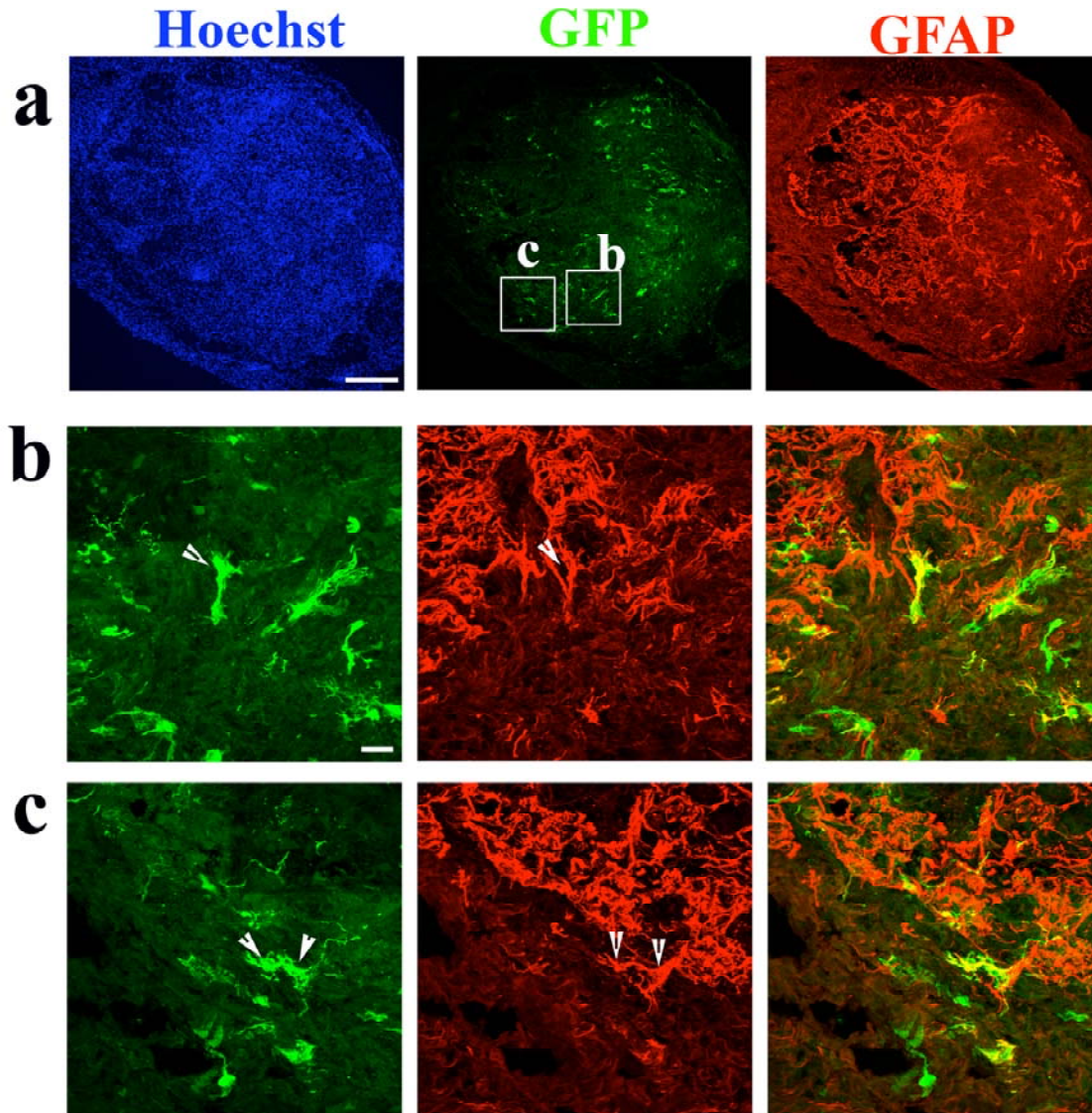
a. Representative sections from Sham and IKVAV PA injected animals at 3 weeks post injury stained for GFAP (red) and Hoechst nuclear stain (blue) showing comparable lesion areas compacted by the astrocytes in both groups. Scale bar : 200µm. **b.** Lesion area measurements show no difference between sham and IKVAV PA injected animals. **c.** Representative images from the two groups stained for CD11b (green) and GFAP (red) shows the reactive astrocytes intermingled with the inflammatory cells. (Scale bar: 20µm) **d.** Quantification of fluorescence intensity for CD11b shows no difference between groups.

Chapter 3, figure 10

**NG2 positive progenitor cells undergo cell divisions after spinal cord injury**

a. Low magnification images of the spinal cord showing retrovirally labeled cells are marked with GFP fluorescence (green) and stained for NG2 at 3 days post injury (see text for details). Note there is labeling in the meninges, but some cells are also labeled in the parenchyma. Scale bar: 200 μ m. **b.** Boxed area in (a) shown at higher magnification. The GFP positive cells in the parenchyma express NG2 (red) but do not express GFAP (pink). Scale bar : 20 μ m. **c.** An area further from the lesion than in (b) that is in the vicinity of reactive astrocytes. Note that the faintly GFP + cells express NG2 (red) but not GFAP (pink).

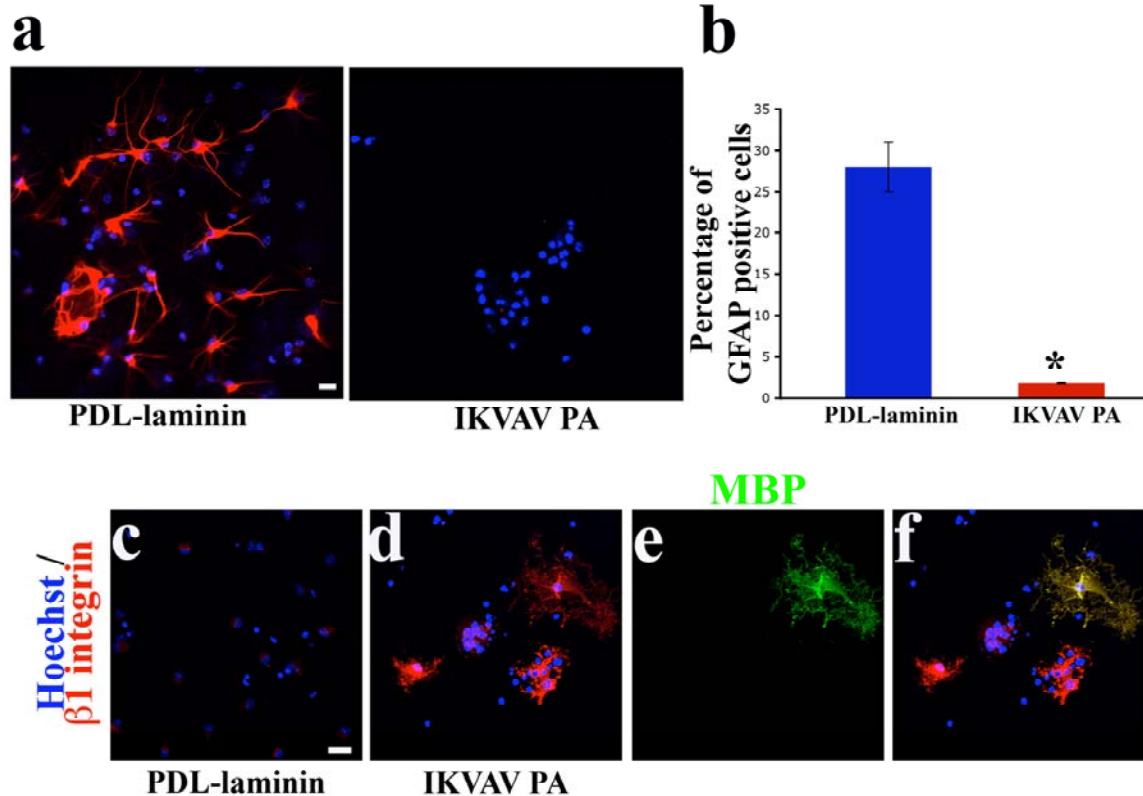
Chapter 3, figure 11



NG2 positive progenitor cells can differentiate into astrocytes after spinal cord injury.

a. Low magnification image of a spinal cord cross sections at 2 weeks post injury stained for GFP (green) and GFAP (red). Scale bar ; 200 μ m **b,c.** Areas boxed in (a) are shown at higher magnification. Some GFP positive cells (arrowheads) are GFAP positive. Scale bar : 20 μ m.

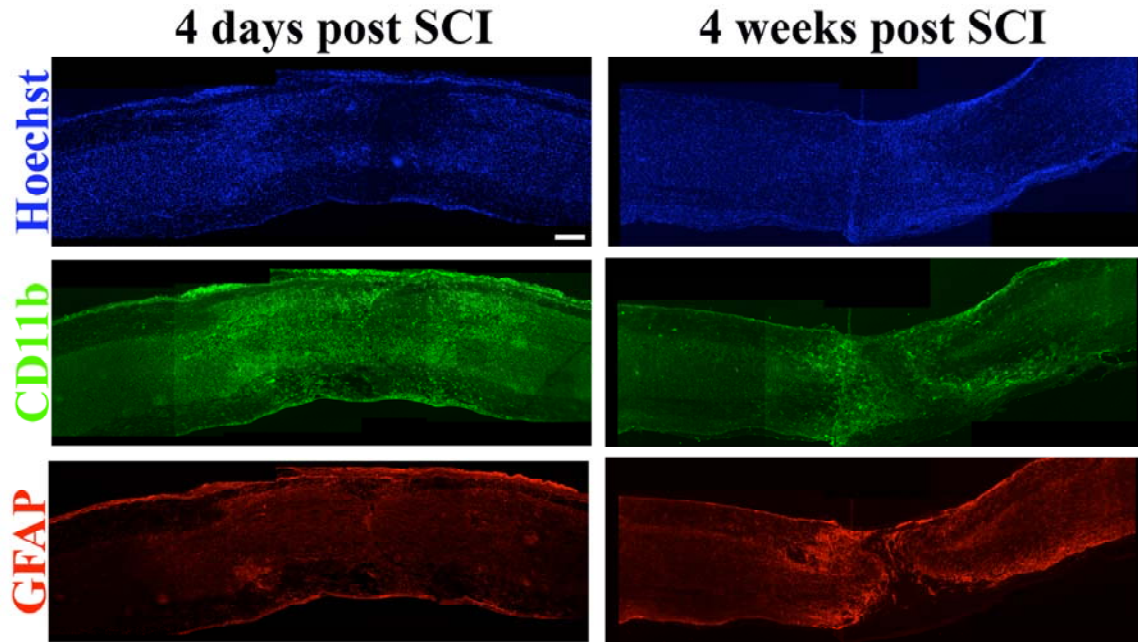
Chapter 3, figure 12



IKVAV PA prevents astroglial lineage commitment from glial progenitors cells.

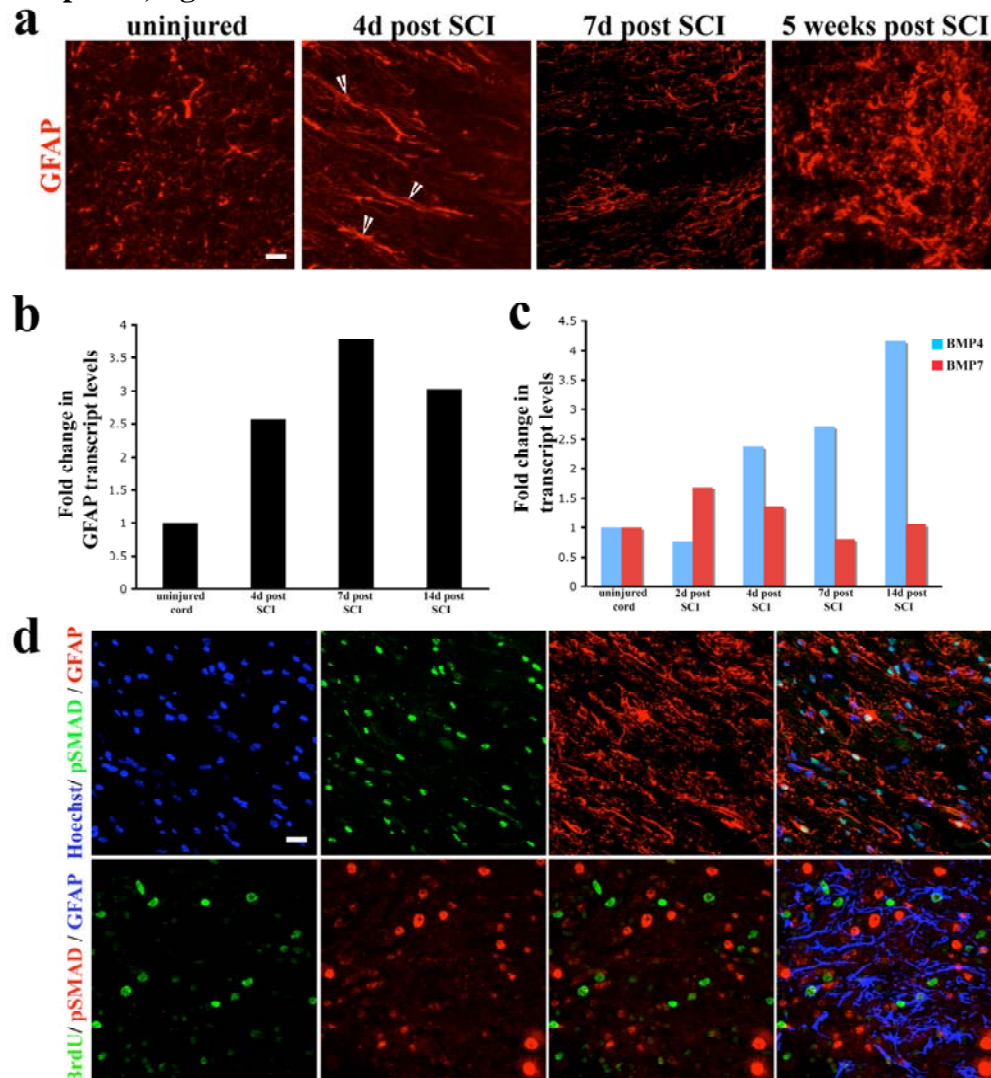
a. O2A progenitor cells cultured on PDL-laminin or IKVAV PA for 3 days in the presence of 20ng/ml BMP4 and stained for GFAP (red) and Hoechst nuclear stain (blue). Representative images for each condition are shown. Note the significant numbers of astrocytes that develop in control (laminin) conditions that are absent when cells are cultured in the IKVAV PA. Scale bar : 20 μ m . **b.** Graph showing percentage of GFAP+ cells observed for the conditions described in (a). * $p < 0.005$ by student's t test **c,d.** Cultures described in a stained for $\beta 1$ integrin (red) showing increased levels in the IKVAV PA. **e,f** A rare cell that expresses MBP, a mature oligodendrocytic marker, that was observed in the IKVAV PA that also stains for $\beta 1$ integrin. (Scale bars in a, c-f : 20 μ m)

Chapter 4, figure 1

**Reactive astrocytes compact inflammatory cells after SCI**

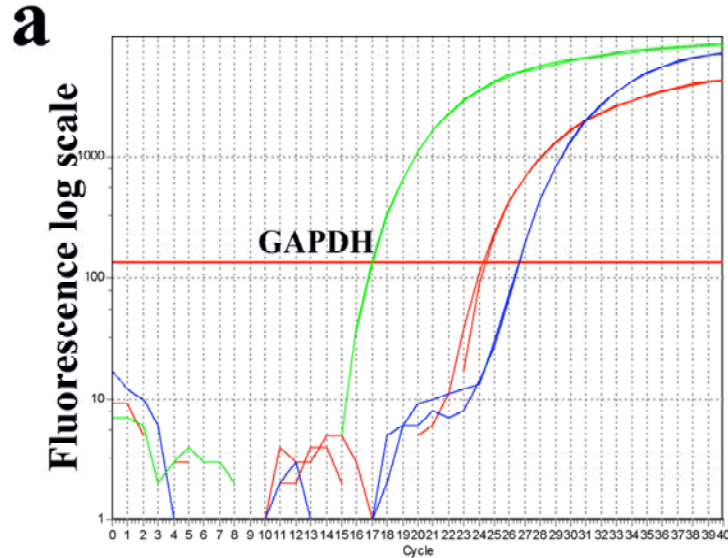
Longitudinal sections of injured spinal cords at 4 days (left column) and 4 weeks (right column) post injury. Sections are stained for CD11b (green), GFAP (red) and Hoechst nuclear stain (blue). Note that the CD11b positive cells have infiltrated great distances into the parenchyma at 4 days post injury, but are compacted by a dense glial scar toward the lesion core by 4 weeks. Scale bar : 200 μ m.

Chapter 4, figure 2

**BMP signaling is active during reactive gliosis after spinal cord contusion injury.**

a. Panels represent uninjured cord versus 4 days, 1 week and 5 weeks post injury. At 4 and 7 days, the reactive astrocytes display long processes (arrowheads). By 5 weeks there is a definite increase in the number of astrocytes at the lesion site. **b.** Transcript levels of GFAP (normalized to GAPDH) fold changes are compared to levels in uninjured controls. **c.** Transcript levels of BMP4 (blue bars) and BMP7 (red bars) were normalized to GAPDH and expressed as fold changes as in **b.** **d.** At 4 days post SCI, nuclear phospho SMAD 1/5/8 (green), is seen in some, GFAP+ astrocytes (red). **e.** Same as (d), shows that BrdU (green), and nuclear phospho SMAD 1/5/8 (red) are exclusive from one another. GFAP + Astrocytes (blue) that are BrdU positive (arrowheads) have weak or low levels of nuclear phospho SMAD. (Scale bar in a,d,e: 20 μ m).

Chapter 4, figure 3

**b**

Animal	BMPR1a (cycle #)	BMPR1b (cycle #)	GAPDH (cycle #)	BMPR1a (cycle diff from GAPDH)	BMPR1b (cycle diff from GAPDH)
1	23.19	25.95	15.32	7.87	10.63
2	24.4	27.43	16.07	8.33	11.36
3	23.27	26.25	15.38	7.89	10.87

BMPR1a is more abundant than BMPR1b in the adult spinal cord.

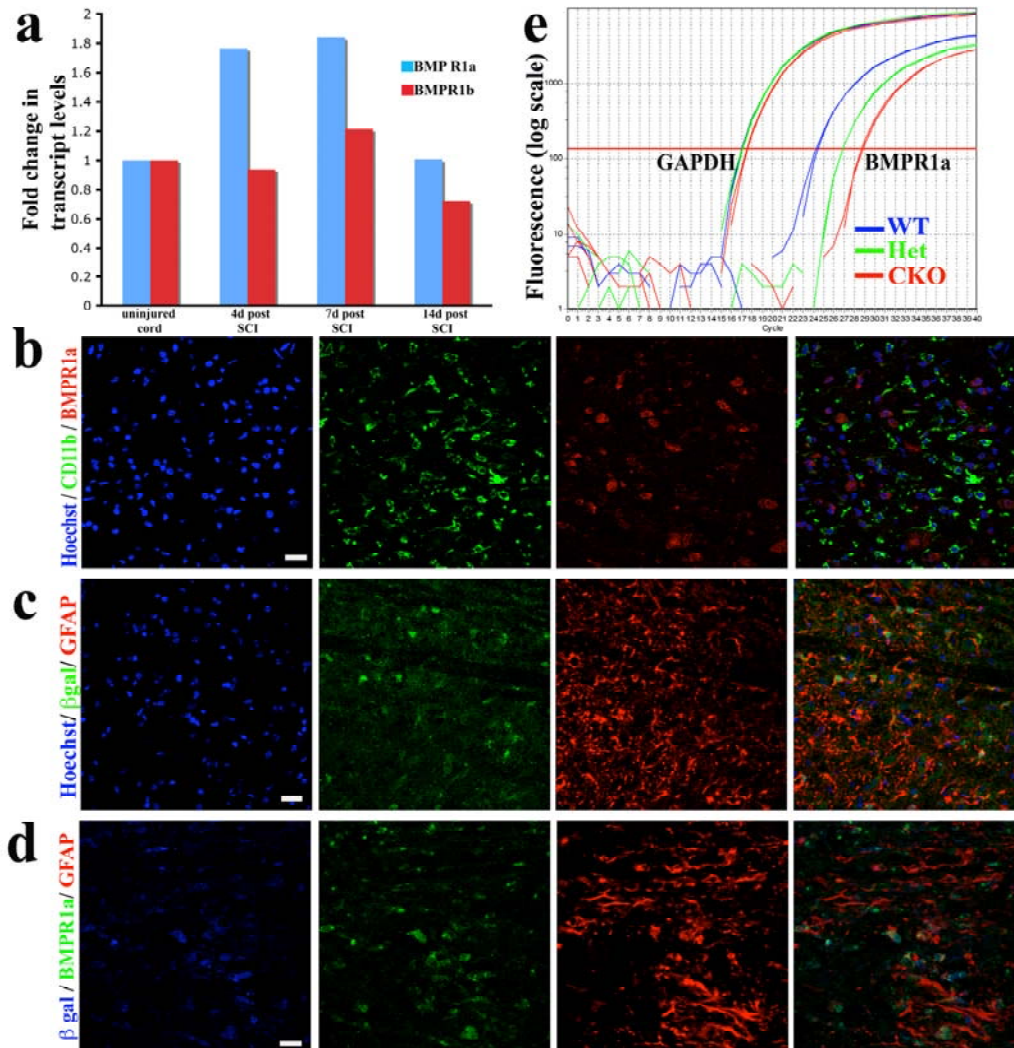
a. Real time PCR amplification plots from RNA extracted from an adult spinal cord showing higher levels of BMPR1a (red plots) versus BMPR1b(blue plots)

b. Different primer sets from (a) were used and the cycle numbers for BMPR1a, BMPr1b and GAPDH from three different adult spinal cords are shown. Again, the levels of BMPR1a transcripts are higher than BMPR1b.

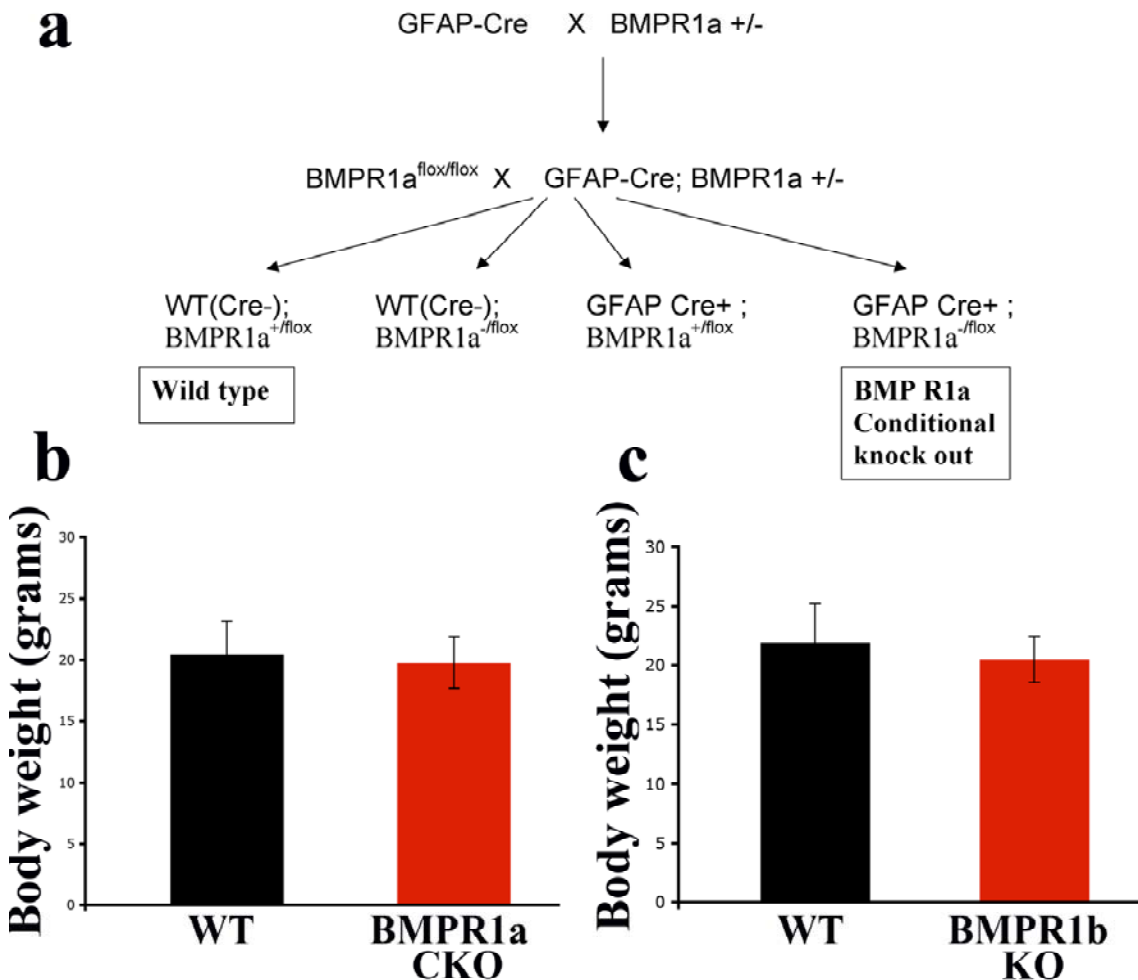
Chapter 4, figure 4**BMPR1a receptor is expressed on reactive astrocytes and not on inflammatory cells.**

a. Transcript levels of BMPR1a (blue bars) and BMPR1b (red bars) were normalized to GAPDH and expressed as fold changes compared to levels in uninjured controls. **b.** Injured spinal cord sections at 4 days post injury stained with Hoechst nuclear stain (blue), Cd11b (green) and BMPR1a (red). Note that the receptor staining does not overlap with the CD11b. **c.** Injured cord (in b) stained with Hoechst nuclear stain (blue), beta galactosidase (green) and GFAP (red) showing that all the beta gal positive cells are in GFAP positive astrocytes. **d.** Sections in b,c stained with beta galactosidase (blue), BMPR1a (green) and GFAP (red). The β gal staining clearly outlines the astrocytic soma, which stains for BMPR1a. **e.** Real time RT-PCR for exon2 of BMPR1a from total RNA extracted from spinal cords of WT, GFAP cre; BMPR1a^{flox/+} (het) and GFAP Cre; BMPR1a^{flox/-} (CKO) mice. GAPDH serves as a loading control. There is a ~4-cycle reduction in the transcript levels of the floxed exon2. (Scale bars in b,c,d : 20 μ m)

Chapter 4, figure 4



Chapter 4, figure 5

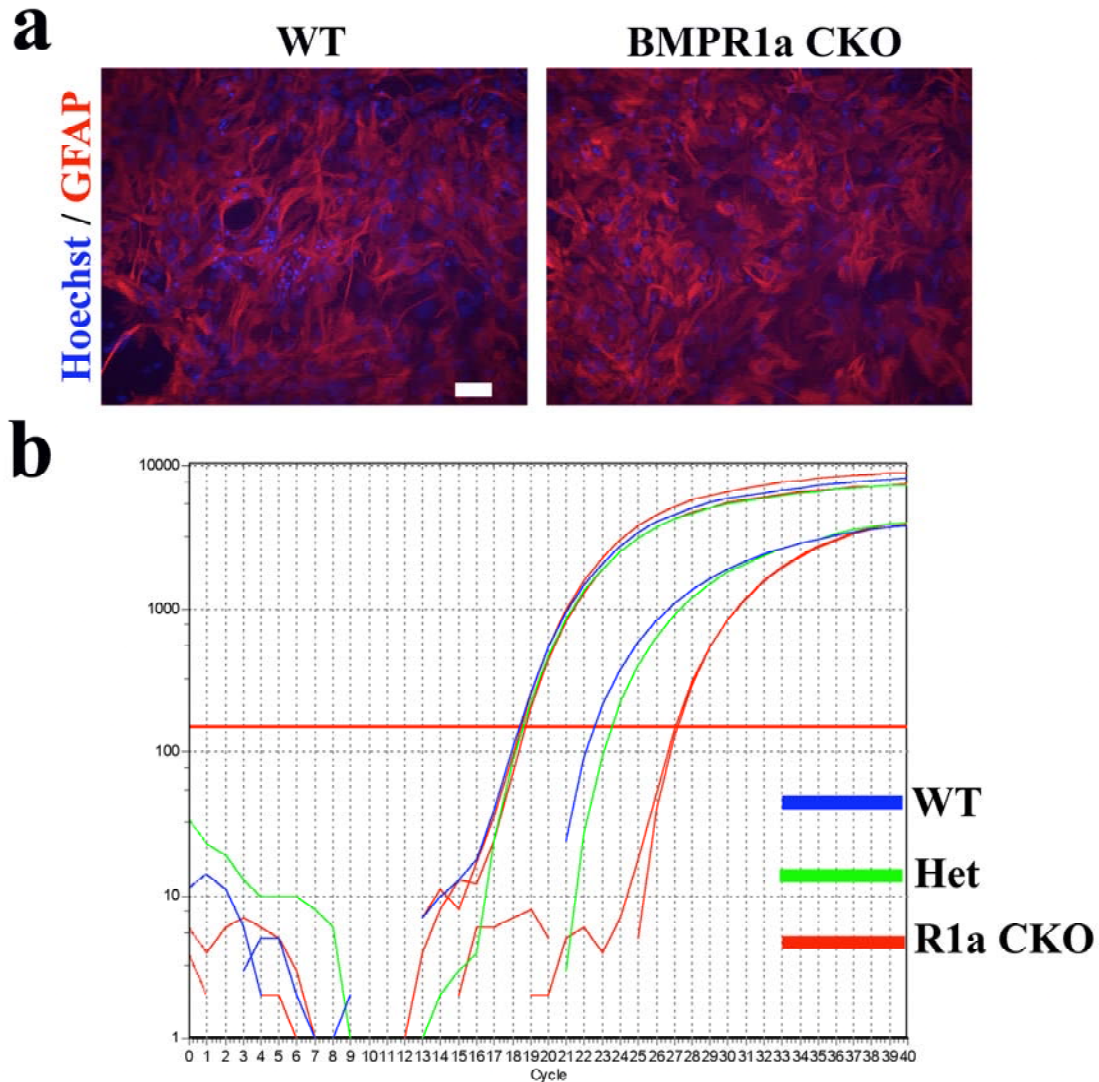
**Strategy to obtain BMPR1a conditional knock out mice**

a. Mating strategy to obtain conditional BMPR1a knock out (BMPR1a CKO) mice.

b. Body weights of 2 month old WT and BMPR1a CKO mice shows no difference between the groups. (n= 24 WT and 31 BMPR1a CKO animals). Graphs are average \pm s.e.m.

c. Body weights of 2 month old WT and BMPR1b KO mice. (n=23 WT and 27 BMPR1b KO animals). Graphs are average weight \pm s.e.m

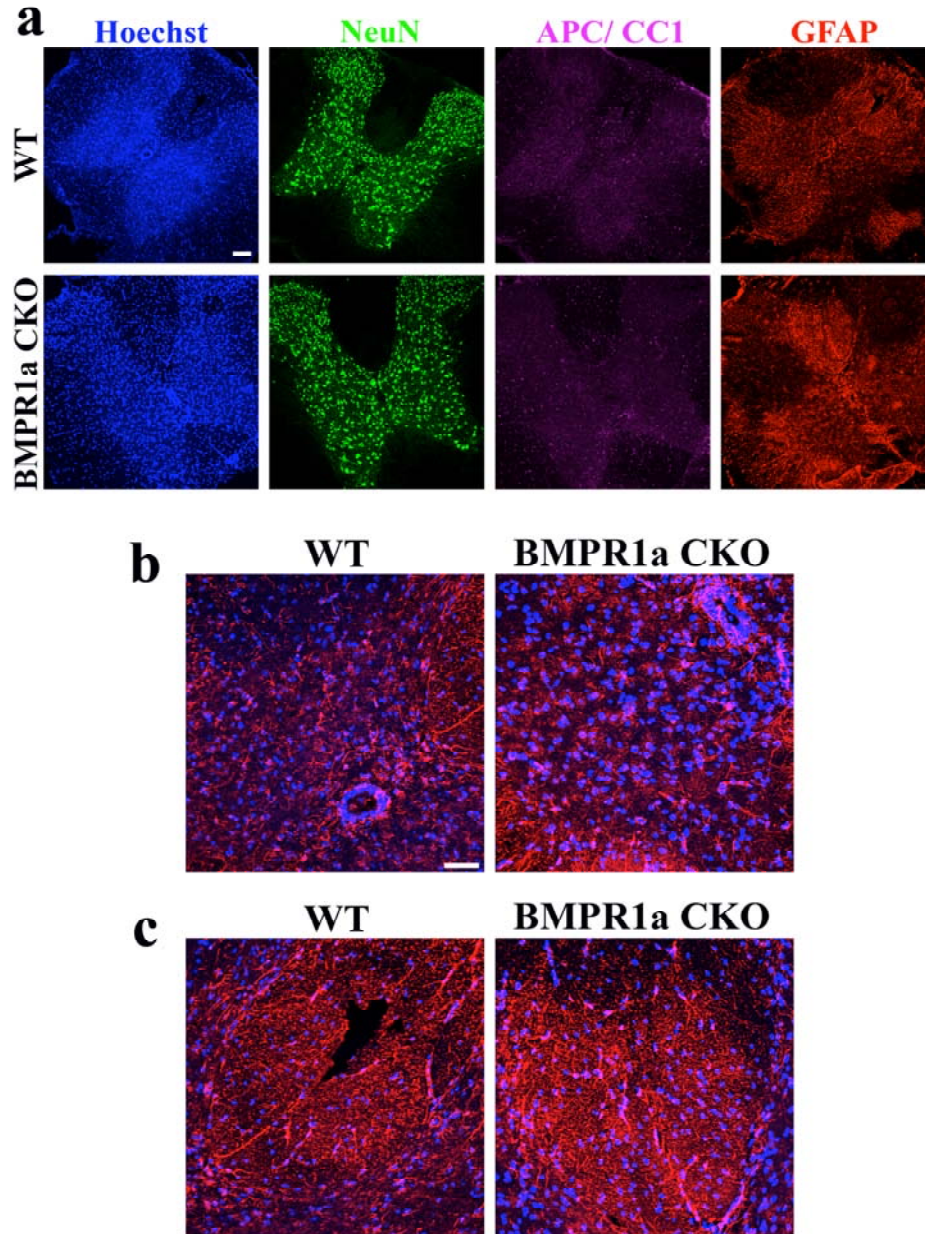
Chapter 4, figure 6

**BMPR1a CKO astrocytes develop normally**

a. Astrocyte monolayers derived from brains of 2 day old WT and BMPR1a CKO animals stained for GFAP (red) and Hoechst nuclear stain (blue). Scale bar : 50 μ m.

b. Real time PCR amplification plots for exon2 of the BMPR1a from the astrocyte monolayers derived from WT, GFAP cre; BMPR1a^{flox/+} (Het), and GFAP Cre; BMPR1a^{flox/-} (BMPR1a CKO) brains.

Chapter 4, figure 7

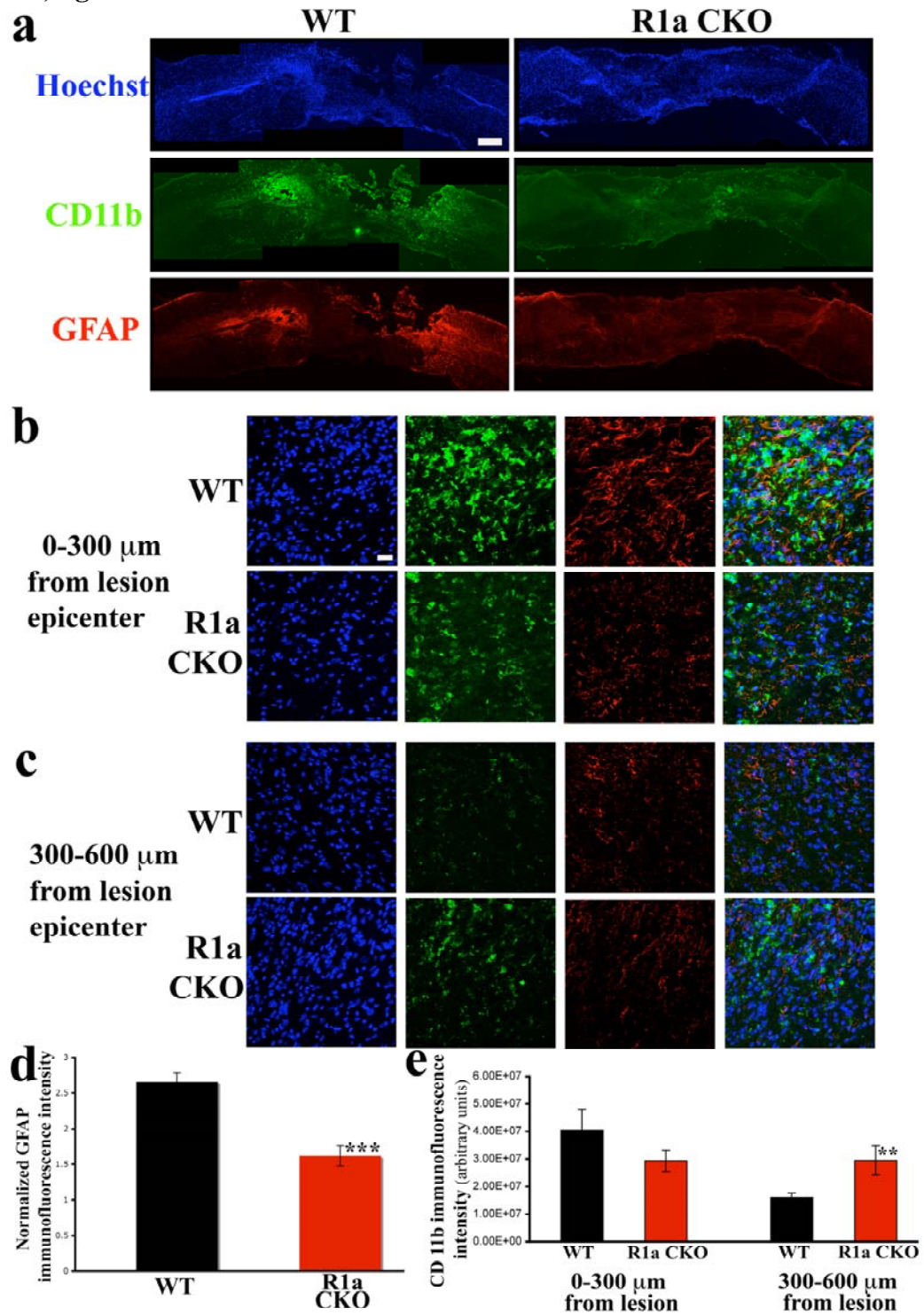


Normal distribution of neurons, astrocytes and oligodendrocytes in BMPR1a CKO spinal cords **a.** Spinal cord cross sections from 2 month old WT and BMPR1a CKO animals stained for neurons-NeuN (green), oligodendrocytes - APC/CC1 (pink), astrocytes – GFAP (red) and Hoechst nuclear stain. Scale bar : 100 μ m. **b.** Higher magnification images of gray matter astrocytes (abutting the central canal) in WT and BMPR1a CKO spinal cords. **c.** Higher magnification images of white matter astrocytes (in the dorsal funiculus) in WT and BMPR1a CKO spinal cords. Scale bar in b,c: 50 μ m

Chapter 4, figure 8**BMPR1a Conditional knock out mice show defective gliosis and increased inflammatory infiltration after spinal cord injury.**

a. Low magnification (10X) montages of longitudinal sections of the injured spinal cord at 1 week post injury from BMPR1a WT and CKO mice stained with Hoechst nuclear stain (blue), CD11b (green) and GFAP (red). Rostral is to the left and dorsal to the top of the images. WT cords show intense GFAP staining at the edge of the lesion indicating reactive gliosis, that is not observed in the BMPR1aCKO mice. The glial scar in the WT mice has in turn condensed the CD11b positive inflammatory cells toward the lesion (intense green seen in and around the GFAP stain while the CD11b positive cells are still diffusely spread throughout the parenchyma in the BMPR1b KO mice. (Scale bar : 200 μ m) **b.** Higher magnification (40X) images taken from the spinal cord sections in (a) (which is to the right of the images). Note that there is intense CD11b staining in this area in the WT mice and the astrocytes have extended long processes. The astrocytes in the BMPR1a CKO mice have smaller, thinner processes. **c.** 40 X images of sections in (a) taken in the region spanning 300-600 μ m from the edge of the lesion. Note the increased CD11b staining that persists in this area in the BMPR1a CKO mice that is comparable to the levels seen in b. (Scale bars in b,c:20 μ m) **d.** Quantification of GFAP intensity in (b) expressed as fold increases over uninjured spinal cord controls. (***) $p < 0.00001$ by student's unpaired t test) **e.** Quantification of the CD11b staining intensity in the regions described in b,c in WT and BMPR1aCKO mice. There is a significantly higher CD11b staining in the region 300-600 μ m from the lesion edge. (***) $p < 0.0039$ by student's unpaired t test)

Chapter 4, figure 8

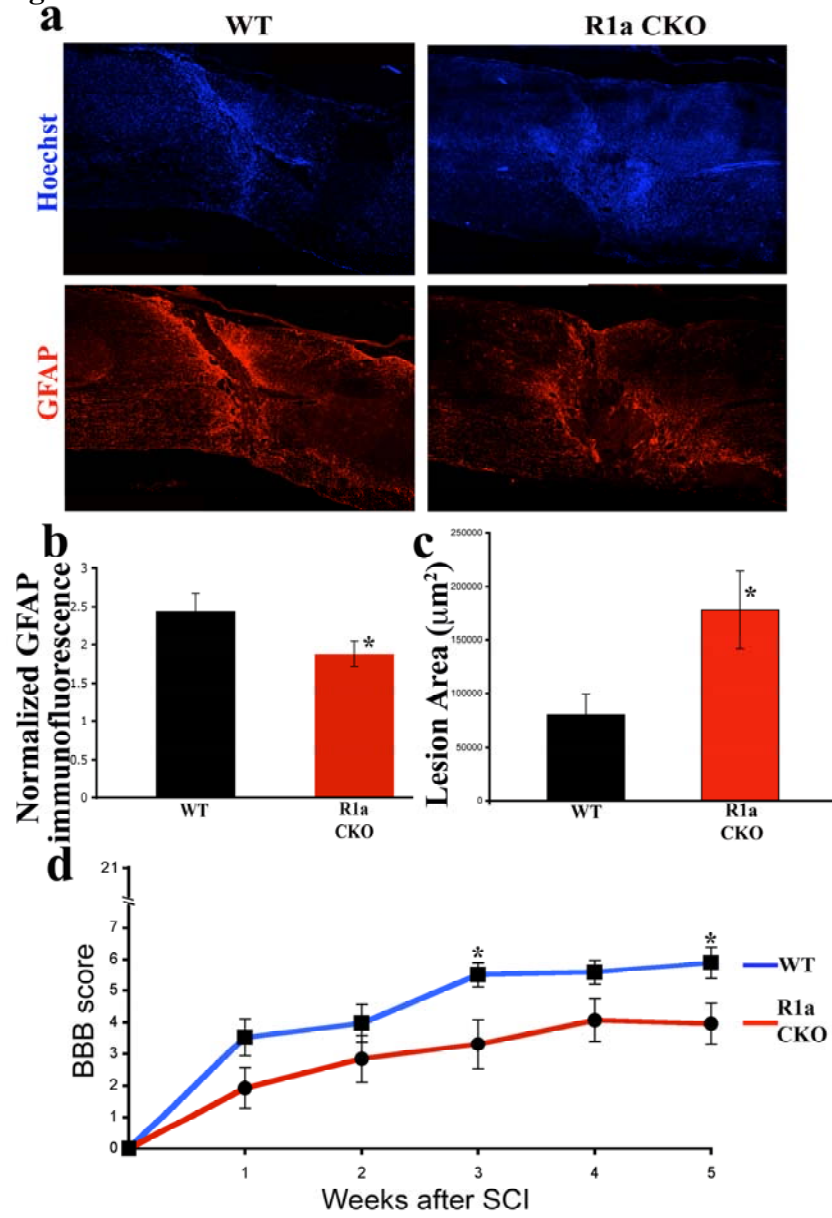


Chapter 4, figure 9

BMPR1a Conditional knock out mice have reduced gliosis and increased lesion volumes in the chronic injured spinal cord and show worsened locomotor recovery.

a. WT and BMPR1a CKO spinal cords at 5 weeks post injury, stained with Hoechst nuclear stain (blue) and GFAP (red). (Scale bar : 200 μ m) **b.** Quantification of GFAP intensity expressed as fold increases over uninjured spinal cord controls. (* $p < 0.06$, by student's unpaired t test) **c.** Quantification of the GFAP negative area flanked by reactive astrocytes in μm^2 . **d.** BBB scores of WT and BMPR1a CKO mice at weekly intervals after injury. The KO animals have significantly lower scores at 5 weeks post injury (WT: 5.89 ± 0.4 , KO: 4.0 ± 0.7 , * $p < 0.05$ by student's unpaired t test, $n = 15$ WT, $n = 12$ R1aCKO animals)

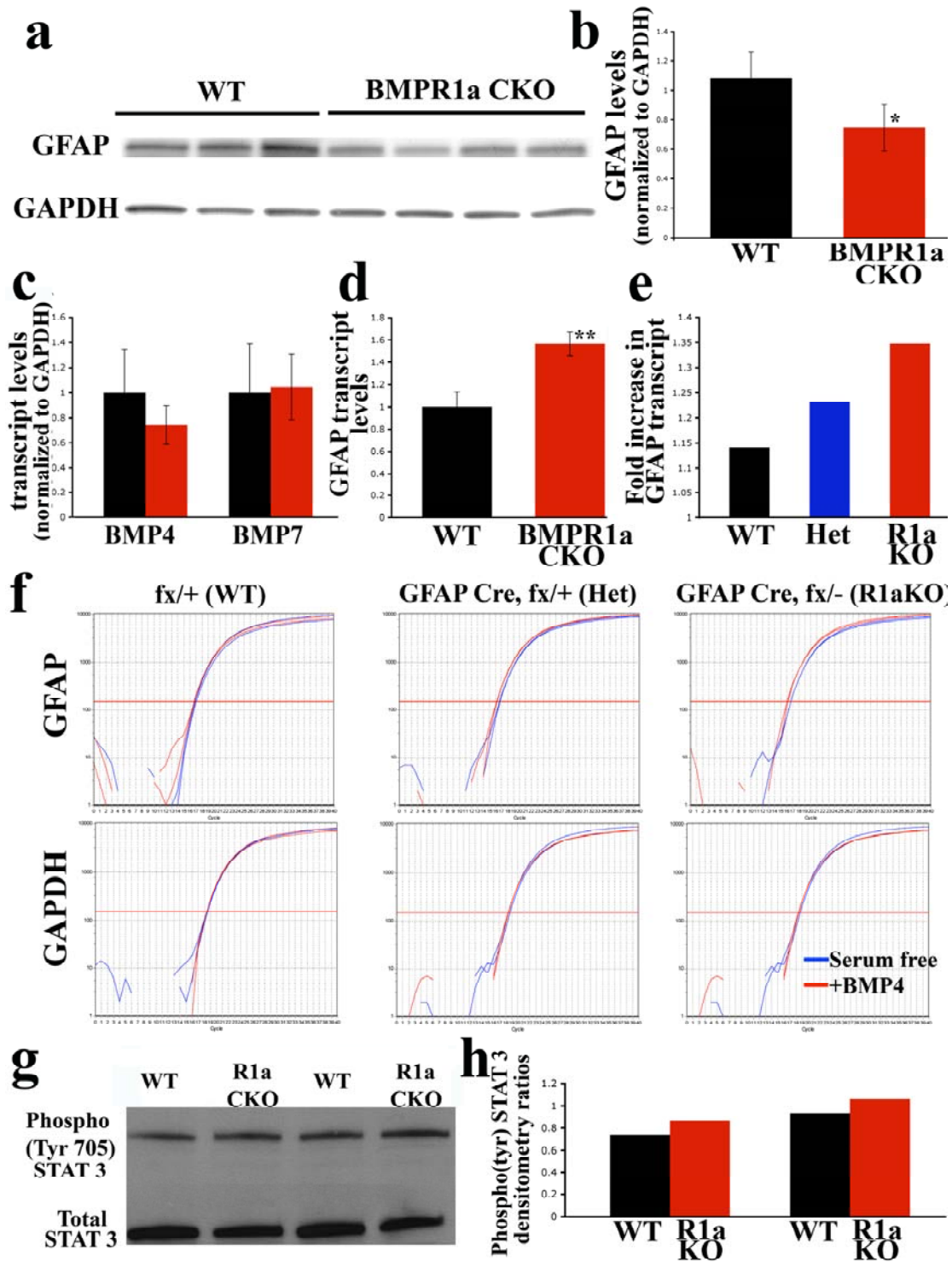
Chapter 4, figure 9



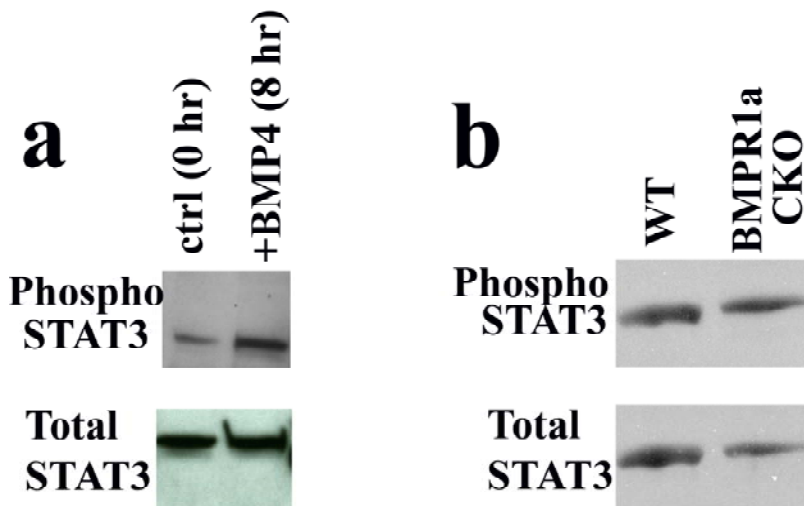
Chapter 4, figure 10**BMPR1a signaling affects post-transcriptional regulation of GFAP.**

a. Western blots for GFAP protein in injured cords from WT and BMPR1a CKO mice at 6 days post SCI. The blot was stripped and re-probed for GAPDH (loading control) **b.** Densitometric analysis of the blot shown in (a) showing reduced levels of GFAP in BMPR1a KO animals. (* $p < 0.06$, by Student's unpaired t test) **c.** Normalized transcript levels of BMP4 and BMP7 in cords from WT and BMPR1a CKO mice at 6 days post SCI showing no significant difference between the groups. **d.** Normalized GFAP transcript levels in the same groups as (a,c) showing significant increase in the BMPR1a CKO mice (* $p < 0.005$ by student's unpaired t test). **e.** Fold increase in GFAP transcript levels upon BMP4 treatment (see methods) in astrocyte monolayers derived from WT, GFAP Cre, BMPR1a $fx/+$ (Het) and GFAP Cre, BMPR1a $fx/-$ (KO) mouse brains. **f.** Real time PCR amplification plots for GFAP and GAPDH in the groups described in (e). Note the increase in the levels of GFAP does occur in the KO animals in BMP4 treated astrocytes (red trace) over serum-free controls (blue trace). **g.** Western blot analysis for Phospho (Tyr) STAT3 and total STAT3 in injured cords from 2 sets of littermates of WT and BMPR1a KO animals at 4 days post SCI. Activated STAT3 is present in the BMPR1a CKO mice. **h.** Densitometric analysis of the individual littermate pairs showing a slight increase in the levels of phospho STAT3 as normalized to total STAT3 in the cords from BMPR1a CKO animals.

Chapter 4, figure 10



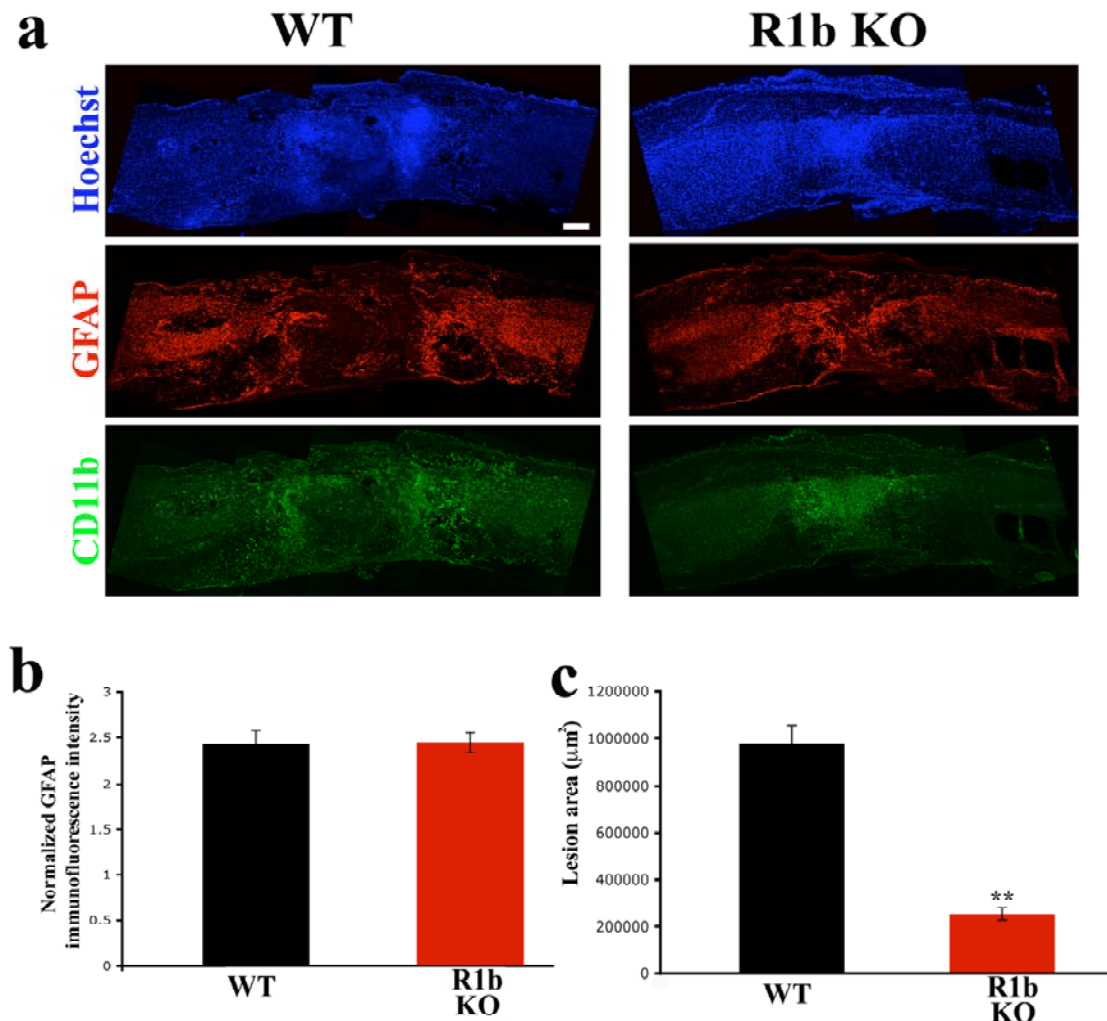
Chapter 4, figure 11

**BMPR1a signaling is not required for STAT3 activation by BMP4 in neural progenitor cells.**

a. Western Blot analysis for Phospho (Tyr 705) STAT3 and total STAT3 on protein extracts from post natal neurospheres. After 8 hours of BMP4 treatment, there is an increase in the levels of phosphorylated STAT3.

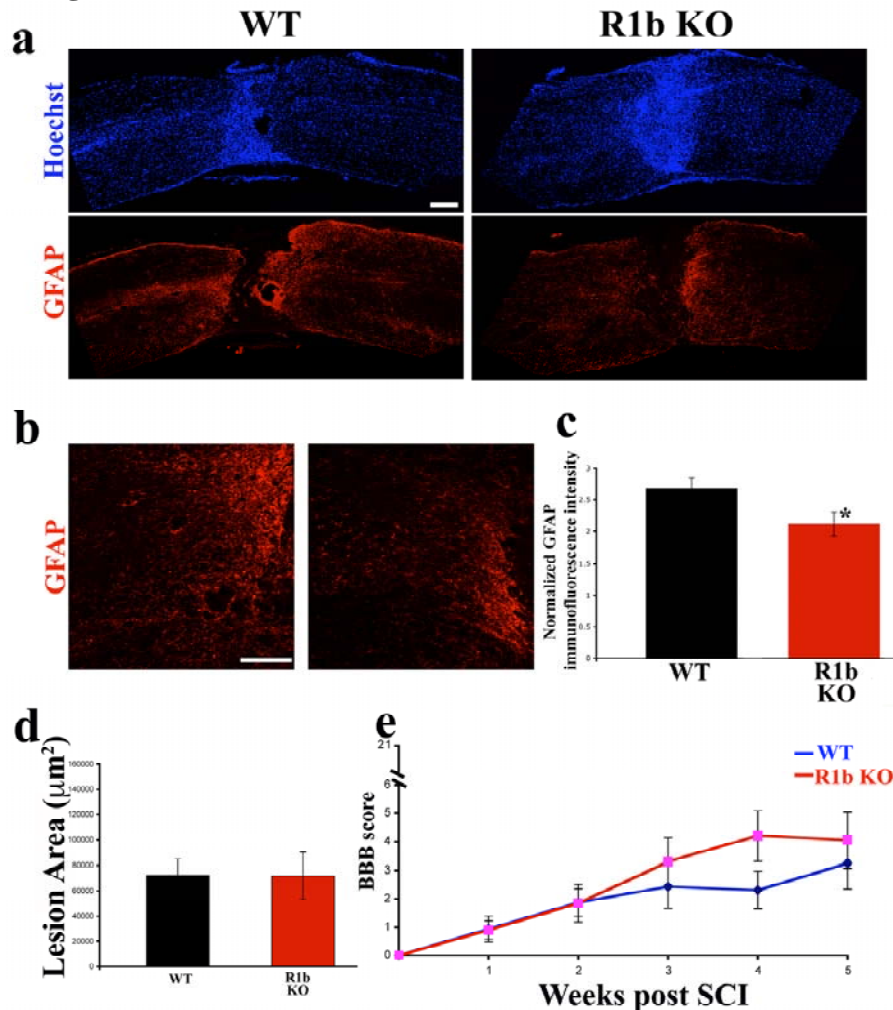
b. 8 hour treatment with BMP4 on neurospheres described above obtained from WT and BMPR1a CKO mice. Note that the activation of STAT3 is still present in the BMPR1a CKO derived neurospheres.

Chapter 4, figure 12

**BMPR1b knock out mice have reduced lesion volumes after spinal cord injury.**

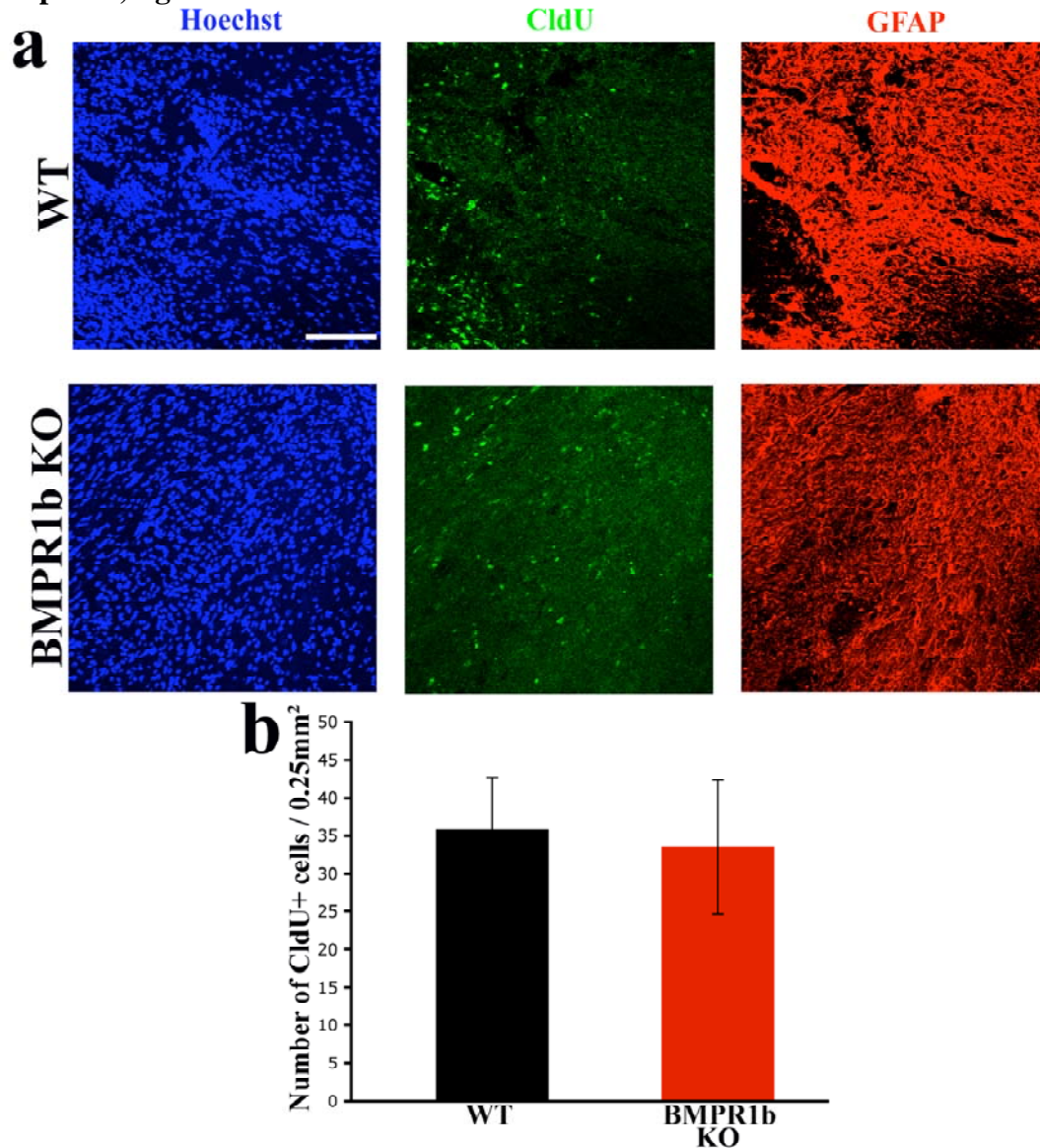
a. Low magnification(10X) montages of longitudinal sections from WT and BMPR1b KO mice at 1 week post injury, stained with Hoechst nuclear stain(blue), CD11b (green) and GFAP (red). Note that the glial scar develops normally at the edge of the lesion in the KO mice. However, the area compacted between the wall of reactive astrocytes is smaller in the KO. Cd11b positive cells have already been largely compacted into this area while this region continues to be mostly acellular in the WT mice as evidenced by the Hoechst stain. (Scale bar : 200 μm). **b.** Quantification of GFAP intensity in the area immediately adjacent to the lesion edge in (a) expressed as fold increases over uninjured spinal cord controls shows no difference between WT and BMPR1bKO . **c.** Quantification of the GFAP negative area flanked by reactive astrocytes in μm^2 . (** $p < 0.00001$ by student's unpaired t test)

Chapter 4, figure 13



BMPR1b knock out mice have reduced glial scar and normal functional recovery after spinal cord injury. **a.** Low magnification (10X) montages of spinal cords from WT and BMPR1b KO mice at 5 weeks post injury, stained with Hoechst nuclear stain (blue) and GFAP (red). There are fewer astrocytes adjacent to the lesion in the KO. (Scale bar: 200µm) **b.** Higher magnification (20X) images of area boxed in a, showing fewer astrocytes in the glial scar in BMPR1b KO mice. (Scale bar: 100µm) **c.** Quantification of GFAP intensity in the area immediately adjacent to the lesion edge in (b) shows a significant reduction in BMPR1bKO mice. (* $p < 0.03$, by student's unpaired t test) **d.** Quantification of the GFAP negative lesion area in WT and BMPR1b KO mice at 5 weeks post injury shows no difference between the groups. **e.** BBB scores of WT and BMPR1b mice at weekly intervals after injury.

Chapter 4, figure 14



BMPR1b KO animals do not show deficits in proliferation in the sub acute phase of spinal cord injury

a. WT and BMPR1b KO animals were given 1 pulse of CldU per day for 7 days beginning from day 7 to day 14 post injury and sacrificed at 5 weeks post injury. Representative images from both groups are shown stained for GFAP (red) and CldU (green). (Scale bar : 100 μ m)

b. Numbers of CldU cells in either groups that were counted in the area of the glial scar spanning a distance of 500 μ m from the edge of the lesion both rostral and caudal to it. There is no difference between the groups.

REFERENCES

- Adrian EK, Jr., Walker BE (1962) Incorporation of thymidine-H3 by cells in normal and injured mouse spinal cord. J Neuropathol Exp Neurol 21:597-609.**
- Ahmed S, Reynolds BA, Weiss S (1995) BDNF enhances the differentiation but not the survival of CNS stem cell-derived neuronal precursors. J Neurosci 15:5765-5778.**
- Alvarez-Buylla A, Garcia-Verdugo JM, Tramontin AD (2001) A unified hypothesis on the lineage of neural stem cells. Nat Rev Neurosci 2:287-293.**
- Araya R, Kudo M, Kawano M, Ishii K, Hashikawa T, Iwasato T, Itohara S, Terasaki T, Oohira A, Mishina Y, Yamada M (2008) BMP signaling through BMPRIA in astrocytes is essential for proper cerebral angiogenesis and formation of the blood-brain-barrier. Mol Cell Neurosci 38:417-430.**
- Balasingam V, Tejada-Berges T, Wright E, Bouckova R, Yong VW (1994) Reactive astrogliosis in the neonatal mouse brain and its modulation by cytokines. J Neurosci 14:846-856.**
- Baldwin SA, Scheff SW (1996) Intermediate filament change in astrocytes following mild cortical contusion. Glia 16:266-275.**
- Balentine JD (1988) Spinal cord trauma: in search of the meaning of granular axoplasm and vesicular myelin. J Neuropathol Exp Neurol 47:77-92.**
- Barnabe-Heider F, Frisen J (2008) Stem cells for spinal cord repair. Cell Stem Cell 3:16-24.**
- Basso DM, Beattie MS, Bresnahan JC (1996a) Graded histological and locomotor outcomes after spinal cord contusion using the NYU weight-drop device versus transection. Exp Neurol 139:244-256.**
- Basso DM, Beattie MS, Bresnahan JC, Anderson DK, Faden AI, Gruner JA, Holford TR, Hsu CY, Noble LJ, Nockels R, Perot PL, Salzman SK, Young W (1996b) MASCIS evaluation of open field locomotor scores: effects of experience and teamwork on reliability. Multicenter Animal Spinal Cord Injury Study. J Neurotrauma 13:343-359.**

- Bauer S, Patterson PH (2006) Leukemia inhibitory factor promotes neural stem cell self-renewal in the adult brain. J Neurosci 26:12089-12099.**
- Beattie MS, Harrington AW, Lee R, Kim JY, Boyce SL, Longo FM, Bresnahan JC, Hempstead BL, Yoon SO (2002) ProNGF induces p75-mediated death of oligodendrocytes following spinal cord injury. Neuron 36:375-386.**
- Blight AR (1992) Macrophages and inflammatory damage in spinal cord injury. J Neurotrauma 9 Suppl 1:S83-91.**
- Bonaguidi MA, McGuire T, Hu M, Kan L, Samanta J, Kessler JA (2005) LIF and BMP signaling generate separate and discrete types of GFAP-expressing cells. Development 132:5503-5514.**
- Bonaguidi MA, Peng CY, McGuire T, Falciglia G, Gobeske KT, Czeisler C, Kessler JA (2008) Noggin expands neural stem cells in the adult hippocampus. J Neurosci 28:9194-9204.**
- Bonni A, Sun Y, Nadal-Vicens M, Bhatt A, Frank DA, Rozovsky I, Stahl N, Yancopoulos GD, Greenberg ME (1997) Regulation of gliogenesis in the central nervous system by the JAK-STAT signaling pathway. Science 278:477-483.**
- Bradbury EJ, Moon LD, Popat RJ, King VR, Bennett GS, Patel PN, Fawcett JW, McMahon SB (2002) Chondroitinase ABC promotes functional recovery after spinal cord injury. Nature 416:636-640.**
- Brederlau A, Faigle R, Elmi M, Zarebski A, Sjoberg S, Fujii M, Miyazono K, Funa K (2004) The bone morphogenetic protein type Ib receptor is a major mediator of glial differentiation and cell survival in adult hippocampal progenitor cell culture. Mol Biol Cell 15:3863-3875.**
- Buffo A, Rite I, Tripathi P, Lepier A, Colak D, Horn AP, Mori T, Gotz M (2008) Origin and progeny of reactive gliosis: A source of multipotent cells in the injured brain. Proc Natl Acad Sci U S A 105:3581-3586.**
- Bunge MB (2001) Bridging areas of injury in the spinal cord. Neuroscientist 7:325-339.**

- Busch SA, Silver J (2007) The role of extracellular matrix in CNS regeneration. *Curr Opin Neurobiol* 17:120-127.**
- Bush TG, Puvanachandra N, Horner CH, Polito A, Ostenfeld T, Svendsen CN, Mucke L, Johnson MH, Sofroniew MV (1999) Leukocyte infiltration, neuronal degeneration, and neurite outgrowth after ablation of scar-forming, reactive astrocytes in adult transgenic mice. *Neuron* 23:297-308.**
- Cahoy JD, Emery B, Kaushal A, Foo LC, Zamanian JL, Christopherson KS, Xing Y, Lubischer JL, Krieg PA, Krupenko SA, Thompson WJ, Barres BA (2008) A transcriptome database for astrocytes, neurons, and oligodendrocytes: a new resource for understanding brain development and function. *J Neurosci* 28:264-278.**
- Calderwood DA, Shattil SJ, Ginsberg MH (2000) Integrins and actin filaments: reciprocal regulation of cell adhesion and signaling. *J Biol Chem* 275:22607-22610.**
- Caley DW, Maxwell DS (1968) An electron microscopic study of neurons during postnatal development of the rat cerebral cortex. *J Comp Neurol* 133:17-44.**
- Campos LS, Leone DP, Relvas JB, Brakebusch C, Fassler R, Suter U, French-Constant C (2004) Beta1 integrins activate a MAPK signalling pathway in neural stem cells that contributes to their maintenance. *Development* 131:3433-3444.**
- Cattaneo E, McKay R (1990) Proliferation and differentiation of neuronal stem cells regulated by nerve growth factor. *Nature* 347:762-765.**
- Chang MY, Park CH, Son H, Lee YS, Lee SH (2004) Developmental stage-dependent self-regulation of embryonic cortical precursor cell survival and differentiation by leukemia inhibitory factor. *Cell Death Differ* 11:985-996.**
- Chen J, Leong SY, Schachner M (2005) Differential expression of cell fate determinants in neurons and glial cells of adult mouse spinal cord after compression injury. *Eur J Neurosci* 22:1895-1906.**
- Cheng X, Wang Y, He Q, Qiu M, Whittemore SR, Cao Q (2007) Bone morphogenetic protein signaling and olig1/2 interact to regulate the differentiation and maturation of adult oligodendrocyte precursor cells. *Stem Cells* 25:3204-3214.**

- Crowe MJ, Bresnahan JC, Shuman SL, Masters JN, Beattie MS (1997) Apoptosis and delayed degeneration after spinal cord injury in rats and monkeys. *Nat Med* 3:73-76.**
- Dimou L, Simon C, Kirchhoff F, Takebayashi H, Gotz M (2008) Progeny of Olig2-expressing progenitors in the gray and white matter of the adult mouse cerebral cortex. *J Neurosci* 28:10434-10442.**
- Doetsch F, Caille I, Lim DA, Garcia-Verdugo JM, Alvarez-Buylla A (1999) Subventricular zone astrocytes are neural stem cells in the adult mammalian brain. *Cell* 97:703-716.**
- Dumont RJ, Okonkwo DO, Verma S, Hurlbert RJ, Boulos PT, Ellegala DB, Dumont AS (2001) Acute spinal cord injury, part I: pathophysiologic mechanisms. *Clin Neuropharmacol* 24:254-264.**
- Ebendal T, Bengtsson H, Soderstrom S (1998) Bone morphogenetic proteins and their receptors: potential functions in the brain. *J Neurosci Res* 51:139-146.**
- Emery E, Aldana P, Bunge MB, Puckett W, Srinivasan A, Keane RW, Bethea J, Levi AD (1998) Apoptosis after traumatic human spinal cord injury. *J Neurosurg* 89:911-920.**
- Enzmann GU, Benton RL, Woock JP, Howard RM, Tsoulfas P, Whitemore SR (2005) Consequences of noggin expression by neural stem, glial, and neuronal precursor cells engrafted into the injured spinal cord. *Exp Neurol* 195:293-304.**
- Faulkner JR, Herrmann JE, Woo MJ, Tansey KE, Doan NB, Sofroniew MV (2004) Reactive astrocytes protect tissue and preserve function after spinal cord injury. *J Neurosci* 24:2143-2155.**
- Fawcett JW, Asher RA (1999) The glial scar and central nervous system repair. *Brain Res Bull* 49:377-391.**
- Filbin MT (2003) Myelin-associated inhibitors of axonal regeneration in the adult mammalian CNS. *Nat Rev Neurosci* 4:703-713.**
- Fitch MT, Doller C, Combs CK, Landreth GE, Silver J (1999) Cellular and molecular mechanisms of glial scarring and progressive cavitation: in vivo and in vitro analysis of inflammation-induced secondary injury after CNS trauma. *J Neurosci* 19:8182-8198.**

- Frade JM, Barde YA (1998) Microglia-derived nerve growth factor causes cell death in the developing retina. *Neuron* 20:35-41.**
- Frederiksen K, McKay RD (1988) Proliferation and differentiation of rat neuroepithelial precursor cells in vivo. *J Neurosci* 8:1144-1151.**
- Friedlander DR, Milev P, Karthikeyan L, Margolis RK, Margolis RU, Grumet M (1994) The neuronal chondroitin sulfate proteoglycan neurocan binds to the neural cell adhesion molecules Ng-CAM/L1/NILE and N-CAM, and inhibits neuronal adhesion and neurite outgrowth. *J Cell Biol* 125:669-680.**
- Frisen J, Johansson CB, Lothian C, Lendahl U (1998) Central nervous system stem cells in the embryo and adult. *Cell Mol Life Sci* 54:935-945.**
- Frisen J, Johansson CB, Torok C, Risling M, Lendahl U (1995) Rapid, widespread, and longlasting induction of nestin contributes to the generation of glial scar tissue after CNS injury. *J Cell Biol* 131:453-464.**
- Fukuda S, Abematsu M, Mori H, Yanagisawa M, Kagawa T, Nakashima K, Yoshimura A, Taga T (2007) Potentiation of astroglialogenesis by STAT3-mediated activation of bone morphogenetic protein-Smad signaling in neural stem cells. *Mol Cell Biol* 27:4931-4937.**
- Gage FH, Ray J, Fisher LJ (1995) Isolation, characterization, and use of stem cells from the CNS. *Annu Rev Neurosci* 18:159-192.**
- Gaiano N, Kohtz JD, Turnbull DH, Fishell G (1999) A method for rapid gain-of-function studies in the mouse embryonic nervous system. *Nat Neurosci* 2:812-819.**
- Garcia AD, Doan NB, Imura T, Bush TG, Sofroniew MV (2004) GFAP-expressing progenitors are the principal source of constitutive neurogenesis in adult mouse forebrain. *Nat Neurosci* 7:1233-1241.**
- Gates MA, Thomas LB, Howard EM, Laywell ED, Sajin B, Faissner A, Gotz B, Silver J, Steindler DA (1995) Cell and molecular analysis of the developing and adult mouse subventricular zone of the cerebral hemispheres. *J Comp Neurol* 361:249-266.**
- Giancotti FG (1997) Integrin signaling: specificity and control of cell survival and cell cycle progression. *Curr Opin Cell Biol* 9:691-700.**

- Giancotti FG, Ruoslahti E (1999) Integrin signaling. Science 285:1028-1032.**
- Goldman S (2003) Glia as neural progenitor cells. Trends Neurosci 26:590-596.**
- Goldshmit Y, Galea MP, Wise G, Bartlett PF, Turnley AM (2004) Axonal regeneration and lack of astrocytic gliosis in EphA4-deficient mice. J Neurosci 24:10064-10073.**
- Gomes WA, Mehler MF, Kessler JA (2003) Transgenic overexpression of BMP4 increases astroglial and decreases oligodendroglial lineage commitment. Dev Biol 255:164-177.**
- Gotz M, Steindler D (2003) To be glial or not-how glial are the precursors of neurons in development and adulthood? Glia 43:1-3.**
- Gregg C, Weiss S (2005) CNTF/LIF/gp130 receptor complex signaling maintains a VZ precursor differentiation gradient in the developing ventral forebrain. Development 132:565-578.**
- Gross RE, Mehler MF, Mabie PC, Zang Z, Santschi L, Kessler JA (1996) Bone morphogenetic proteins promote astroglial lineage commitment by mammalian subventricular zone progenitor cells. Neuron 17:595-606.**
- Gulacsi A, Lillien L (2003) Sonic hedgehog and bone morphogenetic protein regulate interneuron development from dorsal telencephalic progenitors in vitro. J Neurosci 23:9862-9872.**
- Hall AK, Miller RH (2004) Emerging roles for bone morphogenetic proteins in central nervous system glial biology. J Neurosci Res 76:1-8.**
- Hall DE, Reichardt LF, Crowley E, Holley B, Moezzi H, Sonnenberg A, Damsky CH (1990) The alpha 1/beta 1 and alpha 6/beta 1 integrin heterodimers mediate cell attachment to distinct sites on laminin. J Cell Biol 110:2175-2184.**
- Hartgerink JD, Beniash E, Stupp SI (2001) Self-assembly and mineralization of peptide-amphiphile nanofibers. Science 294:1684-1688.**
- Hartgerink JD, Beniash E, Stupp SI (2002) Peptide-amphiphile nanofibers: a versatile scaffold for the preparation of self-assembling materials. Proc Natl Acad Sci U S A 99:5133-5138.**

- He F, Ge W, Martinowich K, Becker-Catania S, Coskun V, Zhu W, Wu H, Castro D, Guillemot F, Fan G, de Vellis J, Sun YE (2005) A positive autoregulatory loop of Jak-STAT signaling controls the onset of astroglialogenesis. *Nat Neurosci* 8:616-625.**
- Heldin CH, Miyazono K, ten Dijke P (1997) TGF-beta signalling from cell membrane to nucleus through SMAD proteins. *Nature* 390:465-471.**
- Herrmann JE, Imura T, Song B, Qi J, Ao Y, Nguyen TK, Korsak RA, Takeda K, Akira S, Sofroniew MV (2008) STAT3 is a critical regulator of astroglialosis and scar formation after spinal cord injury. *J Neurosci* 28:7231-7243.**
- Hjertner O, Hjorth-Hansen H, Borset M, Seidel C, Waage A, Sundan A (2001) Bone morphogenetic protein-4 inhibits proliferation and induces apoptosis of multiple myeloma cells. *Blood* 97:516-522.**
- Horky LL, Galimi F, Gage FH, Horner PJ (2006) Fate of endogenous stem/progenitor cells following spinal cord injury. *J Comp Neurol* 498:525-538.**
- Horner PJ, Thallmair M, Gage FH (2002) Defining the NG2-expressing cell of the adult CNS. *J Neurocytol* 31:469-480.**
- Houle JD (1991) Demonstration of the potential for chronically injured neurons to regenerate axons into intraspinal peripheral nerve grafts. *Exp Neurol* 113:1-9.**
- Hynes RO (1992) Integrins: versatility, modulation, and signaling in cell adhesion. *Cell* 69:11-25.**
- Hynes RO (2002) Integrins: bidirectional, allosteric signaling machines. *Cell* 110:673-687.**
- Jain A, Kim YT, McKeon RJ, Bellamkonda RV (2006) In situ gelling hydrogels for conformal repair of spinal cord defects, and local delivery of BDNF after spinal cord injury. *Biomaterials* 27:497-504.**
- Jensen UB, Lowell S, Watt FM (1999) The spatial relationship between stem cells and their progeny in the basal layer of human epidermis: a new view based on whole-mount labelling and lineage analysis. *Development* 126:2409-2418.**

- Jiang H, Guler MO, Stupp SI (2007) The internal structure of self-assembled amphiphile nanofibers. *Soft Matter* 3.**
- Johansson CB, Momma S, Clarke DL, Risling M, Lendahl U, Frisen J (1999) Identification of a neural stem cell in the adult mammalian central nervous system. *Cell* 96:25-34.**
- Johe KK, Hazel TG, Muller T, Dugich-Djordjevic MM, McKay RD (1996) Single factors direct the differentiation of stem cells from the fetal and adult central nervous system. *Genes Dev* 10:3129-3140.**
- Joshi M, Fehlings MG (2002a) Development and characterization of a novel, graded model of clip compressive spinal cord injury in the mouse: Part 2. Quantitative neuroanatomical assessment and analysis of the relationships between axonal tracts, residual tissue, and locomotor recovery. *J Neurotrauma* 19:191-203.**
- Joshi M, Fehlings MG (2002b) Development and characterization of a novel, graded model of clip compressive spinal cord injury in the mouse: Part 1. Clip design, behavioral outcomes, and histopathology. *J Neurotrauma* 19:175-190.**
- Karimi-Abdolrezaee S, Eftekharpour E, Wang J, Morshead CM, Fehlings MG (2006) Delayed transplantation of adult neural precursor cells promotes remyelination and functional neurological recovery after spinal cord injury. *J Neurosci* 26:3377-3389.**
- Kawamura C, Kizaki M, Yamato K, Uchida H, Fukuchi Y, Hattori Y, Koseki T, Nishihara T, Ikeda Y (2000) Bone morphogenetic protein-2 induces apoptosis in human myeloma cells with modulation of STAT3. *Blood* 96:2005-2011.**
- Keirstead HS, Blakemore WF (1999) The role of oligodendrocytes and oligodendrocyte progenitors in CNS remyelination. *Adv Exp Med Biol* 468:183-197.**
- Keirstead HS, Nistor G, Bernal G, Totoiu M, Cloutier F, Sharp K, Steward O (2005) Human embryonic stem cell-derived oligodendrocyte progenitor cell transplants remyelinate and restore locomotion after spinal cord injury. *J Neurosci* 25:4694-4705.**
- Kigerl KA, McGaughy VM, Popovich PG (2006) Comparative analysis of lesion development and intraspinal inflammation in four strains of mice following spinal contusion injury. *J Comp Neurol* 494:578-594.**

- Kimelberg HK (2004) The problem of astrocyte identity. *Neurochem Int* 45:191-202.**
- Koenig BB, Cook JS, Wolsing DH, Ting J, Tiesman JP, Correa PE, Olson CA, Pecquet AL, Ventura F, Grant RA, et al. (1994) Characterization and cloning of a receptor for BMP-2 and BMP-4 from NIH 3T3 cells. *Mol Cell Biol* 14:5961-5974.**
- Kreutzberg GW (1996) Microglia: a sensor for pathological events in the CNS. *Trends Neurosci* 19:312-318.**
- Lee KK, de Repentigny Y, Saulnier R, Rippstein P, Macklin WB, Kothary R (2006) Dominant-negative beta1 integrin mice have region-specific myelin defects accompanied by alterations in MAPK activity. *Glia* 53:836-844.**
- Leone DP, Relvas JB, Campos LS, Hemmi S, Brakebusch C, Fassler R, Ffrench-Constant C, Suter U (2005) Regulation of neural progenitor proliferation and survival by beta1 integrins. *J Cell Sci* 118:2589-2599.**
- Ligon KL, Kesari S, Kitada M, Sun T, Arnett HA, Alberta JA, Anderson DJ, Stiles CD, Rowitch DH (2006) Development of NG2 neural progenitor cells requires Olig gene function. *Proc Natl Acad Sci U S A* 103:7853-7858.**
- Lillien LE, Raff MC (1990) Differentiation signals in the CNS: type-2 astrocyte development in vitro as a model system. *Neuron* 5:111-119.**
- Liu F, Ventura F, Doody J, Massague J (1995) Human type II receptor for bone morphogenic proteins (BMPs): extension of the two-kinase receptor model to the BMPs. *Mol Cell Biol* 15:3479-3486.**
- Liu XZ, Xu XM, Hu R, Du C, Zhang SX, McDonald JW, Dong HX, Wu YJ, Fan GS, Jacquin MF, Hsu CY, Choi DW (1997) Neuronal and glial apoptosis after traumatic spinal cord injury. *J Neurosci* 17:5395-5406.**
- Lois C, Alvarez-Buylla A (1993) Proliferating subventricular zone cells in the adult mammalian forebrain can differentiate into neurons and glia. *Proc Natl Acad Sci U S A* 90:2074-2077.**
- Lu QR, Sun T, Zhu Z, Ma N, Garcia M, Stiles CD, Rowitch DH (2002) Common developmental requirement for Olig function indicates a motor neuron/oligodendrocyte connection. *Cell* 109:75-86.**

- Mabie PC, Mehler MF, Marmur R, Papavasiliou A, Song Q, Kessler JA (1997) Bone morphogenetic proteins induce astroglial differentiation of oligodendroglial-astroglial progenitor cells. J Neurosci 17:4112-4120.**
- Matsuura I, Taniguchi J, Hata K, Saeki N, Yamashita T (2008) BMP inhibition enhances axonal growth and functional recovery after spinal cord injury. J Neurochem 105:1471-1479.**
- McCarthy KD, de Vellis J (1980) Preparation of separate astroglial and oligodendroglial cell cultures from rat cerebral tissue. J Cell Biol 85:890-902.**
- McKay R (1997) Stem cells in the central nervous system. Science 276:66-71.**
- McTigue DM, Wei P, Stokes BT (2001) Proliferation of NG2-positive cells and altered oligodendrocyte numbers in the contused rat spinal cord. J Neurosci 21:3392-3400.**
- Mehler MF, Rozental R, Dougherty M, Spray DC, Kessler JA (1993) Cytokine regulation of neuronal differentiation of hippocampal progenitor cells. Nature 362:62-65.**
- Mehler MF, Marmur R, Gross R, Mabie PC, Zang Z, Papavasiliou A, Kessler JA (1995) Cytokines regulate the cellular phenotype of developing neural lineage species. Int J Dev Neurosci 13:213-240.**
- Meletis K, Barnabe-Heider F, Carlen M, Evergren E, Tomilin N, Shupliakov O, Frisen J (2008) Spinal cord injury reveals multilineage differentiation of ependymal cells. PLoS Biol 6:e182.**
- Menet V, Prieto M, Privat A, Gimenez y Ribotta M (2003) Axonal plasticity and functional recovery after spinal cord injury in mice deficient in both glial fibrillary acidic protein and vimentin genes. Proc Natl Acad Sci U S A 100:8999-9004.**
- Milev P, Maurel P, Haring M, Margolis RK, Margolis RU (1996) TAG-1/axonin-1 is a high-affinity ligand of neurocan, phosphacan/protein-tyrosine phosphatase-zeta/beta, and N-CAM. J Biol Chem 271:15716-15723.**
- Milev P, Friedlander DR, Sakurai T, Karthikeyan L, Flad M, Margolis RK, Grumet M, Margolis RU (1994) Interactions of the chondroitin sulfate proteoglycan phosphacan, the extracellular domain of a receptor-type protein tyrosine**

- phosphatase, with neurons, glia, and neural cell adhesion molecules. *J Cell Biol* 127:1703-1715.
- Milner R, Campbell IL (2002) The integrin family of cell adhesion molecules has multiple functions within the CNS. *J Neurosci Res* 69:286-291.
- Mishina Y (2003) Function of bone morphogenetic protein signaling during mouse development. *Front Biosci* 8:d855-869.
- Mishina Y, Suzuki A, Ueno N, Behringer RR (1995) Bmpr encodes a type I bone morphogenetic protein receptor that is essential for gastrulation during mouse embryogenesis. *Genes Dev* 9:3027-3037.
- Mishina Y, Hanks MC, Miura S, Tallquist MD, Behringer RR (2002) Generation of Bmpr/Alk3 conditional knockout mice. *Genesis* 32:69-72.
- Molne M, Studer L, Tabar V, Ting YT, Eiden MV, McKay RD (2000) Early cortical precursors do not undergo LIF-mediated astrocytic differentiation. *J Neurosci Res* 59:301-311.
- Moon LD, Asher RA, Rhodes KE, Fawcett JW (2001) Regeneration of CNS axons back to their target following treatment of adult rat brain with chondroitinase ABC. *Nat Neurosci* 4:465-466.
- Mothe AJ, Tator CH (2005) Proliferation, migration, and differentiation of endogenous ependymal region stem/progenitor cells following minimal spinal cord injury in the adult rat. *Neuroscience* 131:177-187.
- Murphy M, Drago J, Bartlett PF (1990) Fibroblast growth factor stimulates the proliferation and differentiation of neural precursor cells in vitro. *J Neurosci Res* 25:463-475.
- Nishiyama A, Watanabe M, Yang Z, Bu J (2002) Identity, distribution, and development of polydendrocytes: NG2-expressing glial cells. *J Neurocytol* 31:437-455.
- Nohno T, Ishikawa T, Saito T, Hosokawa K, Noji S, Wolsing DH, Rosenbaum JS (1995) Identification of a human type II receptor for bone morphogenetic protein-4 that forms differential heteromeric complexes with bone morphogenetic protein type I receptors. *J Biol Chem* 270:22522-22526.

- Nomizu M, Weeks BS, Weston CA, Kim WH, Kleinman HK, Yamada Y (1995) Structure-activity study of a laminin alpha 1 chain active peptide segment Ile-Lys-Val-Ala-Val (IKVAV). *FEBS Lett* 365:227-231.
- Okada S, Nakamura M, Katoh H, Miyao T, Shimazaki T, Ishii K, Yamane J, Yoshimura A, Iwamoto Y, Toyama Y, Okano H (2006) Conditional ablation of Stat3 or Socs3 discloses a dual role for reactive astrocytes after spinal cord injury. *Nat Med* 12:829-834.
- Oohira A, Matsui F, Tokita Y, Yamauchi S, Aono S (2000) Molecular interactions of neural chondroitin sulfate proteoglycans in the brain development. *Arch Biochem Biophys* 374:24-34.
- Palmer TD, Ray J, Gage FH (1995) FGF-2-responsive neuronal progenitors reside in proliferative and quiescent regions of the adult rodent brain. *Mol Cell Neurosci* 6:474-486.
- Panchision DM, Pickel JM, Studer L, Lee SH, Turner PA, Hazel TG, McKay RD (2001) Sequential actions of BMP receptors control neural precursor cell production and fate. *Genes Dev* 15:2094-2110.
- Parnavelas JG, Nadarajah B (2001) Radial glial cells. are they really glia? *Neuron* 31:881-884.
- Pekny M, Johansson CB, Eliasson C, Stakeberg J, Wallen A, Perlmann T, Lendahl U, Betsholtz C, Berthold CH, Frisen J (1999) Abnormal reaction to central nervous system injury in mice lacking glial fibrillary acidic protein and vimentin. *J Cell Biol* 145:503-514.
- Pitman M, Emery B, Binder M, Wang S, Butzkueven H, Kilpatrick TJ (2004) LIF receptor signaling modulates neural stem cell renewal. *Mol Cell Neurosci* 27:255-266.
- Popovich PG, Wei P, Stokes BT (1997) Cellular inflammatory response after spinal cord injury in Sprague-Dawley and Lewis rats. *J Comp Neurol* 377:443-464.
- Pringle NP, Guthrie S, Lumsden A, Richardson WD (1998) Dorsal spinal cord neuroepithelium generates astrocytes but not oligodendrocytes. *Neuron* 20:883-893.
- Privat A (1975) Postnatal gliogenesis in the mammalian brain. *Int Rev Cytol* 40:281-323.

- Privat A, Leblond CP (1972) The subependymal layer and neighboring region in the brain of the young rat. J Comp Neurol 146:277-302.**
- Qin L, Wine-Lee L, Ahn KJ, Crenshaw EB, 3rd (2006) Genetic analyses demonstrate that bone morphogenetic protein signaling is required for embryonic cerebellar development. J Neurosci 26:1896-1905.**
- Raff MC, Miller RH, Noble M (1983a) A glial progenitor cell that develops in vitro into an astrocyte or an oligodendrocyte depending on culture medium. Nature 303:390-396.**
- Raff MC, Abney ER, Cohen J, Lindsay R, Noble M (1983b) Two types of astrocytes in cultures of developing rat white matter: differences in morphology, surface gangliosides, and growth characteristics. J Neurosci 3:1289-1300.**
- Rajan P, Panchision DM, Newell LF, McKay RD (2003) BMPs signal alternately through a SMAD or FRAP-STAT pathway to regulate fate choice in CNS stem cells. J Cell Biol 161:911-921.**
- Rakic P (1971) Neuron-glia relationship during granule cell migration in developing cerebellar cortex. A Golgi and electronmicroscopic study in Macacus Rhesus. J Comp Neurol 141:283-312.**
- Rao MS, Noble M, Mayer-Proschel M (1998) A tripotential glial precursor cell is present in the developing spinal cord. Proc Natl Acad Sci U S A 95:3996-4001.**
- Rash JE, Yasumura T, Hudson CS, Agre P, Nielsen S (1998) Direct immunogold labeling of aquaporin-4 in square arrays of astrocyte and ependymocyte plasma membranes in rat brain and spinal cord. Proc Natl Acad Sci U S A 95:11981-11986.**
- Reynolds BA, Weiss S (1992) Generation of neurons and astrocytes from isolated cells of the adult mammalian central nervous system. Science 255:1707-1710.**
- Reynolds BA, Weiss S (1996) Clonal and population analyses demonstrate that an EGF-responsive mammalian embryonic CNS precursor is a stem cell. Dev Biol 175:1-13.**

- Reynolds BA, Tetzlaff W, Weiss S (1992) A multipotent EGF-responsive striatal embryonic progenitor cell produces neurons and astrocytes. *J Neurosci* 12:4565-4574.
- Richardson PM, McGuinness UM, Aguayo AJ (1980) Axons from CNS neurons regenerate into PNS grafts. *Nature* 284:264-265.
- Rosenzweig BL, Imamura T, Okadome T, Cox GN, Yamashita H, ten Dijke P, Heldin CH, Miyazono K (1995) Cloning and characterization of a human type II receptor for bone morphogenetic proteins. *Proc Natl Acad Sci U S A* 92:7632-7636.
- Samanta J, Kessler JA (2004) Interactions between ID and OLIG proteins mediate the inhibitory effects of BMP4 on oligodendroglial differentiation. *Development* 131:4131-4142.
- Samanta J, Burke GM, McGuire T, Pisarek AJ, Mukhopadhyay A, Mishina Y, Kessler JA (2007) BMPR1a signaling determines numbers of oligodendrocytes and calbindin-expressing interneurons in the cortex. *J Neurosci* 27:7397-7407.
- Schense JC, Bloch J, Aebischer P, Hubbell JA (2000) Enzymatic incorporation of bioactive peptides into fibrin matrices enhances neurite extension. *Nat Biotechnol* 18:415-419.
- Schmechel DE, Rakic P (1979) A Golgi study of radial glial cells in developing monkey telencephalon: morphogenesis and transformation into astrocytes. *Anat Embryol (Berl)* 156:115-152.
- Schwab ME (2002) Repairing the injured spinal cord. *Science* 295:1029-1031.
- Schwab ME, Bartholdi D (1996) Degeneration and regeneration of axons in the lesioned spinal cord. *Physiol Rev* 76:319-370.
- See J, Mamontov P, Ahn K, Wine-Lee L, Crenshaw EB, 3rd, Grinspan JB (2007) BMP signaling mutant mice exhibit glial cell maturation defects. *Mol Cell Neurosci* 35:171-182.
- Sephel GC, Tashiro KI, Sasaki M, Greatorex D, Martin GR, Yamada Y, Kleinman HK (1989) Laminin A chain synthetic peptide which supports neurite outgrowth. *Biochem Biophys Res Commun* 162:821-829.

- Setoguchi T, Yone K, Matsuoka E, Takenouchi H, Nakashima K, Sakou T, Komiya S, Izumo S (2001) Traumatic injury-induced BMP7 expression in the adult rat spinal cord. *Brain Res* 921:219-225.**
- Setoguchi T, Nakashima K, Takizawa T, Yanagisawa M, Ochiai W, Okabe M, Yone K, Komiya S, Taga T (2004) Treatment of spinal cord injury by transplantation of fetal neural precursor cells engineered to express BMP inhibitor. *Exp Neurol* 189:33-44.**
- Shimazaki T, Shingo T, Weiss S (2001) The ciliary neurotrophic factor/leukemia inhibitory factor/gp130 receptor complex operates in the maintenance of mammalian forebrain neural stem cells. *J Neurosci* 21:7642-7653.**
- Shinohara T, Avarbock MR, Brinster RL (1999) beta1- and alpha6-integrin are surface markers on mouse spermatogonial stem cells. *Proc Natl Acad Sci U S A* 96:5504-5509.**
- Shuman SL, Bresnahan JC, Beattie MS (1997) Apoptosis of microglia and oligodendrocytes after spinal cord contusion in rats. *J Neurosci Res* 50:798-808.**
- Silva GA, Czeisler C, Niece KL, Beniash E, Harrington DA, Kessler JA, Stupp SI (2004) Selective differentiation of neural progenitor cells by high-epitope density nanofibers. *Science* 303:1352-1355.**
- Silver J, Miller JH (2004) Regeneration beyond the glial scar. *Nat Rev Neurosci* 5:146-156.**
- Skoff RP (1990) Gliogenesis in rat optic nerve: astrocytes are generated in a single wave before oligodendrocytes. *Dev Biol* 139:149-168.**
- Sofroniew MV (2005) Reactive astrocytes in neural repair and protection. *Neuroscientist* 11:400-407.**
- Steward O, Zheng B, Tessier-Lavigne M (2003) False resurrections: distinguishing regenerated from spared axons in the injured central nervous system. *J Comp Neurol* 459:1-8.**
- Stokes BT, Fox P, Hollinden G (1983) Extracellular calcium activity in the injured spinal cord. *Exp Neurol* 80:561-572.**

- Stokols S, Tuszynski MH (2004) The fabrication and characterization of linearly oriented nerve guidance scaffolds for spinal cord injury. *Biomaterials* 25:5839-5846.**
- Stokols S, Tuszynski MH (2006) Freeze-dried agarose scaffolds with uniaxial channels stimulate and guide linear axonal growth following spinal cord injury. *Biomaterials* 27:443-451.**
- Storck T, Schulte S, Hofmann K, Stoffel W (1992) Structure, expression, and functional analysis of a Na(+)-dependent glutamate/aspartate transporter from rat brain. *Proc Natl Acad Sci U S A* 89:10955-10959.**
- Talbott JF, Loy DN, Liu Y, Qiu MS, Bunge MB, Rao MS, Whitemore SR (2005) Endogenous Nkx2.2+/Olig2+ oligodendrocyte precursor cells fail to remyelinate the demyelinated adult rat spinal cord in the absence of astrocytes. *Exp Neurol* 192:11-24.**
- Tashiro K, Sephel GC, Weeks B, Sasaki M, Martin GR, Kleinman HK, Yamada Y (1989) A synthetic peptide containing the IKVAV sequence from the A chain of laminin mediates cell attachment, migration, and neurite outgrowth. *J Biol Chem* 264:16174-16182.**
- Temple S (2001) The development of neural stem cells. *Nature* 414:112-117.**
- ten Dijke P, Yamashita H, Sampath TK, Reddi AH, Estevez M, Riddle DL, Ichijo H, Heldin CH, Miyazono K (1994) Identification of type I receptors for osteogenic protein-1 and bone morphogenetic protein-4. *J Biol Chem* 269:16985-16988.**
- Teng YD, Lavik EB, Qu X, Park KI, Ourednik J, Zurakowski D, Langer R, Snyder EY (2002) Functional recovery following traumatic spinal cord injury mediated by a unique polymer scaffold seeded with neural stem cells. *Proc Natl Acad Sci U S A* 99:3024-3029.**
- Thuret S, Moon LD, Gage FH (2006) Therapeutic interventions after spinal cord injury. *Nat Rev Neurosci* 7:628-643.**
- Trivedi A, Olivas AD, Noble-Haesslein LJ (2006) Inflammation and Spinal Cord Injury: Infiltrating Leukocytes as Determinants of Injury and Repair Processes. *Clin Neurosci Res* 6:283-292.**
- Tysseling-Mattiace VM, Sahni V, Niece KL, Birch D, Czeisler C, Fehlings MG, Stupp SI, Kessler JA (2008) Self-assembling nanofibers inhibit glial scar**

- formation and promote axon elongation after spinal cord injury. *J Neurosci* 28:3814-3823.
- Vescovi AL, Reynolds BA, Fraser DD, Weiss S (1993) bFGF regulates the proliferative fate of unipotent (neuronal) and bipotent (neuronal/astroglial) EGF-generated CNS progenitor cells. *Neuron* 11:951-966.
- Viti J, Feathers A, Phillips J, Lillien L (2003) Epidermal growth factor receptors control competence to interpret leukemia inhibitory factor as an astrocyte inducer in developing cortex. *J Neurosci* 23:3385-3393.
- Walz W (2000) Controversy surrounding the existence of discrete functional classes of astrocytes in adult gray matter. *Glia* 31:95-103.
- Watanabe T, Yamamoto T, Abe Y, Saito N, Kumagai T, Kayama H (1999) Differential activation of microglia after experimental spinal cord injury. *J Neurotrauma* 16:255-265.
- Wilhelmsson U, Li L, Pekna M, Berthold CH, Blom S, Eliasson C, Renner O, Bushong E, Ellisman M, Morgan TE, Pekny M (2004) Absence of glial fibrillary acidic protein and vimentin prevents hypertrophy of astrocytic processes and improves post-traumatic regeneration. *J Neurosci* 24:5016-5021.
- Xu C, Inokuma MS, Denham J, Golds K, Kundu P, Gold JD, Carpenter MK (2001) Feeder-free growth of undifferentiated human embryonic stem cells. *Nat Biotechnol* 19:971-974.
- Yamauchi K, Phan KD, Butler SJ (2008) BMP type I receptor complexes have distinct activities mediating cell fate and axon guidance decisions. *Development* 135:1119-1128.
- Yi SE, Daluiski A, Pederson R, Rosen V, Lyons KM (2000) The type I BMP receptor BMPRII is required for chondrogenesis in the mouse limb. *Development* 127:621-630.
- Ying QL, Nichols J, Chambers I, Smith A (2003) BMP induction of Id proteins suppresses differentiation and sustains embryonic stem cell self-renewal in collaboration with STAT3. *Cell* 115:281-292.
- Yong VW, Moudjian R, Yong FP, Ruijs TC, Freedman MS, Cashman N, Antel JP (1991) Gamma-interferon promotes proliferation of adult human astrocytes

in vitro and reactive gliosis in the adult mouse brain in vivo. Proc Natl Acad Sci U S A 88:7016-7020.

Zhou Q, Anderson DJ (2002) The bHLH transcription factors OLIG2 and OLIG1 couple neuronal and glial subtype specification. Cell 109:61-73.

Zhu AJ, Haase I, Watt FM (1999) Signaling via beta1 integrins and mitogen-activated protein kinase determines human epidermal stem cell fate in vitro. Proc Natl Acad Sci U S A 96:6728-6733.

Zhu X, Bergles DE, Nishiyama A (2008) NG2 cells generate both oligodendrocytes and gray matter astrocytes. Development 135:145-157.

Zuo J, Neubauer D, Dyess K, Ferguson TA, Muir D (1998) Degradation of chondroitin sulfate proteoglycan enhances the neurite-promoting potential of spinal cord tissue. Exp Neurol 154:654-662.